T H E S I S

APPLICATION OF THE THEORY OF BENDING TO THE STRUCTURAL MEMBERS OF SHIPS

by

I. M. YUILLE, B.Sc., A.M.I.N.A.

University of Glasgow

1956

PREFACE

On my return to employment in a shipyard design office after graduating in 1947, I was required to solve many problems of a non-routine nature. These were associated with almost every branch of naval architecture, but structural strength problems predominated and most of the latter were concerned with the local strength of the structural members of ships rather than strength of the hull as a whole. It seemed to be generally accepted that knowledge of the application of the theory of bending was inadequate and cynics went so far as to state that no matter what theoretical stresses were obtained, they would bear little relation to those which actually occurred. This unhappy state of affairs led me to enquire what shortcomings there might be in the usual theory of flexure and a survey of relevant literature revealed a formidable list. Although there were many theories covering the whole range of possibilities there seemed to be very little experimental evidence to enable one to decide which of the possible causes of error was important in shipbuilding, although it was possible to make a reasonable guess. An exception was the vast amount of experimental research at Glengarnock, which had been started by the Welding Research Council just before the last war to compare welded and riveted stiffened plating under conditions which simulated those in a ship. Throughout this work (which is still going on) interim factual reports were issued, but the investigators appeared to have shelved the task of analysis. When the opportunity arose for me to carry out research at the University it was not unnatural that I should chose to examine this problem.

The main objective was to decide what precautions must be taken when using the theory of elastic bending to analyse the strength of the structural members of ships and to formulate a suitable theory which could be applied in the design offices of shipyards. With the latter end in view it was necessary that the final theory should be as simple as possible and, bearing in mind that in general neither the loads applied to most ship structures nor the strength characteristics of the materials used were accurately known, it was permissible to omit refinements of the theory which would affect the results by less than a few per-cent. To achieve this object the stresses and deflections measured in the experiments at Glengarnock were compared with those predicted by the theory of bending, and the theory was modified until it could be made to agree with the measurements with reasonable accuracy. This analysis was supplemented by some experimental work on board ship which showed that the theories developed could be applied also in practice. Although the research did not necessarily proceed in a straightforward manner the results are presented in this thesis in a logical sequence. There are five main chapters with a review of the work in a sixth chapter, and an Appendix.

Two problems which were peculiar to shipbuilding appeared to be important. The first of these was the difficulty of deciding what degree of constraint there was at the ends of the structural members of ships. To enable this to be taken into account I modified one of the most useful tools of structural analysis - the method of moment distribution. An early version of the theory was sent to the Institution

of Naval Architects in an interim report on the research and was published in 1952 (ref. A1), but later revisions were so extensive that a full account of the final theory is given in Chapter I of the thesis. The theory allows for the constraint at the ends of loaded beams which may be straight or curved in the plane of the applied loads and may have constant or variable cross sections.

The second problem was that of shear lag in stiffened plating. This occurs in ships and aircraft and had received a good deal of theoretical attention. Many of the theories indicated conflicting results and hardly any experimental work had been published; the Glengarnock results were inconclusive. I therefore investigated the matter by theory and experiment, and the results were published in 1955 by the Institution of Naval Architects. A copy of this paper, together with the discussion, is bound as an Appendix at the end of the thesis and a summary (and one small extension which has a bearing on later work) is given in Chapter II. It is shown that shear lag is usually unimportant in shipbuilding, but a new method of calculating shear lag effects is described for use when required.

With this foundation it was found to be possible to commence an analysis of the Glengarnock results and this is discussed in Chapter III. Altogether the results of about 300 experiments were examined. It was found to be possible to correlate a large number of these by means of the theory described in Chapter I. Further modifications or additions to the theory of bending were required in order to account for discrepancies noted in certain classes of specimen, and these are discussed as they arise. An attempt to predict the experimental results entirely from theoretical considerations met with a fair amount of success. A paper on the analysis is nearly ready for submission to the Institution of Naval Architects.

In Chapter IV there is a description of some experiments which I carried out on board ship. Measured deflections are compared with those predicted theoretically and, although agreement is not perfect, it is shown that it is possible to estimate fairly accurately the constraint at the ends of a bulkhead stiffener with welded brackets, at any rate in this particular case, by the theory outlined in Chapter I.

The theories described are all based on elastic analysis of beams but in Chapter V there is a brief discussion of the possibilities of using the theory of plastic bending in shipbuilding. This is followed in Chapter VI by a review of the research and some conclusions and suggestions for further work.

The list of references at the end of the thesis includes all work previously published which came to my notice and which was of use to me during the research. References are given in the text where appropriate by a letter followed by a number; the letter indicates the group in which the paper is classified and the number refers to its position in that group of the list. Articles etc. which were found to

contain faulty theories or which were of little use for other reasons, have been omitted unless they are of historical interest or the faults noted led me to an advance in knowledge.

I would like to express my gratitude to the staff of the University for the help and encouragement I was given throughout the period of my research. I have the most pleasant memories of the friendliness with which I was received by all those from whom I sought assistance.

My research also benefitted considerably by the help given by the British Shipbuilding Research Association. I was allowed to consult the field results of the Glengarnock experiments, and received many useful papers and articles which would otherwise have been difficult to obtain. Messrs. Alexander Stephen and Sons very kindly permitted me to carry out experiments in two ships during construction and the firm's generous assistance at that time is much appreciated. (See also footnote on page 116). The remainder of my experiments were carried out in the James Watt Engineering Laboratories of the University, by permission of their Director, Prof. J. Small, and I am most grateful to Mr. E. J. Fair for his assistance during those which concerned shear lag.

Lastly, I am indebted to the Institution of Naval Architects and the Royal Commission for the Exhibition of 1851 for awarding me their Post Graduate Research Scholarship in Naval Architecture.

J. M. Quille.

Research Student at the University of Glasgow,

October 1949 - September 1952.

CONTENTS

CHAPTER I

CONSTRAINT AT THE ENDS OF STRUCTURAL MEMBERS OF SHIPS.

1) Introduction.

The classical beam theories enable investigations to be undertaken regarding the strength of loaded beams of two types:

a) Those with ends completely fixed or encastré.

b) Those with ends freely supported.

In a ship these conditions are rarely fulfilled and beams in an intermediate condition are said to be partially constrained at the ends. It is customary in shipyards to analyse the strength of partially constrained beams in a somewhat unscientific manner. It is generally recognised that the incomplete constraint is due mainly to the flexibility of the structure to which the beams are connected and to a lesser extent to distortion of the connections, and that the strength of loaded parts of the structure should be calculated by considering them to be parts of the continuous structure of the ship. Owing to the prohibitive amount of work involved in considering a large part of the ship as a continuous structure merely to find the bending moments acting in a loaded small part of it, recourse is usually had to other methods. Often the bending moments are calculated on the assumption that the ends of the beams are completely fixed and then the fixing moments are reduced by an empirical amount, the value of which is often assumed to depend upon the size of bracket or other connection of the beams to the surrounding structure. Even when the analysis is carried out by an experienced man the results can be little better than guesswork. The main purpose of the research described in this chapter was to develop a more rational method which would enable the strength of a loaded portion of a ship to be calculated after correctly taking account of the constraint afforded by the surrounding structure.

Structural members of ships are almost always statically indeterminate and there are three general methods by which they may be analysed: strain energy, slope-deflection, or relaxation. There are several variations of each of these but all the methods lead eventually to the same results. When applied to structures which involve several members the first two methods become very laborious on account of the large numbers of simultaneous equations involved. The last is in fact an iterative method of solving equivalent simultaneous equations but it has the great advantage that convergence may be accelerated at the initiative of the computer. A reasonable approximation to the correct solution of a problem, or even an intuitive guess, may usually be made and this may be used as a starting point. After the artificial restraints have been relaxed to the extent indicated unbalanced forces (residuals) remain which simply constitute a new problem, and the solution of this may again be approximated

and the cycle repeated. Whatever approximations are made - good or bad - the relaxation method leads eventually to the correct solution. It should not be inferred that the relaxation method requires good intuitional powers. If the relaxation of restraints is carried out in any predetermined sequence it becomes simply an iterative process. The operator can vary the process to any extent which his skill permits. (When deflections of the joints do not occur the relaxation method applied to continuous beams becomes the moment distribution method and convergence is sufficiently rapid to give a solution without resort to additional techniques of this kind). The relaxation method has the additional advantages that it is possible to visualize the process as it is carried out and that the work can be stopped as soon as the solution is within the accuracy of the assumptions upon which it is based. These considerations influenced the choice of relaxation as the method of analysis to be used.

The amount of arithmetical work in any problem of the sort under discussion increases very rapidly as the number of joints between beam spans is increased. This chapter is concerned with a new technique which reduces the amount of arithmetical work by reducing the number of moments and forces to be considered in the relaxation process. Instead of distributing moments through the complete structure, the effects of the unloaded members surrounding the loaded portion are expressed by coefficients of constraint and the relaxation process is confined to the loaded members only. A number of variations of the technique, all aimed at reducing the arithmetical work, are illustrated in the examples.

Consider a continuous beam which is to be analysed by moment distribution. If the extreme ends of the beam are completely fixed they do not require to be alternately released and fixed during the distribution process; the moments carried over simply remain. On the other hand, if the ends are freely supported the moments carried over to them have to be repeatedly reduced to zero by releasing the artificial restraints at the freely supported ends. As pointed out by Hardy Cross in his original paper (ref. R 1) the process may be simplified by keeping sunh ends permanently free throughout the distribution. The initial fixed-end moments must be altered accordingly and a modified value of the stiffness must be used when calculating the manner in which the unbalanced moment at the adjacent joint is to be distributed. For a straight prismatic beam with a fixed end the stiffness at the other end is $K = 4\ EI/L$ and the carry-over factor is 1/2, but if one end is freely supported the stiffness at the other end is $K = 3\ EI/L$ and the carry-over is zero.

In a ship the extreme ends of a loaded part of the structure which it is desired to analyse are generally neither completely fixed nor freely supported, but are partially constrained by the surrounding structure of the ship. In order to avoid extending the analysis to a number of points beyond the loaded part of the structure the constraint at its extremities may be evaluated. When analysing the whole continuous structure by the normal moment distribution methods change of slope is prevented at all joints except the one at which an artificial restraint is released during a step in the process. In the new method, artificial restraints are placed only at joints within the loaded structure: changes of slope (but not deflection) are permitted at all joints at the extremities of the loaded structure and, with certain exceptions, at all joints in the surrounding unloaded structure. The surrounding structure resists changes of

slope at the extremities of the loaded part of the structure and the stiffness etc. of the outside members of the latter must be modified accordingly. The bending moments in the loaded members may then be found without further regard to the constraining structure surrounding them. The theory is a logical development of the method used for freely supported ends mentioned in the last paragraph.

2) Straight Prismatic Beam - Moment Distribution Equations.

I Change of Slope imposed at one end.

The basic equations required in the application of relaxation methods will be derived by the slope-deflection method (see, for example, ref. B 3) and the following sign convention will be used: "Loads applied downwards ..... , bending moments tending to produce concavity downwards ..... , and downwards deflections, are considered to be positive."

Consider a beam AB of length L and moment of inertia of cross section I, and let a change of slope θ be imposed at B ($x = L$) by a moment M_B while the other end A ($x = 0$) is constrained against rotation by structure having stiffness, or moment per unit change of slope, K_E. Let the deflection be zero at both ends of the beam and let the change of slope at A be ϕ and the bending moment in the beam at A associated with constraint applied by the end structure, be M_A. Then the slope-deflection equations are:

$$\theta - \phi = \frac{1}{E I} \int_A^B M.dx \qquad (2\cdot1)$$

$$L\theta = \frac{1}{E I} \int_A^B Mx.dx \qquad (2\cdot2)$$

The bending moments M in the beam arise from the application of moments at the ends of the beam only. Hence the shear forces must be constant along the beam and the bending moments must vary linearly from A to B so that:

$$\int_A^B M.dx = \text{Area under bending moment diagram from A to B} = \frac{L}{2}(M_A + M_B) \qquad (2\cdot3)$$

$$\int_A^B Mx\cdot dx = \text{Moment of area under bending moment diagram about A} = \frac{L^2}{6}(M_A + 2M_B) \qquad (2\cdot4)$$

Since the moment M_A is associated with the presence of the constraining structure at A, $M_A/\phi = K_E$, by definition of K.

or $$\phi = M_A/K_E \qquad (2\cdot5)$$

Hence equations 2·1 and 2·2 become:

$$\theta - \frac{M_A}{K_E} = \frac{L}{2EI}(M_A + M_B) \qquad (2\cdot6)$$

$$L\theta = \frac{L^2}{6EI}(M_A + 2M_B) \qquad (2\cdot7)$$

Solution of these simultaneous equations leads to the results:

Stiffness K_B of beam at B $$= \frac{M_B}{\theta} = (3 + c)\frac{EI}{L} \qquad (2\cdot8)$$

Carry-over factor from B to A $$= \frac{M_A}{M_B} = -\frac{2c}{(3 + c)} \qquad (2\cdot9)$$

where c is a coefficient which expresses the constraint at end A of the beam and is defined by:

$$c = \frac{1}{1 + \frac{4EI}{K_E L}} = \frac{K_E}{\frac{4EI}{L} + K_E} \qquad (2\cdot10)$$

Hereafter "c" will be referred to as the "coefficient of constraint." If the beam is completely fixed at A, c = 1, and if the beam is freely supported at A, c = 0. Note that in these two extreme cases equations 2·8 and 2·9 reduce to the usual Hardy Cross relationships.

II Deflection imposed at one end.

Consider a similar beam AB and let a change of level δ_B be imposed at B while no change of slope is permitted at B, and let the other end A be maintained at its original level while changes of slope are resisted by structure of stiffness K_E. Let the change of slope at A be ϕ and the bending moment in the beam at A associated with constraint applied by the end structure be M_A, and let the bending moment at B be M_B. Then the slope-deflection equations are:

$$-\phi = \frac{1}{EI}\int_A^B M.dx \qquad (2\cdot11)$$

$$-\delta_B = \frac{1}{EI}\int_A^B Mx.dx \qquad (2\cdot12)$$

Using the relationships 2·3, 2·4 and 2·5, these equations become:

$$-\frac{M_A}{K_E} = \frac{L}{2EI}(M_A + M_B) \qquad (2\cdot13)$$

$$-\delta_B = \frac{L^2}{6EI}(M_A + 2M_B) \qquad (2\cdot14)$$

Solution of these simultaneous equations yields the results:

$$M_B = -3(1+c)\frac{EI}{L^2}\delta_B \qquad (2\cdot15)$$

$$M_A = +6c\frac{EI}{L^2}\delta_B \qquad (2\cdot16)$$

where c is given by equation 2·10.

Equations 2·8, 2·9, 2·10, 2·15 and 2·16 are generalisations of the usual equations required for the analysis of structures made of straight prismatic beams by relaxation methods. Examples of the use of these equations will be given in Sections 5 and 6. It will be noted that the manner in which the stiffness of the end structure arises has not been specified. The end structure need not consist of beams for which the stiffness K is known; the resistance to rotation may arise in a number of other ways.

3) General Equation for End Moments in a Loaded Prismatic Beam with Both Ends Partially Constrained.

Consider a beam AB which is loaded so that the bending moments at the ends of the span would be M_{FA} and M_{FB} if the ends were completely fixed. If the ends are only partially constrained, let the end moments be M_A and M_B. Then from equation 2·1:

$$\theta - \phi = \int_0^L \frac{M_I}{EI}\,dx + \int_0^L \frac{M_S}{EI}\,dx$$

$$= \frac{L}{2EI}(M_A + M_B) + \int_0^L \frac{M_S}{EI}\,dx \qquad (3\cdot1)$$

where M_S represents the bending moments associated with the loads applied to the beam if it was statically determinate, and M_I represents the bending moments associated with end constraint.

For completely fixed ends:

$$\int_0^L \frac{M_I}{EI}\,dx + \int_0^L \frac{M_S}{EI}\,dx = 0$$

$$\therefore \int_0^L \frac{M_S}{EI}\,dx = -\frac{L}{2EI}(M_{FA} + M_{FB})$$

Substituting in equation 3·1:

$$\theta - \phi = \frac{L}{2EI}(M_A + M_B) - \frac{L}{2EI}(M_{FA} + M_{FB}) \qquad (3\cdot2)$$

Similarly, using equation 2·2 it may be shown that:

$$L\theta = \frac{L^2}{6EI}(M_A + 2M_B) - \frac{L^2}{6EI}(M_{FA} + 2M_{FB}) \qquad (3\cdot3)$$

If K_A and K_B are the stiffnesses of the constraining

structures beyond A and B respectively:

$$\phi = M_A/K_A \qquad \text{and} \qquad \theta = -M_B/K_B$$

The negative sign is used in the second expression because in general the sign of θ is opposite to that of M_B. Substituting these expressions into equations 3·2 and 3·3 the following equations are obtained:

$$-\frac{M_A}{K_A} - \frac{M_B}{K_B} = \frac{L}{2EI}(M_A + M_B) - \frac{L}{2EI}(M_{FA} + M_{FB})$$

$$-\frac{M_B L}{K_B} = \frac{L^2}{6EI}(M_A + 2M_B) - \frac{L^2}{6EI}(M_{FA} + 2M_{FB})$$

Solving these two simultaneous equations it is found that:

$$M_B = \frac{4 c_B M_{FB} + 2 c_B (1 - c_A) M_{FA}}{4 c_B + (1 - c_B)(3 + c_A)} \qquad (3·4)$$

$$M_A = \frac{4 c_A M_{FA} + 2 c_A (1 - c_B) M_{FB}}{4 c_B + (1 - c_B)(3 + c_A)} \qquad (3·5)$$

where $c_A = \dfrac{K_A}{\frac{4EI}{L} + K_A}$ $\qquad$ $c_B = \dfrac{K_B}{\frac{4EI}{L} + K_B}$

Note that the denominator of equations 3·4 and 3·5 has an alternative form:

$$4 c_B + (1 - c_B)(3 + c_A) = 4 c_A + (1 - c_A)(3 + c_B)$$

A particular case of some importance is that of a beam which is completely fixed at one end and partially constrained at the other. If end A is completely fixed ($c_A = 1$) and the coefficient of constraint at end B is c_B the equations become:

$$M_B = c_B M_{FB} \qquad (3·6)$$

$$M_A = M_{FA} + \frac{(1 - c_B) M_{FB}}{2} \qquad (3·7)$$

4) Application of Theory.

The moment distribution or relaxation process is used for only that part of the structure to which loads are applied. The first step is to calculate the coefficients of constraint c at the ends of the members at the extremities of the loaded part of the structure. Values of c are calculated by starting at a point remote from the loaded structure, either where c is known or where possible variations will give final results within the required degree of accuracy. Proceeding towards the loaded part of the structure, stiffnesses and coefficients of constraint are found alternately member by member, until a boundary of the loaded structure is reached. The procedure is repeated until the coefficients of constraint have been found at the ends of all the outside members of the loaded part of the structure. The adjusted stiffnesses of these members are then calculated using equation 2·8. The stiffnesses of all members within the loaded part of the structure are calculated in the usual way. The fixed end moments are then found in the usual way (except that those in the members just within the boundary of the loaded part of the structure are found by using equations 3·6 and 3·7), and unbalanced end moments are balanced in the usual way. The moments carried over to the partially constrained ends are computed at the end of the calculation, using the modified carry-over factor (equation 2·9), and these in turn are distributed to the members beyond them in ratio of their adjusted stiffnesses and carried over the next span, and so on until they become too small to be taken into account further. The processes will be clarified by means of examples in the following sections.

A difficulty may arise in the calculation of the coefficients of constraint in closed frameworks, such as a ship with one or more rows of pillars, where a point sufficiently remote from the loaded structure to enable the coefficients of constraint to be calculated accurately, cannot be found. In these cases it is possible to create points at which the constraint is known by disposing artificial restraints at one or more "strategic" joints in the unloaded framework. Starting at these it is possible to calculate the coefficients of constraint and to proceed as before. At the end of the computation, moments carried over to these "strategic" joints are unbalanced. It only remains to carry out a further analysis in which these joints are treated as a loaded structure, considering one or two other joints as fixed when necessary. If sizeable moments remained unbalanced after this, the cycle could be repeated until a satisfactory solution was obtained. The process is generally not as prolonged as might be supposed, for each time a moment is carried over an unloaded span it is multiplied by a carry-over factor less than one half, and in most problems the moments diminish very rapidly indeed. In many cases it is found that it is unnecessary to start calculating the coefficients of constraint more than two or three spans from the boundaries of the loaded part of the structure, and that any reasonable assumption for the value of c to start the calculation of the coefficients will yield a sufficiently accurate estimate of constraint nearer the loaded structure. In this the only reliable guide is experience.

It is convenient when using relaxation methods to fix one's attention on the moments and forces applied to the ends of the spans by the artificial restraints instead of on the bending moments in the beams themselves, particularly when considering a structure in which there

are both horizontal and vertical members, and the following sign convention is useful. A moment applied to the end of a beam is regarded as positive if it tends to rotate the end of the beam in a clockwise direction, and negative if it tends to rotate it counter-clockwise. After the bending moments in the individual members have been found by applying the formulae in the previous Sections (with the usual sign convention) it is a simple matter to find the moments applied to the ends of each span using the new sign convention. The main noticable difference is that the carry-over factor is positive in the working of the problem, instead of negative.

5) Example 1. Strength of Stiffeners in an Oil Tanker.

Fig. 1 A shows a longitudinal section through an all welded oil tander of similar construction to that of the "Neverita" (ref. X 1). The ship is longitudinally framed and the diagram represents one of the many parallel longitudinals at deck and bottom, together with the vertical stiffeners on the bulkheads which separate each oil tank. It is required to find the effect on these members of filling one tank.

Each tank is 378 in. long and 422 in. high. The moment of inertia of the deck longitudinals is 210 $in.^4$, that of the bottom longitudinals 980 $in.^4$, and that of the bulkhead stiffeners 317 $in.^4$ The The deck and bottom longitudinals are continuous along the length of the ship and the bulkhead stiffeners are continuous from top to bottom of the bulkheads and are rigidly connected to the longitudinals. In each tank there are two heavy transverse frames 139 in. from the bulkheads, which so stiffen the deck and bottom of the vessel that points on the longitudinals such as A, A', F and F' may be assumed to be supported rigidly so that they do not deflect under load. Similarly there are two sets of horizontal girders 127 in. and 237 in. above keel, which so stiffen the bulkheads that points such as C', C, S, D', D and T may be assumed to be supported rigidly so that they do not deflect under load. It is assumed, however, that the longitudinals and bulkhead stiffeners are free to change slope at the points at which they are so supported. The relaxation process in such cases becomes simply one of moment distribution.

Suppose that tank B B' E' E is filled with sea water ballast (35 ft^3/ton) and that several identical tanks fore and aft of this tank remain empty, (but weight is removed elsewhere so that the draught of the ship is unchanged). The problem of calculating the bending moments in the longitudinals and bulkhead stiffeners is greatly simplified by the fact that both the load and structure are symmetrical about a plane midway between the transverse frames A F and A'F'. Only one half of the structure needs to be analysed; the bending moments in the other half are identical. The procedure is to find the bending moments in the loaded part of the structure ABCDE by moment distribution methods modified to take account of the structure FEWXYZ, PQRSTU..... which, although there is no load applied to it, affords a certain amount of constraint to the joints B and E.

The coefficients of constraint at E and P are calculated as a preliminary. The constraining structure is a closed one,

so that it is necessary to chose joints which may be assumed to be completely fixed during the moment distribution process, as explained in Section 4. In this example joint T is suitable for this purpose. It is considered that the structure beyond U and Z is sufficiently remote not to affect the bending moments significantly. In order to calculate the coefficient of constraint at E start from T and Z. Assuming that T is completely fixed, the stiffness of YT at Y is

$$K_{YT} = \frac{4 E I_{YT}}{L_{YT}}$$

$$= 4 \times \frac{517}{185} E = 6{\cdot}85 E \text{ tons in./radian}$$

For numerical convenience it is preferable not to substitute the value of Young's modulus E.

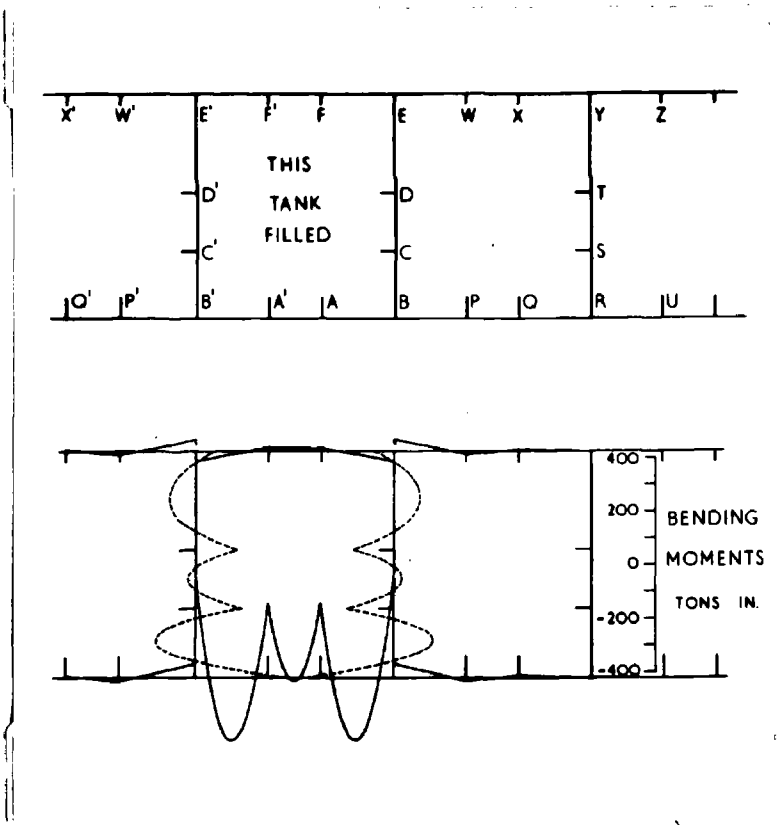

Fig. 1 To illustrate Example 1.

A Diagram of structure.

B Bending moments deduced as a result of analysis.

Assuming that the coefficient of constraint at Z is 0·5, the stiffness of YZ at Y is

$$K_{YZ} = (3 + c_{ZY}) \frac{E I_{YZ}}{L_{YZ}}$$

$$= 3{\cdot}5 \times \frac{210}{139} E = 5{\cdot}285 \text{ tons in./radian}$$

Then the coefficient of constraint for span XY at Y is

$$c_{YX} = \frac{\sum K_Y}{4 EI_{XY}/L_{XY} + \sum K_Y}$$

$$= \frac{6{\cdot}85 + 5{\cdot}285}{6{\cdot}04 + (6{\cdot}85 + 5{\cdot}285)} = 0{\cdot}668$$

Using this coefficient, the stiffness of span XY at X is

$$K_{XY} = (3 + c_{YX}) \frac{E I_{XY}}{L_{XY}}$$

$$= 3{\cdot}668 \times \frac{210}{139} E = 5{\cdot}54 E \text{ tons in./radian}$$

Similarly, the coefficient of constraint for span WX at X is

$$c_{XW} = \frac{K_X}{4 EI_{WX}/L_{WX} + K_X}$$

$$= \frac{5{\cdot}54}{8{\cdot}4 + 5{\cdot}54} = 0{\cdot}397$$

Proceeding in this manner towards E it is found that

$$K_{WX} = 7{\cdot}15 E \text{ tons in./radian}$$

$$c_{WE} = 0{\cdot}542$$

$$K_{EW} = 5{\cdot}35 E \text{ tons in./radian}$$

Because of symmetry the span F F' may be treated by the method described in most textbooks on moment distribution (see, for

example, paras. 1·10 and 1·17 of ref. R 3). Stiffness of span F F' is

$$K_{FF'} = \frac{2\,E\,I_{FF'}}{L_{FF'}} = 4{\cdot}2\,E \text{ tons in./radian}$$

Then the coefficient of constraint for span E F at F is

$$c_{FE} = \frac{K_F}{4\,EI_{EF}/L_{EF} + K_F} = 0{\cdot}410$$

The stiffness of span E F at E is

$$K_{EF} = (3 + c_{FE})\frac{E\,I_{EF}}{L_{EF}} = 5{\cdot}05\,E \text{ tons in./radian}$$

The coefficient of constraint for span DE at E may now be calculated:

$$c_{ED} = \frac{\Sigma K_E}{4\,EI_{DE}/L_{DE} + \Sigma K_E}$$

$$= \frac{5{\cdot}05 + 5{\cdot}35}{6{\cdot}85 + (5{\cdot}05 + 5{\cdot}35)} = 0{\cdot}603$$

These computations can be performed rapidly and conveniently on a slide rule. In a similar manner the coefficient of constraint for span BP at P and the stiffness of span BP at B may be estimated. Starting from T which is assumed to be completely fixed, and U where the coefficient of constraint is assumed to be 0·5, the figures are:

$K_{ST} = 11.52\,E$ tons in./radian — $c_{SR} = 0{\cdot}536$

$K_{RS} = 8{\cdot}81\,E$ tons in./radian

$K_{RU} = 24{\cdot}68\,E$ tons in./radian — $c_{RQ} = 0{\cdot}543$

$K_{QR} = 25{\cdot}0\,E$ tons in./radian — $c_{QP} = 0{\cdot}389$

$K_{PQ} = 33{\cdot}2\,E$ tons in./radian — $c_{PB} = 0{\cdot}541$

$K_{BP} = 24{\cdot}98\,E$ tons in./radian

After this preparatory work the main calculation of moments in the loaded part of the structure is carried out in Table I (p. 13),

TABLE I

MOMENT DISTRIBUTION APPLIED TO LOADED PART OF STRUCTURE SHOWN IN FIG. 1 A.

1	Joint	A		B			C		D	
2	Member	AA'	AB	BA	BP	BC	CB	CD	DC	DE
3	Distribution factors	0·410	0·592	0·446	0·396	0·158	0·465	0·535	0·651	0·349
4	Initial moments (tons in.)	+192	-371	+371	0	-273	+254	-138	+126	-195
5	Distribution A	+ 73	+106							
6	Carry-over			+ 53						
7	Distribution C						- 54	- 62		
8	Carry-over					- 27			- 31	
9	Distribution B			- 55	- 49	- 20				
10	Carry-over		- 27				- 10			
11	Distribution D								+ 65	+ 35
12	Carry-over							+52		
13	Distribution A	+ 11	+ 16							
14	Carry-over			+ 8						
15	Distribution C						- 10	- 12		
16	Carry-over					- 5			- 6	
17	Distribution D								+ 4	+ 2
18	Carry-over							+ 2		
19	Distribution B			- 1	- 1	0				
20	Distribution C						- 1	- 1		
21	Final moments (Tons in.)	+276	-276	+376	- 50	-325	+179	-179	+158	-158

in much the same way as ordinary moment distribution. Artificial restraints are applied at A,B,C and D and the distribution factors at each are found in the usual way by dividing the stiffness of each adjoining member in turn by the sum of the stiffnesses of all members meeting at that joint, and are entered in line 3. The fixing moments at A,B,C and D are calculated from the loading and entered in line 4. The following points are noteworthy:

a) The sign convention is that mentioned at the end of Section 4.

b) Because of symmetry the stiffness of AA' at A is $2\ EI_{AA'}/L_{AA'}$

c) The sum of the stiffnesses at B includes the stiffness of BP taking account of the coefficient of constraint at P as described above.

d) Although a load is applied to span DE it is necessary to apply an artificial restraint only at D, where the adjoining span is also under load. The fixing moments applied to the ends of span DE would be 172 tons in. (counter clockwise) at D and 115 tons in. (clockwise) at E, if both ends were completely fixed. The joint E is not completely fixed, however, but is partially constrained by spans EF and EW and the end moments are calculated by using equations 3·6 and 3·7, thus:

$$M_E = 0{\cdot}603 \times 115$$

$$= 69 \text{ tons in.} \quad \text{(clockwise)}$$

$$M_D = 172 + \frac{(1 - 0{\cdot}603)}{2} \times 115$$

$$= 195 \text{ tons in.} \quad \text{(counter clockwise)}$$

The end moments at A,B,C and D may then be balanced by the normal processes of moment distribution, which require no description here. This work is set out in Table I and the final moments applied to the members meeting at A,B,C and D are given in line 21.

The moments carried over into the unloaded part of the structure are then calculated as follows. The change in moment at B in span BP is 50 tons in. and the moment carried over to P is

$$\frac{2\ c_{PB}}{3 + c_{PB}} \times (50) = \frac{2 \times 0{\cdot}541 \times 50}{3{\cdot}541}$$

$$= 15 \text{ tons in.}$$

Similarly, the moment carried over to Q is

$$\frac{2\,c_{qr}}{3 + c_{qr}} \times (15) = 3 \text{ tons in.}$$

- and the moment carried over to R is

$$\frac{2\,c_{qo}}{3 + c_{qo}} \times (5) = 1 \text{ ton in.}$$

Turning now to the deck: the moment at E was 69 tons in. initially, and during the distribution process the moment carried over to E was (see last column of Table I):

$$\frac{2 \times 0{\cdot}603}{3{\cdot}603} \times (35 + 2) = 12 \text{ tons in.}$$

Hence the total moment at E is 81 tons in. This is balanced by moments distributed between EF and EW in ratio of their stiffnesses

To EF	39 tons in.	Carry over to F	9 tons in.
To EW	42 tons in.		

Carry over to W	13 tons in.
Carry over to X	3 tons in.
Carry over to Y	1 ton in.

The moments carried over to joint T are insignificant, and it is therefore unnecessary to release the artificial restraint which was assumed to act there when the calculation of the effects of constraint was commenced. In practice, unless a very accurate result is required, it is usually unnecessary to consider more than two or three spans beyond the loaded part of the structure when calculating the coefficients of constraint, and in this example one could have started at joints Y and R.

The final bending moments in the structure, associated with the filling of the tank, are shown in fig. 1 B, on page 10.

6) Example 2. Transverse Strength of a Cargo Liner.

It sometimes happens that the problems may be so simplified by means of the coefficients of constraint that the solution may be obtained without resorting to a table of moment distributions. This will be illustrated by reference to the strength of an idealized cross section of a cargo liner.

Fig. 2 A shows half of the transverse section through a cargo vessel with hold and four decks. The section has been simplified on the lines suggested by Hay (ref. X 2), the main assumption being that there is a sharp corner at the bilge and all structural members are straight and of uniform cross section, (see Example 4 for a comment on this). It is assumed that the section considered is at the mid-length of a long hold and that the stiffness of the longitudinal keel is negligible compared with the stiffness of the transverse floors so that transverse forces are resisted by the transverse framing alone. The rigidity of the side plating and bottom plating of the ship under shearing forces in their own planes is assumed to be very large so that deflections in the plane of the plating are negligible compared with those perpendicular to the plating. Thus if a perpendicular load is applied to the transverse floor it will be resisted by the floor, which will bend, and the load is reacted at the ends of the floor by shearing actions in the vertical plating such that the ends B and B' do not deflect. A similar reasoning applies to the side plating and frames, and to the decks and beams. The inner ends of the beams at D, F, H and K are assumed to be simply supported by the hatch girders. Under these assumptions the structure can be analysed in the same way as a portal frame.

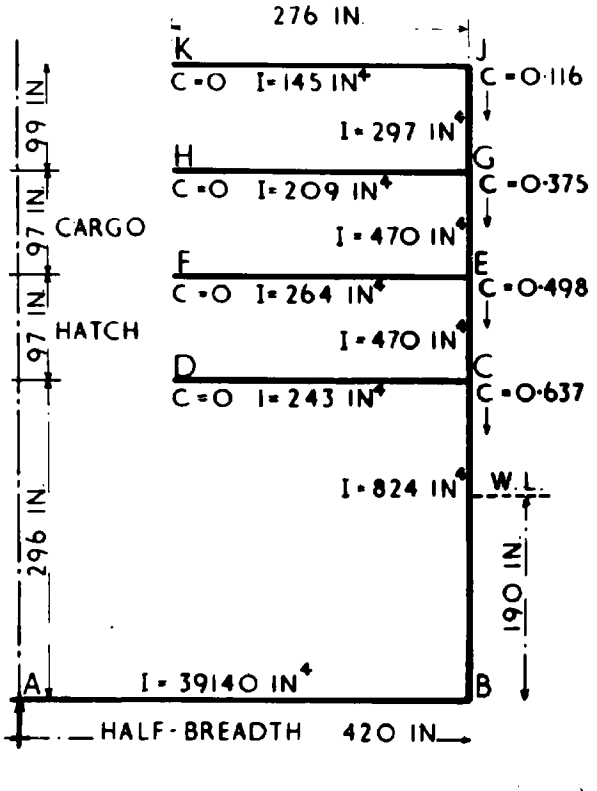

Fig. 2A. Structure analysed in Example 2. Idealized Cross Section of Cargo Liner near Amidships.

Consider the changes in bending moments which arise when dry docking the ship, which was floating initially at a draught of 190 in. (waterline shown dotted in fig. 2 A). The loads due to water pressure on the sides and bottom of the ship are removed and replaced by a single concentrated load acting vertically upwards at the centre keel A. The changes in load all take place beneath the level of deck CD and the first step is to find the coefficient of constraint at the top of the frame BC by the process described in Example 1. Starting at K, where $c_{KJ} = 0$ because it was assumed that the end of the deck beam is freely supported, the stiffness of the deck beam is calculated, using equation 2·8, and then the coefficient of constraint at J is calculated using equation 2·10. After this the stiffnesses of frame GJ and deck beam GH are found, followed by the coefficient of constraint at G. The process is continued down through E, to C where the coefficient of constraint is found to be 0·637. The numerical values are shown in fig. 2 A, and full details of the computations are to be found in ref. A 1.

Consider next the change of bending moments in the frame BC associated with the removal of water pressure on one frame space. If both ends of the frame are completely fixed, the end fixing moments in the frame are found to be:

$$M_{fc} = + 123 \text{ tons in.}$$

$$M_{fB} = + 300{\cdot}5 \text{ tons in.}$$

It has been assumed that moments which tend to bend the frame concave to the right are positive. Assume that joint B is rigidly held, temporarily, by an artificial restraint so that $c_B = 1$. Then if the coefficient of constraint at C is $c_c = 0{\cdot}637$, the moments at the ends of the frame may be calculated by means of equations 3·6 and 3·7. They are:

$$M_c = 0{\cdot}637 \times 123 = + 78{\cdot}5 \text{ tons in.}$$

$$M_B = 300{\cdot}5 + \frac{(1 - 0{\cdot}637)}{2} \times 123$$

$$= + 323 \text{ tons in.}$$

Consider next the floor and assume that the ends B and B' at the opposite sides of the ship, are held completely fixed, temporarily, by artificial restraints. With the ends thus fixed, the bending moments in the floor, associated with the removal of water pressure and its substitution by an equal and opposite concentrated load due to keel blocks at the centre line A, may be calculated by the usual methods. The end fixing moment is found to be - 3048 tons in. (Negative, because the moment tends to bend the floor concave upwards).

It is clear that the artificial restraint at B applies a moment to the end of the frame equal to 323 tons in. counter clockwise, and to the end of the floor a moment equal to 3048 tons in.

counter clockwise. The corresponding restraint at B' at the other side of ship applies an equal pair of moments of opposite sense. The total moment applied by the artificial restraint at B is (3048 + 323) = 3371 tons in. counterclockwise. When the artificial restraint at B and the corresponding one at B', are removed these unbalanced moments are distributed between the floor and frames in the same manner as in a moment distribution calculation.

With the top end of the frame partially constrained, the stiffness of the frame at B is

$$K_{BC} = (3 + c_{CB}) \frac{E I_{BC}}{L_{BC}}$$

$$= 10{\cdot}12\ E \text{ tons in./radian}$$

In view of symmetry of the ship and loads about the centre line, the stiffness of the floor at B is

$$K_{BB'} = 2 \frac{E I_{BB'}}{L_{BB'}}$$

$$= 98{\cdot}18\ E \text{ tons in./radian}$$

Hence

$$\text{Moment distributed to BB'} = \frac{98{\cdot}18}{98{\cdot}18 + 10{\cdot}12} (3371)$$

$$= 3041 \text{ tons in. (clockwise)}$$

and the total moment applied to end B of the floor is

$$M_{BB'} = -3048 + 3041$$

$$= -7 \text{ tons in. (counter clockwise)}$$

$$\text{Moment distributed to BC} = \frac{10{\cdot}12}{98{\cdot}18 + 10{\cdot}12} (3371)$$

$$= 330 \text{ tons in. (clockwise)}$$

and the total moment applied to end B of the frame is

$$M_{BC} = -323 + 330$$

$$= +7 \text{ tons in.} \quad \text{(clockwise)}$$

$$\text{Moment carried over to C} = \frac{2 \times 0{\cdot}637}{3 + 0{\cdot}637} \times (330)$$

$$= 116 \text{ tons in.} \quad \text{(clockwise)}$$

$$\text{and the total moment at C} = +116 + 78{\cdot}5$$

$$= +194{\cdot}5 \text{ tons in.} \quad \text{(clockwise)}$$

This moment at C is distributed between CD and CE in ratio of their stiffnesses and carried over to E in the same way as explained in Example 1. The final changes in bending moment are shown in fig. 2 B.

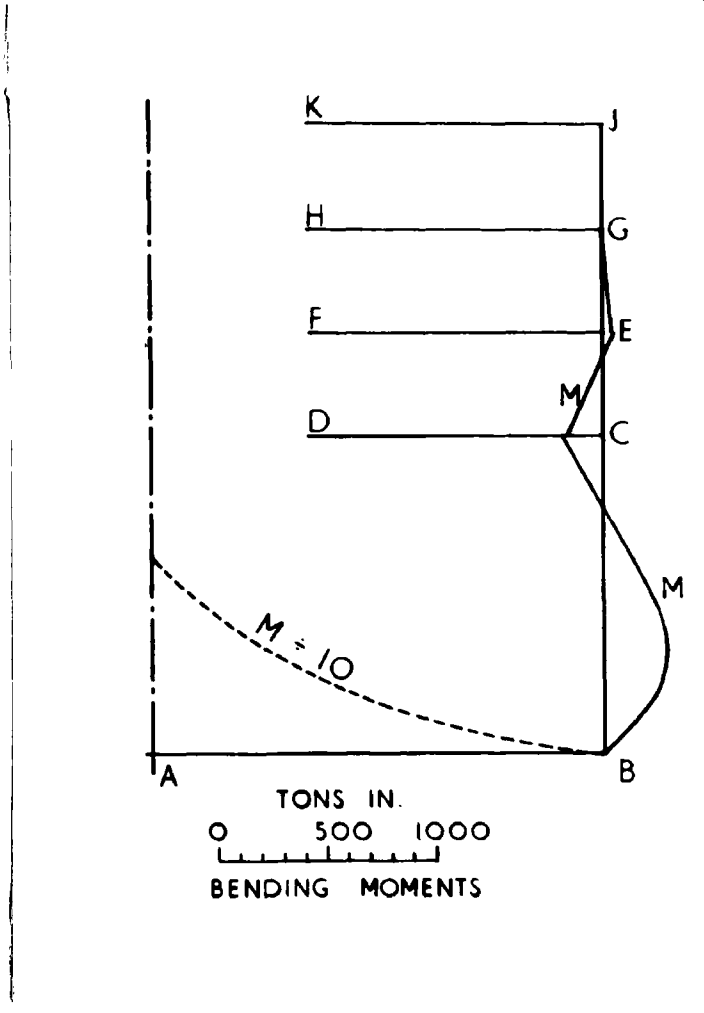

Fig. 2B. Changes of Bending Moment calculated in Example 2.

It will be observed that by ordinary methods of analysis by moment distribution the computation would have involved moment distribution between five joints, viz: B, C, E, G and J. By use of the constraint coefficient method the number of joints at which moment distribution was required was reduced to one, and only one distribution was needed. At the same time the advantage of being able to visualize the steps in the calculation was retained.

If only one span is under load, the coefficients of constraint at each end may be calculated. The bending moments may then be found directly by use of equations 3·4 and 3·5. In a structure in which many spans are under load it would be possible to analyse each span independently and then find the total bending moments by superposition, but little advantage is gained in this case and it is better to analyse the loaded part of the structure by moment distribution as explained in Example 1.

7) Analysis of Structures Containing Non-uniform Curved Beams.

In this and following sections, a theory will be developed to enable end constraint to be allowed for in beams of arbitrary initial curved shape in one plane, with cross sections which are not uniform along the length of the beam. Equations will be developed to make possible the analysis by the normal relaxation methods, of frames consisting of such beams. It will be seen that these equations are the same as the ones used in the column analogy method (ref. C 1), but the analogy has been dropped and the equations given here are developed for beams, and are applied directly to them. Subsequently it will be shown how these equations may be applied in the analysis of partially constrained beams and beams joined together by semi-rigid connections. In the original theory (ref. A 1) the coefficient of constraint method was extended but the method given in Section 11 is simpler to apply.

It is assumed that strains and deflections of the beams arise entirely from bending actions, and that strains due to forces acting along the axis of the beam, shear across its axis, etc., may be neglected. It is assumed that the non-uniformity of cross sections of the beams is sufficiently gradual not to require the use of the tapered beam theory, a condition not always realised in practice. It is also assumed that the initial radius of curvature at any point along the central longitudinal axis of the beam is greater than 10 times the depth of the beam and that the theory of bending of beams having a small initial radius of curvature need not therefore be applied. (This will give sufficiently accurate results when the bending moments in most ship's framing are calculated; in other cases modifications based on the curved beam theory give a better approximation when the equations developed below are used : see ref. C 1).

The sign convention adopted enables the equations to be applied to straight or curved beams alike. When considering straight beams, loads acting downwards were considered to be positive, and bending moments tending to produce concavity downwards were positive; downward

deflections were also positive. If the beam is curved turn it, in imagination, so that a line joining its extreme ends is horizontal and call the left hand end A and the right hand end B. Choose rectangular co-ordinate axes x and y which may be orientated in any direction with respect to the curved beam provided that the same sign convention applies to the line joining A and B. Measure s from A to B along the curved axis of the beam, and the signs of loads, and bending moments are the same with respect to the direction of s in the curved beam as they are with respect to x in a straight beam. Changes of slope and deflection are measured with respect to the initial axis of the beam. The position of the origin of the x-y co-ordinate axes will be chosen later.

The general theory will be developed with reference to a curved beam AB and the equations will apply directly to this case. A similar argument may be used to obtain simpler equations applying to straight beams, or these equations may be obtained by making obvious simplifications to the more general equations.

8) Non-uniform Curved Beams - Moment Distribution Equations.

I Change of Slope imposed at one end.

Consider a beam AB held at A so that no change of slope or deflection may take place there. At B no deflection is permitted but an external moment is applied there such that the change of slope is θ radians. Let $x_B y_B$ be the co-ordinate of B. Then if M is the change of bending moment at any point, associated with the moment of the applied couple:

$$\int_A^B \frac{M}{E I}\, ds = \theta \qquad (8\cdot1)$$

$$\int_A^B \frac{M}{E I}\, (x_B - x)\, ds = 0$$

or

$$\int_A^B \frac{M}{E I}\, x\, ds = \theta\, x_B \qquad (8\cdot2)$$

from equation 8·1, since x_B is constant.

Similarly

$$\int_A^B \frac{M}{E I}\, y\, ds = \theta\, y_B \qquad (8\cdot3)$$

These bending moments arise from the application of moments at the ends of the beam only, so that the shear forces must be constant along the beam and the bending moments along the beam must vary linearly across the xy plane.

i.e: $$M = N + Px + Qy \qquad (8\cdot4)$$

where N, P and Q are constants to be determined.

Hence

$$\left.\begin{aligned} N\int_A^B \frac{1}{EI}\,ds + P\int_A^B \frac{x}{EI}\,ds + Q\int_A^B \frac{y}{EI}\,ds &= \theta \\ N\int_A^B \frac{x}{EI}\,ds + P\int_A^B \frac{x^2}{EI}\,ds + Q\int_A^B \frac{xy}{EI}\,ds &= \theta\, x_B \\ N\int_A^B \frac{y}{EI}\,ds + P\int_A^B \frac{xy}{EI}\,ds + Q\int_A^B \frac{y^2}{EI}\,ds &= \theta\, y_B \end{aligned}\right\} (8\cdot5)$$

Consider now a diagram of values of 1/EI plotted along the central longitudinal axis of the beam. If the xy plane were horizontal the values of 1/EI could be plotted vertically, one half of each ordinate being above and the other half below the xy plane. If the origin of co-ordinates is taken at the centroid of this diagram:

$$\int_A^B \frac{x}{EI}\,ds = 0 \qquad \text{and} \qquad \int_A^B \frac{y}{EI}\,ds = 0$$

The remaing integrals in equations8·5 are also geometrical properties of the 1/EI diagram and it is convenient to replace these by the following symbols:

$$\int_A^B \frac{ds}{EI} = a \qquad \int_A^B \frac{x^2}{EI}\,ds = i_y \qquad \int_A^B \frac{y^2}{EI}\,ds = i_x \qquad \int_A^B \frac{xy}{EI}\,ds = i_{xy}$$

The symbol a denotes the area of the 1/EI diagram, and i_y, i_x and i_{xy} denote the moments of inertia and product of

inertia of the diagram about the y and x axes through its centroid. Then equations 8·5 become:

$$N\,a = \theta$$

$$P\,i_y + Q\,i_{xy} = \theta\,x_B$$

$$P\,i_{xy} + Q\,i_x = \theta\,y_B$$

Hence

$$N = \frac{\theta}{a}$$

$$P = \frac{(x_B i_x - y_B i_{xy})}{(i_x i_y - i_{xy}^2)}\,\theta$$

$$Q = \frac{(y_B i_y - x_B i_{xy})}{(i_x i_y - i_{xy}^2)}\,\theta$$

The bending moments in the beam are found by substituting these values in equation 8·4.

$$M = \frac{\theta}{a} + \frac{(x_B i_x - y_B i_{xy})\,\theta\,x + (y_B i_y - x_B i_{xy})\,\theta\,y}{(i_x i_y - i_{xy}^2)} \qquad (8·6)$$

By substituting the appropriate values of x and y in equation 8·6 the moments at A and B may be calculated. The stiffness at B is given by M_B/θ and the carry-over factor from B to A is equal to M_A/M_B.

When the beam is straight and coincides with the x axis equation 8·6 simplifies to:

$$M = \frac{\theta}{a} + \frac{\theta\,x_B}{i_y}\,x \qquad (8·7)$$

II Deflection Imposed at One End.

Consider a beam AB, held at A so that no change of slope or deflection may take place there. At B no change of slope is permitted but a change in position of B, with components δ_y in the y direction and δ_x in the x direction, is imposed there. Let $x_B y_B$ be the co-ordinates of B. If M is the bending moment at any point due to the imposed movement at B:

$$\int_A^B \frac{M}{E I}\, ds = 0 \qquad (8\cdot8)$$

$$\int_A^B \frac{M}{E I}\,(x_B - x)\, ds = \delta_y$$

or

$$\int_A^B \frac{M}{E I}\, x\, ds = -\delta_y \qquad (8\cdot9)$$

by equation 8·8, because x_B is constant.

Similarly

$$\int_A^B \frac{M}{E I}\, y\, ds = -\delta_x \qquad (8\cdot10)$$

Since the bending moments M arise from the application of moments and forces to the ends of the beam only, the bending moments must vary linearly across the xy plane.

i.e:

$$M = N + Px + Qy \qquad (8\cdot11)$$

Hence

$$\left.\begin{aligned} N\int_A^B \frac{1}{E I}\, ds + P\int_A^B \frac{x}{E I}\, ds + Q\int_A^B \frac{y}{E I}\, ds &= 0 \\ N\int_A^B \frac{x}{E I}\, ds + P\int_A^B \frac{x^2}{E I}\, ds + Q\int_A^B \frac{x y}{E I}\, ds &= -\delta_y \\ N\int_A^B \frac{y}{E I}\, ds + P\int_A^B \frac{x y}{E I}\, ds + Q\int_A^B \frac{y^2}{E I}\, ds &= -\delta_x \end{aligned}\right\} \qquad (8\cdot12)$$

If the origin of co-ordinates is taken at the centroid of the $1/EI$ diagram and if the integrals are written in terms of the symbols defined in I above equation 8·12 becomes:

$$Na = 0$$

$$Pi_y + Qi_{xy} = -\delta_y$$

$$Pi_{xy} + Qi_x = -\delta_x$$

The solution of these three simultaneous equations is:

$$N = 0$$

$$P = \frac{(i_{xy}\delta_x - i_x\delta_y)}{(i_x i_y - i_{xy}^2)}$$

$$Q = \frac{(i_{xy}\delta_y - i_y\delta_x)}{(i_x i_y - i_{xy}^2)}$$

The bending moments in the beam are found by substituting these values in equation 8·11 and are given by:

$$M = \frac{(i_{xy}\delta_x - i_x\delta_y)\,x + (i_{xy}\delta_y - i_y\delta_x)\,y}{(i_x i_y - i_{xy}^2)} \qquad (8\cdot13)$$

By substituting the appropriate values of x and y in equation 8·13 the bending moments at A and B may be calculated.

When the beam is straight equation 8·13 simplifies to:

$$M = -\frac{(\delta_y)}{i_y}\,x \qquad (8\cdot14)$$

9) <u>End Fixing Moments in a Non-uniform Curved Beam acted on by Forces in its Plane.</u>

Before carrying out an analysis of a framework by relaxation methods if is necessary to calculate the end fixing moments in each loaded beam in the structure. Consider a beam AB which has both ends fixed so that no rotation or displacement may occur at either end. Then if M is the total bending moment acting at any point along the beam:

$$\int_A^B \frac{M}{E\,I}\,ds = 0 \qquad (9\cdot1)$$

$$\int_A^B \frac{M}{EI} x \, ds = 0 \qquad (9\cdot2)$$

$$\int_A^B \frac{M}{EI} y \, ds = 0 \qquad (9\cdot3)$$

With its ends completely fixed the beam is statically indeterminate and the total bending moment at any point cannot be found directly. Make the beam statically determinate by inserting a gap, or a number of hinges (two in a straight beam, three in a curved one), and calculate the statically determinate bending moments M_S due to the loads acting on the beam in this condition. The moments M_S will cause changes of slope and deflection of the beam, and discontinuities will appear at the gap or hinges. Continuity of the beam must be restored by the application of shearing forces and bending moments at the point or points of discontinuity. These result in further bending moments M_I acting on the beam which must vary linearly across the xy plane.

Then $$M_I = N + Px + Qy \qquad (9\cdot4)$$

and $$M = M_s + M_I$$

$$= M_s + N + Px + Qy$$

Substitute for M in equations 9·1, 9·2 and 9·3 and they become:

$$\left.\begin{aligned} -\int_A^B \frac{M_S}{EI} ds &= N\int_A^B \frac{1}{EI} ds + P\int_A^B \frac{x}{EI} ds + Q\int_A^B \frac{y}{EI} ds \\ -\int_A^B \frac{M_S x}{EI} ds &= N\int_A^B \frac{x}{EI} ds + P\int_A^B \frac{x^2}{EI} ds + Q\int_A^B \frac{xy}{EI} ds \\ -\int_A^B \frac{M_S y}{EI} ds &= N\int_A^B \frac{y}{EI} ds + P\int_A^B \frac{xy}{EI} ds + Q\int_A^B \frac{y^2}{EI} ds \end{aligned}\right\} \qquad (9\cdot5)$$

The integrals on the left hand side may be interpreted in terms of differences of slope and deflection of the beam in the

statically determinate condition and will be denoted by:

$$-\int_A^B \frac{M_s}{E\,I}\,ds = \beta \qquad -\int_A^B \frac{M_s x}{E\,I}\,ds = \Delta_y \qquad -\int_A^B \frac{M_s y}{E\,I}\,ds = \Delta_x$$

Again, if the origin of co-ordinates is placed at the centroid of the $1/EI$ diagram and the integrals on the right hand side which are not equal to zero are replaced by the symbols in Section 8, the equations expressing continuity of the beam become:

$$\beta = Na$$

$$\Delta_y = Pi_y + Qi_{xy}$$

$$\Delta_x = Pi_{xy} + Qi_x$$

Hence

$$N = \frac{\beta}{a}$$

$$P = \frac{(i_x\Delta_y - i_{xy}\Delta_x)}{(i_x i_y - i_{xy}^2)}$$

$$Q = \frac{(i_y\Delta_x - i_{xy}\Delta_y)}{(i_x i_y - i_{xy}^2)}$$

Substituting these values in equation 9·4, it is found that the equation for the statically indeterminate moments is:

$$M_I = \frac{\beta}{a} + \frac{(i_x\Delta_y - i_{xy}\Delta_x)\,x + (i_y\Delta_x - i_{xy}\Delta_y)\,y}{(i_x i_y - i_{xy}^2)} \qquad (9\cdot6)$$

The end fixing moments are found by substituting the co-ordinates of A and B into equation 9·6, calculating M_I and adding the values of M_s (if not zero) at these points.

When the beam is straight equation 9·6 simplifies to:

$$M_I = \frac{\beta}{a} + \frac{\Delta_y\,x}{i_y} \qquad (9\cdot7)$$

10) Semi-rigid Joints.

Suppose a beam has in its length one or more joints. The joints will be referred to as "rigid joints" if they permit neither relative deflections nor relative changes of slope between the two ends joined together (e.g: welded joints). If, under the action of a bending moment, the joint permits a certain amount of difference to occur between the slopes of the two ends joined together, but still maintains both ends at the same level whatever the shearing forces applied, it will be referred to as a "semi-rigid" joint. Examples of the latter are riveted and bolted joints. As a first approximation it may be assumed that changes of slope in a semi-rigid joint are directly proportional to the changes in bending moment acting on the joint. (In Chapter III of this thesis it will be shown that riveted connections found in shipbuilding behave in this manner, after the first load has been applied. See also discussion of the use of a bi-linear relationship, in chapter 11 of ref. B 11).

If a bending moment M acting over a length δs of the joint causes a change of slope $\delta\theta$, then:

$$\delta\theta = M f \delta s$$

where f is a factor which expresses the flexibility per unit length of the joint. The quantity Mf is equivalent to M/EI in a beam and the semi-rigid connection may be treated in the same way as a reduced cross section of the beam. To take account of the flexibility of a joint the ordinates of the 1/EI diagram for the beam could be modified accordingly provided that the distribution and magnitude of f along the length of the joint is known. When this is done the bending moments in a beam with one or more semi-rigid joints may be found directly by the equations developed in the last two Sections.

It is more likely in practice, however, that only an overall value for the flexibility of the semi-rigid joint as a whole will be known or obtainable from experiments. In this case if a constant bending moment M_o applied between the ends of the joint produces a total change of slope θ measured between the ends of the joint:

$$\int d\theta = M_o \int f.ds$$

where the integration extends over the length of the joint.

or $$\theta = M_o F \qquad (10\cdot1)$$

where F denotes the total flexibility of the joint.

Both M_o and θ may be found by experiment and F may be obtained from the relationship

$$F = \theta/M_o \qquad (10\cdot2)$$

A beam with semi-rigid joints may be analysed by

the methods described in previous Sections if it is assumed that the change of slope of the joint under bending moments which vary along its length is the same as that produced by a constant bending moment equal to that acting at a suitably chosen point along the length of the joint. This assumption is usually justified because of the relatively short length of most joints in practice. The quantity F is added to the diagram of 1/EI for the beam at the co-ordinates of the chosen point along the joint, when calculating the position of centroid of the diagram and the quantities a and i etc. The variation f along the joint is not required any more than is the variation of force when considering an impulse in some dynamic problems.

11) Beam which is Partially Constrained at the Ends.

The simple concept explained in this short Section is the basis of the method of allowing for partial constraint at the ends of beams which are curved or of non-uniform cross section. It rests on the discussion of a semi-rigid joint in the previous Section. The use of the method will be explained by examples in the following two Sections. The principle is that, when it is desired to find the statically indeterminate bending moments in a loaded beam which is partially constrained at its ends, the end structures are replaced by rigid structures at the ends of the beam to which the latter is attached by semi-rigid joints having the same stiffness as the end structures they are assumed to replace.

Suppose that a beam AB is attached at A (and/or B) to an unloaded structure which, while preventing deflections at the end of the beam, allows it to change slope there but opposes such changes of slope by reason of its stiffness. Let the stiffness of the end structure at one end be K_ϵ. This quantity is defined (as before) to be the moment per unit change of slope:

$$K_\epsilon = \frac{M_\epsilon}{\theta}$$

where M_ϵ is the moment required to produce a change in slope θ of the end structure.

The effect upon the beam is identical to the effect of a semi-rigid connection of very short length between the beam and a rigid structure beyond A (or B), if the flexibility of the connection is given by:

$$F_\epsilon = \frac{\theta}{M_\epsilon} = \frac{1}{K_\epsilon} \qquad (11\cdot1)$$

Thus the constraint associated with an end structure to which the beam AB is attached at A, may be taken into account by adding the reciprocal of the stiffness of the end structure to the 1/EI diagram at the co-ordinates of end A when calculating the properties of the diagram, viz: a, i, etc. The effect of the end structure at the other end B may be taken into account similarly. If the modified properties

of the 1/EI diagram are calculated in this way, beams partially constrained their ends may be analysed with very little additional labour than if they were completely fixed at the ends.

12) Example 3. Strength of Mast.

Fig. 3 shows the mast of a large passenger liner. Its cross section varies along its length and it is supported at the deck and at different heights by three forestays. The mast will deflect when loaded because of the sag and elasticity of the forestays. The structure below deck is not rigid so the mast cannot be considered to be completely fixed at its lower end. It is desired to find the effect on the mast and stays of applying a test load of 20 tons to the derrick.

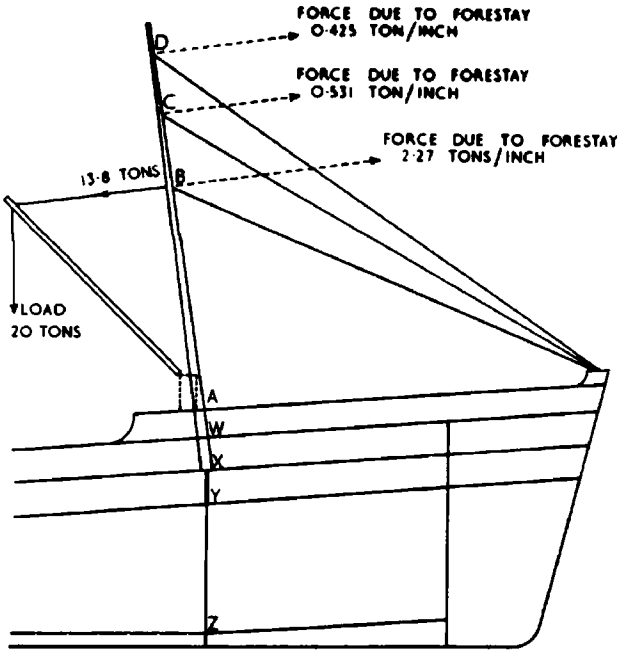

Fig. 3.

The first step in the analysis of the problem is to estimate the stiffness of the structure below the bottom of the mast at A. This is done by a similar process to that described in Example 1. After passing through two decks at W and X the base of the mast trunk rests on the top of a heavy stiffener which runs down one of the main bulkheads to the bottom of the hull. The stiffness of the keel of the ship is such that the bulkhead stiffener may be assumed to be completely fixed at its lower end. The stiffness of the stiffener between Z and Y is calculated using the equation $K = 4EI/L$ and the resulting value is used to find the coefficient of constraint at Y. The stiffness of stiffener between X and Y is then calculated using the equation $K = (3 + c)EI/L$ and the resulting value is used to find the coefficient of constraint at X. The process is repeated for the mast trunk between W and X, and again for the section between A and

W, taking account of the taper of the mast trunk. The final result of this calculation was that the stiffness of the structure below A was 331 E tons in./radian at A.

Fig. 4.

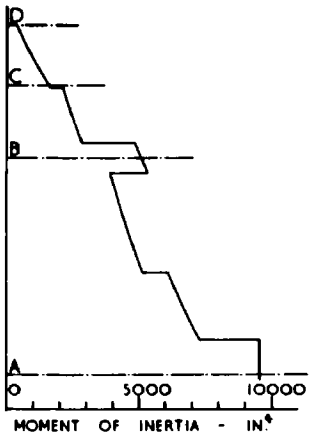

The next step is to calculate the stiffness of the mast itself. Fig. 4 shows the shape of the diagram of moments of inertia of cross section and it is necessary to calculate, for each of sections AB, BC, and CD, the values of the integrals represented by the symbols a and i etc. defined in Section 8. This may be done graphically, numerically or by any other suitable method depending upon the problem; the results for section AB were:

$$a = \frac{0{\cdot}15073}{E} \text{ radian/ton.in.}$$

$$i = \frac{6733{\cdot}6}{E} \text{ radian. in./ton}$$

$x_B = 339{\cdot}3$ in. $\quad x_A = -450{\cdot}9$ in. $\quad L = 790{\cdot}2$ in.

It is now necessary to find the modified values taking account of the constraint at A. Since the stiffness of the structure below A is 331 E tons in./radian, the corresponding value of F_A may be found from equation 11·1, and is:

$$F_A = \frac{1}{331\,E} = \frac{0{\cdot}00302}{E} \text{ radians/ton.in.}$$

The symbols a and i stand for integrals which represent the area, and second moment of area of the diagram of 1/EI respectively, and the usual rules apply to them when an area is added to the diagram.

Denoting the modified values by superscripts, it

is found that:

$$a' = \frac{0{\cdot}15073}{E} + \frac{0{\cdot}00302}{E} = \frac{0{\cdot}15375}{E} \text{ radians/ton.in.}$$

Taking moments about original centroid of diagram of 1/EI :

$$\text{Shift of centroid} = \frac{0{\cdot}00302 \times 450{\cdot}9}{0{\cdot}15375} = 8{\cdot}86 \text{ inches}$$

Hence $x'_B = 348{\cdot}16$ in. $x'_A = -442{\cdot}02$ in.

And by the theorem of parallel axes:

$$i' = (6733{\cdot}6 + 0{\cdot}00302 \times 450{\cdot}9^2 - 0{\cdot}15375 \times 8{\cdot}86^2)/E$$

$$= \frac{7335{\cdot}6}{E} \text{ radian in./ton}$$

The calculation of the effects of a change of slope and of deflections at B is straightforward:

Using equation 8·7

$$K_B = \frac{M_B}{\theta} = \frac{E}{0{\cdot}15375} + \frac{(348{\cdot}16 \times 348{\cdot}16)\,E}{7335{\cdot}6} = +23{\cdot}03\,E \text{ ton in./radian}$$

$$\frac{M_A}{\theta} = \frac{E}{0{\cdot}15375} + \frac{(348{\cdot}16 \times 442{\cdot}04)\,E}{7335{\cdot}6} = -14{\cdot}48\,E \text{ ton in./radian}$$

Forces for equilibrium: 0·0475 E ton to right at A
0·0475 E ton to left at B

Using equation 8·14, and assuming that the value of E = 13,400 tons/in² for mast steelwork:

$$M_B = \frac{348{\cdot}16}{7555{\cdot}6}\,E = +636{\cdot}1 \text{ tons in./inch deflection to left at B}$$

$$M_A = -\frac{442{\cdot}04}{7355{\cdot}6}\,E = +807{\cdot}6 \text{ tons in./inch deflection to left at B}$$

Forces for equilibrium: 1·826 ton to right at A
1·826 ton to left at B

Similar calculations are made for the rest of the mast and the figures are used to construct the first part of Table II (the signs being changed in accordance with the convention that moments applied to the sections of the mast are to be considered positive if clockwise, and forces and deflections to left are positive). The forces necessary to overcome the resistance of the forestays were calculated assuming an effective modulus of elasticity = 5,000 tons/in^2 and are entered in the column headed "forestays." From this part of Table II the upper part of Table III is constructed representing the forces and moments applied by the artificial restraints to effect the standard operations indicated. Line 1 of Table III corresponds to line 1 of Table II, the only difference being that the total moment applied at B is entered in column B. Line 1A is obtained from line 1 by proportion and shows the effect of 100·0 tons in. applied at B. (This figure is underlined to draw attention to the fact). The remainder of the Operations Table is constructed in a similar manner, down to line 5A. Three special operations were added which were found to speed up the relaxation process. Line 6 was obtained from line 5 by balancing, once for all, the moments -3318·5 and -2983·0 by means of lines 1A and 2A, and calculating the resulting forces. Lines 7 and 8 were obtained from lines 4 and 5 in a similar manner. By means of these last three operations attention is concentrated on the forces at B, C and D when forces are applied to these points and changes of slope there are not prevented. The force in the topping lift is + 13·8 tons and is resisted initially by an equal force in the opposite direction applied by the artificial restraint at B, which is entered in line a of Table IV. It is necessary to find what deflections must be applied to the mast in order to distribute this between the mast and forestays and reduce the forces in the artificial restraints to zero, using lines 6, 7 and 8 of the Operations Table.

Starting the relaxation process, a very rough approximation shows that the mast may deflect about 2 in. at B and C, and less at D, and lines b, c and d are computed on this basis. (Line b is simply twice line 6, and so on). The algebraic sum of each column is then calculated, and if the approximation had been correct the forces in the restraints would be zero. It was not, however, and a new approximation is required. It is clear from the forces remaining that the relative deflection of D was not great enough, and line f represents the result of an increase of 0·5 in. there. The sum of the columns, line g, shows that the original estimate of deflections was too low and in lines h, j and k they are increased by 50%. The sum of the residuals, line l shows that an improvement would be made if the deflections of C and D were increased relative to B and lines m and n show this. Examination of the residuals in line p and comparison with the operation in line c indicates that a further deflection of 0·02 in. at C would reduce the residuals at C and D nearly to zero. In line r the residuals are very like those which existed at the start of the problem in line a, except that the force at B has been reduced to just over half a ton. This is about one twentieth of the original force at B and suggests that a considerable improvement would result if all the deflections were increased by one twentieth of their present values. Lines s, t and u show this and the residuals left after finding the sum of the columns, line v, are negligibly small so that the problem may be considered to be solved. The complete solution is entered in the second part of Table II. The lines 9. 10 and 11 simply record the effect of the total deflections found in Table IV, using lines 3, 4 and 5 of

TABLE II - Moments (Tons in.)

Operation	A	B		C	
		BA	BC	CB	CD
1 Unit rotation at B	+14·48	+23·03	+55·72	+23·95	
2 Unit rotation at C			+23·95	+36·15	+16·38
3 Deflection 1·0 inch at B	+807·5	+636	-3954·5	-2983	
4 Deflection 1·0 inch at C			+3954·5	+2983	-1016
5 Deflection 1·0 inch at D					+1016
Relaxation Solution (After Table IV)					
6 Initial actions.					
7 Rotation at B	-605	-962	-2328	-1001	
8 Rotation at C			+372	+561	+254
9 Deflection B = 3·15 in.	+2544	+2005	-12457	-9396	
10 Deflection C = 3·381 in.			+13370	+10086	-3435
11 Deflection D = 2·8875 in.					+2934
12 Totals	+1939	+1041	-1043	+250	-247

TABLE II - Forces (Tons)

Operation	A	B	C	D	Fore-
		AC	BD		stays
1 Unit rotation at B	-0·0475	-0·2476	+0·2951		
2 Unit rotation at C		-0·2226	+0·1468	+0·0758	
3 Deflection 1·0 inch at B	-1·826	+27·52	-25·695		+2·27
4 Deflection 1·0 inch at C		-25·695	+30·40	-4·705	+0·53
5 Deflection 1·0 inch at D			-4·705	+4·705	+0·425
Relaxation Solution (After Table IV)					
6 Initial actions.		-15·8			
7 Rotation at B	+1·98	+10·34	-12·33		
8 Rotation at C		-5·45	+2·28	+1·18	
9 Deflection B = 3·15 in.	-5·74	+86·69	-80·93		+7·15
10 Deflection C = 3·381 in.		-86·87	+102·78	-15·91	+1·79
11 Deflection D = 2·8875 in.			-13·58	+13·58	+1·23
12 Totals	-3·76	-7·09	-1·78	-1·15	

TABLE III

Operations Table.

		Moments (Tons in.)		Forces (Tons)		
		B	C	B	C	D
1	Unit rotation at B	+78·75	+23·95	-0·2476	+0·2951	
1A		+100·00	+30·41	-0·3144	+0·3747	
2	Unit rotation at C	+23·95	+52·53	-0·2226	+0·1468	+0·0758
2A		+45·59	+100·00	-0·4238	+0·2794	+0·1444
3	Deflection 1·0 inch at B	-3318·5	-2983·0	+29·79	-25·695	
3A		-1114·0	-1001·5	+10·00	-8·65	
4	Deflection 1·0 inch at C	+3954·5	+1967·0	-25·695	+30·93	-4·705
4A		+1278·5	+636·0	-8·31	+10·00	-1·52
5	Deflection 1·0 inch at D		+1016·0		-4·705	+5·13
5A			+1981·0		-9·17	+10·00
6	Deflection 1·0 inch at B with moments balanced.	0	0	+12·93	-10·775	+3·31
7	Deflection 1·0 inch at C with moments balanced.	0	0	-10·775	+15·15	-5·985
8	Deflection 1·0 inch at D with moments balanced.	0	0	+3·31	-5·985	+3·425

TABLE IV

RELAXATION TABLE.

		Forces (Tons)		
		B	C	D
a	Initial actions	- 13·80		
b	Deflection = 2 in. at B	+ 25·86	- 21·55	+ 6·61
c	Deflection = 2 in. at C	- 21·55	+ 30·30	- 11·97
d	Deflection = 1 in. at D	+ 3·31	- 5·985	+ 3·425
e	Residuals	- 6·18	+ 2·765	- 1·935
f	Deflection = 0·05 in. at D	+ 1·655	- 2·99	+ 1·71
g	Residuals	- 4·525	- 0·225	- 0·225
h	Deflection = 1·00 in. at B	+ 12·93	- 10·775	+ 3·31
j	Deflection = 1·00 in. at C	- 10·775	+ 15·15	- 5·985
k	Deflection = 0·75 in. at D	+ 2·48	- 4·49	+ 2·57
l	Residuals	+ 0·11	- 0·34	- 0·33
m	Deflection = 0.50 in. at D	+ 1·655	- 2·99	+ 1·71
n	Deflection = 0·20 in. at C	- 2·155	+ 3·03	- 1·195
p	Residuals	- 0·39	- 0·30	+ 0·185
q	Deflection = 0·2 in. at C	- 0·205	+ 0·30	- 0·12
r	Residuals	- 0·595	0·0	+ 0·065
s	Deflection = 0·1500 in. at B	+ 1·94	- 1·615	+ 0·495
t	Deflection = 0·1610 in. at C	- 1·735	+ 2·44	- 0·965
u	Deflection = 0·1375 in. at D	+ 0·455	- 0·82	+ 0·47
v	Residuals	+ 0·065	- 0·005	+ 0·065

Table II. The unbalanced moments which result may be balanced by use of lines 1A and 2A of Table III and the result is recorded in lines 7 and 8 of Table II. It will be noted that the moments and forces on either side of B are balanced, similarly at C and D. Table II is the only one which need be retained for record purposes. The solution of the problem is illustrated in fig. 5.

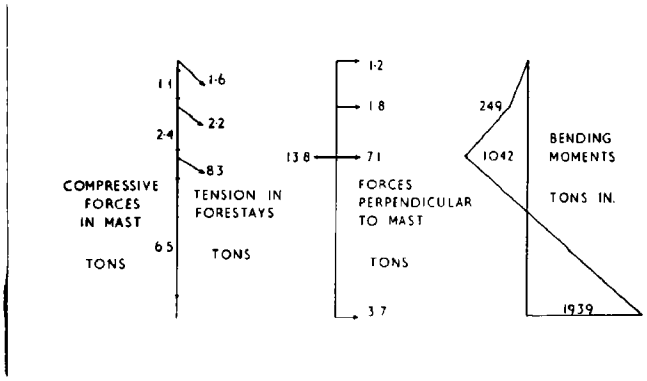

Fig. 5.

This example has been described in some detail in order to demonstrate some of the advantages of the method described. It is, ofcourse, obvious that other methods could have been used to obtain the solution; one of these gave the following:

	Deflections (in.)	Forces applied to Mast (Tons)	Bending Moments (Tons in.)
D	2·7856	1·18	0
C	3·52011	1·77	255
B	3·12095	7·08	1052
A	0	3·78	1933

It will be seen that the solution by relaxation is in error by only a few per cent, but it should be remembered that the "precise" solution is only correct if the assumptions on which it is based are correct. The value (3000 tons/in^2) of the modulus of elasticity of the forestays is particularly open to question; some authorities quote 4000 and even 5000 tons/in^2. For practical purposes, therefore, the relaxation solution is quite accurate enough.

The method described here for taking account of the partial constraint need not be combined with the relaxation method of solution; in this example, other methods were quicker. The advantages of the relaxation method grows as the number of joints is increased. It is not the purpose of the example to show this, but only to illustrate a method which can be used to solve more complicated problems in which partial constraint is a factor.

13) Example 4. Transverse Strength (continued).

In this example the structure to be analysed has one member which is curved, of non-uniform cross section, and is partially constrained at both ends. The structure and loading are identical to that analysed in Example 2 (page 16) except that the bilge frame is curved instead of having a square corner. The structure is shown in fig. 6A. It differs from that of example 2 by having a radius of bilge equal to 190 in. (This particular value was chosen to be equal to the draught of the ship afloat, for mathematical convenience), and is representative of that part of the ship which is some distance from midships. The problem is the same as in example 2, viz: to find the change in bending moments when the ship is dry docked. The analysis of the frame-floor arch CBAB'C' is carried out using the equations in Section 9 after calculating the stiffness, and hence the flexibility, of the constraining structure beyond C and C'.

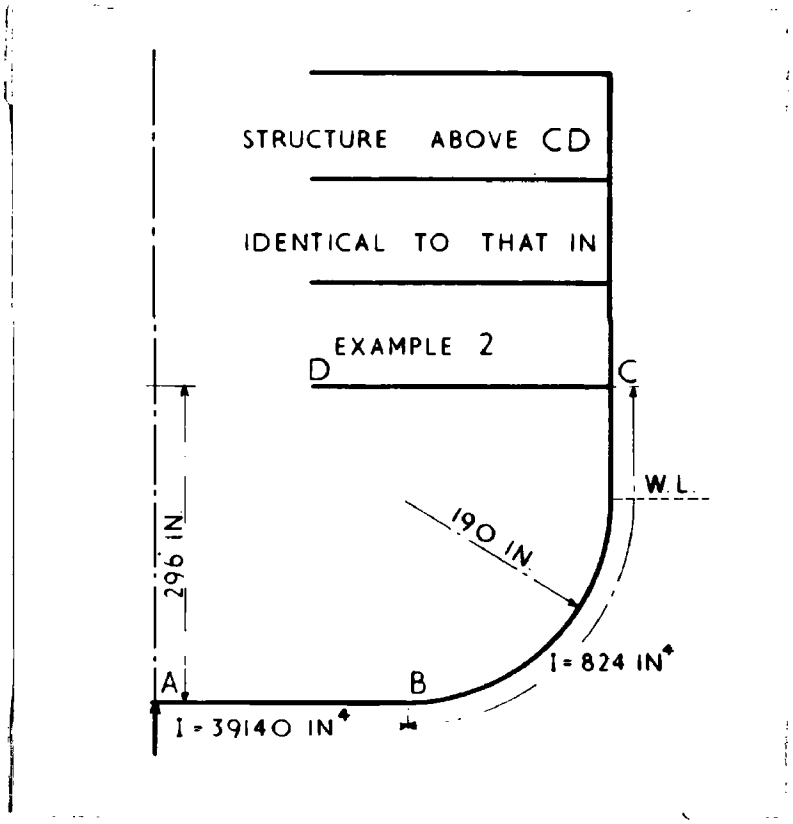

Fig. 6A.

Structure analysed in Example 4.

The first step is to assume that there are three hinges at C, A and C'. The statically determinate bending moments are then calculated by the usual method of analysis of three-pinned arches (see, for example, ref. B4, Art. 194). By integrating these bending moments, with respect to distance measured round the frame, the values of β and Δ_{α} are found:

$$\beta = -\int_{C'}^{C} \frac{M_s}{E\,I}\,ds = +\frac{4592}{E} \text{ radians.}$$

By evaluating $-\int_{C'}^{C} \frac{M_s y}{E I}\, ds$ and dividing by β it is found that the centroid of the diagram of M_s/EI is 119·5 in. below the waterline when the ship was afloat, i.e: 70·5 in. above the keel. Hence Δ_x may be calculated when the centre of area of the diagram of $1/EI$ has been located.

Next calculate the required properties of the diagram of $1/EI$. The easiest way to do this is to consider the diagram in convenient parts, calculate the values for each component separately, and then to compute the figures for whole diagram. The latter is most conveniently carried out in a table; the work in this problem is summarized in Table V.

TABLE V

CALCULATION OF PROPERTIES OF $1/EI$ DIAGRAM (BOTH SIDES OF SHIP).

Item	a	$\bar{y}$	$a\bar{y}$	$a\bar{y}^2$	i
Floor	0·0118	-190·0	- 2·24	+ 426	-
Bilge frames	0·7240	-121·0	- 87·60	+ 10600	2476
Side frames	0·2574	+ 53·0	+ 13·65	+ 723	2888
2 x Flexibility at C	0·1022	+106·0	+ 10·83	+ 1149	-
	1·0954	- 59·7	- 65·36	12898	5364

This preliminary work is simple and consists of four calculations of a, i and centroid of diagrams of $1/EI$ of each of the following:

i) Floor. (Straight. $I = 39140$ in.^{4})

ii) Two side frames. (Straight. $I = 824$ in.^{4})

iii) Two bilge frames. (Quadrant of circle. $I = 824$ in.^{4})

iv) Flexibility at C and C'.

Only the last of these requires explanation. The structure above C is identical to that in example 2 and the stiffnesses of

deck CD and frame CE are found by the methods described when discussing examples 1 and 2. They are:

$$K_{cD} = 2{\cdot}64\ E \text{ tons in./radian}$$

$$K_{cE} = 16{\cdot}95\ E \text{ tons in./radian}$$

The flexibility F_c at C is the reciprocal of the stiffness of the end structure:

$$F_c = \frac{1}{2{\cdot}64\ E + 16{\cdot}95\ E} = \frac{0{\cdot}0511}{E} \text{ radian/ton in.}$$

For an assumed axis at the waterline of the ship afloat, the properties of the diagram of $1/EI$ are summarized in Table V. Note that the fact that the ends of the frames are partially constrained at C and C' involves no more than a rapid estimate of the flexibility of the end structures above C and C', and an extra line in Table V.

From the algebraic sum of the columns in Table V the properties of the diagram of $1/EI$ were found to be:

$$a' = \frac{1{\cdot}0954}{E} \text{ radian/in. ton}$$

$$i' = (5364 + 12898 - 59{\cdot}7 \times 65{\cdot}56)/E$$

$$= \frac{14364}{E} \text{ radian in./ton}$$

The centroid of area of the diagram of M_s/EI was found previously to be 119·5 in below the waterline so that it is 59·8 in. below the centroid of the diagram of $1/EI$:

Hence $\Delta_x = -\frac{4592 \times 59{\cdot}8}{E}$ radian in.

Ofcourse $\Delta_y = 0$ by symmetry.

The statically indeterminate bending moments M_I associated with the restoration of continuity of slope of the structure at C, A and C' are obtained by substituting in equation 9·6:

$$M_I = \frac{\beta}{a} + \frac{\Delta_x y}{i_x} = \frac{4592}{1{\cdot}0954} - \frac{(4592 \times 59{\cdot}8)\ y}{14364}$$

$$= 4190 - 19{\cdot}12\ y \text{ tons in.}$$

where y is measured positively upwards from a horizontal axis 130·3 in. above keel.

The total bending moments are given by the sum of M_S + M_I and are shown diagramatically in fig. 6B. The full line shows the change in bending moments (measured perpendicular to the outline of the cross section) when the upper ends of the frames are partially constrained, and the two dotted lines indicate the changes in bending moments which would occur if the frames were either completely fixed at C and C', or freely supported at C and C'. These three curves show the effect of the constraint on the bending moments in the frames and floor.

It is interesting to compare the bending moments shown by the full lines in fig. 6B with those shown in fig. 2B. The latter represent the same ship under the same change of load calculated on the usual assumption that the cross section may be approximated by straight uniform structural members. It will be observed that the approximation made in example 2 is not a very good one if the radius of bilge is not small.

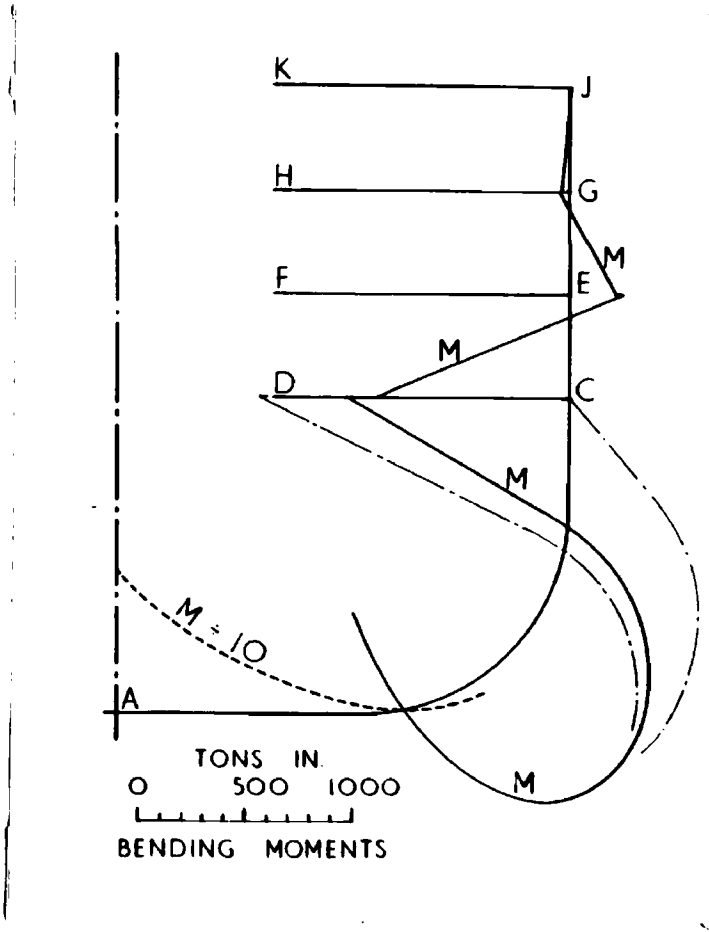

Fig. 6B Changes of Bending Moment calculated in Example 4.

CHAPTER II

SHEAR LAG IN STIFFENED PLATING

Note This chapter contains a summary of the paper on this subject which was published by the Institution of Naval Architects in 1955, together with a note on some work not mentioned in the paper. The paper and discussion are bound as an appendix at the end of this thesis.

14) Introduction.

In Chapter I it was assumed that the flexural properties of the beam cross sections (moment of inertia etc.) were known or could be calculated. Most of the structure of a ship, however, consists of panels of plating stiffened by rolled bars. When a panel is bent out of its plane the stiffeners act as beams and it is clear that the plating between them must act as a flange to each stiffener. When the stiffeners are widely spaced these flanges are very broad, and it is known that the usual assumption, that plane cross sections of a beam at right angles to the plane of bending remain plane after bending, may not be accurate. (Shear strains associated with the shearing stresses across a wide flange cause decrease in its efficiency, and the problem is known as that of shear lag. A more detailed explanation will be found on pages 2 and 5 of the Appendix.) The question then arises - how much of the plate may be considered to act as a flange of the stiffener ? This is a problem which faces the naval architect every time he tries to calculate the strength of a panel of stiffened plating, and a similar problem arises in the design of aircraft.

Many papers have been written about shear lag and their very number indicates an unsatisfied desire for information on the subject. An examination of a large number of the papers (refs. S 1 to S 16 are representative but by no means exhaustive), showed that there were several gaps in knowledge of the subject and very little experimental verification of the various theories had been attempted. Much confusion appeared to have been caused by the lack of a detailed explanation of the mechanism of shear lag and by the fact that instability can also cause weakness of thin plating (when it is in compression). It may be shown that, after local instability of plating on the compression side of a beam has been established, the effective width of plate is a function of its thickness. Pietzker (ref. S 1) introduced into naval architecture the idea of an effective breadth of plate which depended upon the thickness but he incorrectly applied this criterion to plating in tension also. Unfortunately this ill conceived method is very easy to apply and many naval architects still use it for plating in both tension and compression (and in any case omit to calculate the stress at which buckling of the plating would commence). Modern authors such as Schade (ref. S 9) and Vedeler

(ref. R 7) distinguished between local instability of plating and shear lag, and Schade introduced a notation which will undoubtedly clarify the situation. The lack of a clear description of the causes of shear lag has also enabled it to gain prominence in cases where its neglect would be justified. Schade was content to say "The plate is loaded only by virtue of the transmission of shear through the plate from the web of the stiffener, and therefore the direct stress diminishes as distance from the web increases". Most of the mathematical authors, however, have neither explanation nor diagram to help their readers, while the papers that described the more approximate methods usually contained only a brief description of the action of shear, upon which the theory rests. In consequence the practical man frequently spends valuable time trying to estimate an effective breadth of plate to be associated with a stiffener in circumstances where shear lag is likely to be negligible, and measured departures from the simple beam theory due to unknown causes are often ascribed to shear lag when there is in fact no reason to expect shear lag to be important (see for example refs. G 2 to G 9). It must be clearly understood that the effects of shear lag only become noticeable when the breadth of plate is so large that shear strains can cause warping of the cross sections which are able to affect the direct stresses, and that the effect upon the direct stresses is dependent upon the rate of change of shear force with respect to distance along the beam, i.e: upon the distribution of load on the beam. A full appreciation of this fact is essential if the results of shear lag theory are to be applied correctly in practice.

Ever since the introduction of the idea of an effective breadth much effort had been expended in the evaluation of this quantity for the benefit of the practical man. In some modern work the concept appeared to have been carried too far. In many papers diagrams of effective breadth associated with shear lag were published without comment on their significance and some were not a little obscure. Vedeler, for example, included in a recent paper (fig. 8 of ref. R 7) several diagrams of effective breadths of plating associated with beams consisting of a stiffener attached to an infinitely wide plate, under various conditions of loading. Considering a uniformly loaded beam he showed that when there were no constraining moments at the ends of the beam the effective breadth did not vary much along the span, but when the same beam was completely fixed at the ends the effective breadth varied considerably along the span and tended to infinity near the points of zero bending moment. It was difficult to understand how bending moments applied at the ends of a beam could have such a large effect on shear lag throughout its length. Furthermore, the difference between the effective breadths in the two cases indicated an apparently insuperable difficulty when calculating the integrals represented by symbols a and i in Chapter I, prior to finding the bending moments which acted upon a beam. It was clear that the concept of an effective breadth must be examined more closely if it led to difficulties of this nature.

Many papers contained results expressed in terms of infinite series of trigonometrical terms. If the origin was at one end of the beam, series of sine terms were used to represent the stresses in simply supported beams, and series of cosine terms applied similarly to beams which were completely fixed at the ends. The stiffened plating in a ship is constrained at its boundaries in some manner intermediate between these conditions, and in general the amount of constraint at the ends of the stiffeners has a far greater effect on the stresses in them than shear

lag in the plating. Clearly any shear lag theory used in practice must be applicable to beams which are partially constrained at the ends, but the sine or cosine series in the papers examined did not include this case.

Experimental work should, in my opinion, always follow theoretical analysis and it is surprising that so few experiments have been performed on wide flanged beams when so much time has been devoted to the publication of theoretical papers. Quite a lot of the experimental work which has been done has been divorced from thorough theoretical analysis with the result that many of the theoretical conclusions were not properly checked.

The earliest experiments were made by Miller (ref. S 4) who carried out some systematic experiments apparently under Metzer. His specimens were between 30 and 100 cm. long. Two specimens were milled from solid blocks of steel, two consisted of aluminium I-bars riveted to plates 1 mm. thick, and one was made of wood. The steel and wooden specimens consisted of single bars of rectangular cross section with wide flanges. The ratio of length to breadth of flange was the main variable. An ordinary tensile testing machine was adapted to apply a load at the centre of span, and the ends were simply supported. Deflections were measured, and also strains in the steel specimens only. Various experimental difficulties were experienced but the results were claimed to show some agreement with Metzer's theoretical work (ref. S 3).

Winter (ref. S 7) carried out some experiments with wide flanged I-bars and, although details of the experiments were omitted from his paper, it was stated that the results indicated a general agreement with his method of calculating the effective breadth of flange.

Hartman and Moore (ref. S 14) made a systematic experimental investigation of shear lag in panels of stiffened plating which might be found in aircraft. The specimens were of aluminium and the stiffeners had cross sections commonly used in the aircraft industry. The investigators started with single stiffeners at the centre of very wide plates. Two further stiffeners were added later at the extreme edges of the plates, and later still two stiffeners were added at intermediate positions so that the final specimens consisted of a plate with five equally spaced stiffeners. In this way the ratio of length to breadth of plate was varied. Strain gauges were fitted so that in the final specimens there was a line of gauges along each stiffener and one along the plate between each stiffener. Results from the single stiffener specimens showed that there was considerable deflection of the plate so that its distance from the neutral surface of the beam was not constant (Miller also experienced this difficulty). The three-stiffener specimens represented a case intermediate between the two theoretical extremes usually considered and were not comparable with either. The five-stiffener specimens had insufficient gauges to show the distribution of stress in the plate between each stiffener, but the maximum and minimum stresses were indicated and agreed fairly well with theory.

To sum up, the number of theoretical papers that had been published about shear lag greatly exceeded those which described experimental work, and there had been inadequate correlation between the

two. After studying all the papers, there were still a number of anomalies and several queries left unanswered. Shear lag in stiffened plating where the stiffeners were partially constrained at the ends seemed to be a particularly fruitful field for investigation.

15) Summary of Investigation into Shear Lag in Stiffened Plating.

The examination of the various theories of shear lag, the formulation of a rational exposition of the subject and some extensions of previous theories, werecarried out concurrently with a set of experiments designed to exhibit the main features of the phenomenon with particular reference to beams which were partially constrained at their ends. This work was fully described in a paper published in 1955 by the Institution of Naval Architects and a copy of this paper, together with the discussion, is bound as an appendix at the end of this thesis. It is the purpose of this Section to discuss the research in general terms and to call attention to advances made in the knowledge of the subject.

The paper is in three parts. The first part was written for the practising naval architect and desoribes the investigation in a manner which was intended to appeal to persons with limited mathematical knowledge. In this way it was hoped that some of the mystery which had surrounded the subject would be removed and that this would lead to a proper application of shear lag theory when, and only when, necessary. (Remarks in the discussion showed that this was appreciated). The second part of the paper deals with the theory and includes one or two extensions of it which will be mentioned later in this Section. The third part describes experiments carried out in the James Watt Engineering Laboratories of the University. These were the first experiments to be carried out in which the effects of shear lag were clearly demonstrated, and compared with theory.

The usual theory of shear lag is set out in articles 7 to 13 of the Appendix, and a summary is given in article 5. The theory given is based on the work of Chwalla (ref. S 5). The basis of the solution is the use of the Airy stress function to describe the stresses in the wide plates and to satisfy the boundary conditions along their junctions with the stiffeners or along the plate edges parallel to them. In this way the condition that plane cross sections of the stiffened plating remain plane after bending is removed so that it no longer applies to the wide plating. (Plane sections across the stiffener alone are assumed to remain plane after bending).

In all previous papers which had been examined, the boundary conditions at the ends of the plate had not been discussed. At the end of article 10 it is shown that the choice of sine or cosine for the term in x of the product solution, governs the boundary conditions which may be satisfied at the ends of the plate, i.e: at $x = 0$ and $x = L$. In article 11, when the elementary solution is extended in the usual way by means of Fourier series, this distinction between the end conditions is clearly made. (The fact that a half range series of either sine, or cosine terms can be made to represent any bending moment diagram was also emphasised because this point had not been made clear in previous papers).

The other advance in the theory may be appreciated better after considering the experimental results. The experiments are described in Part III of the Appendix and were carried out on a beam which was specially designed to exhibit measurable shear lag effects. Figs. 16 to 19 of the Appendix show very clearly the effects of shear lag and demonstrated that the theory agrees well with the experiments, except possibly at the theoretical extreme ends of a beam. The difficulty of designing a beam such that the ends would satisfy either of the theoretical end conditions is discussed an article 17, and in fig. 22 the actual conditions achieved are compared with the two theoretical end conditions, treating section K as if it were one end of the beam KK'. A qualitative comparison is also to be found in figs 1B and 1C and fig. 21 (Experiment I).

In Experiments I, II and IV an identical load, approximately uniform, was applied to the span KK' while the constraining moments applied at K and K' were varied considerably. Observe that between sections A and G the difference between the stresses associated with the ordinary bending theory (shown by dotted lines) and those which include shear lag (shown by full lines) is identical in each experiment and the effect is uniform along the span. In Experiment III, in which no load was applied between sections K and K', there was no shear lag between sections A and G. In each of these experiments the shear lag effect of a concentrated load at K (in this case a negative load due to reaction at the support) was clearly shown, and was demonstrated to be a local effect associated with the diffusion of the disturbance into the beam. These experiments demonstrate clearly that shear lag is associated with the distribution of load along the beam and is directly proportional to its magnitude. Originally it had been intended to compare the various approximate theories of shear lag with the exact theory and the experiments, but time did not permit this. It is interesting to note, however, that the early approximate method of Lockwood-Taylor (ref. S 13) predicts results of this nature, (but incorrectly in detail - see page 41 of Appendix), whereas the papers of v. Karman, Metzer, Chwalla, Sandorff etc. give mathematically correct solutions but fail to express the results in such a way as to call attention to the salient features of the phenomenon.

The obscurity of many of the more mathematical papers seems to be associated with the pre-occupation of the authors with the calculation of "quasi-"* effective breadths of plate. The bending stresses calculated by the ordinary theory of bending (i.e: assuming plane cross sections remain plane) are directly proportional to the bending moments, which depend upon the combined action of the applied load and reactions together with the constraining moments. But the modifications to these stresses caused by shear lag depend upon the local variation of load along the beam and, in general, these effects are not linked in any simple way to the variation of bending moments. It seems illogical,

---

* The "quasi" effective breadth is called the "overall" effective breadth in the Appendix but the word "quasi" is used here in deference to Prof. Schade's criticism on page 37, - see author's reply on page 41.

therefore, to attempt to evaluate the modified stresses entirely in terms of the bending moments. This suggests that more rational results would be achieved if the stresses due to bending and to shear lag were considered separately, and this is done in article 14 of the Appendix by the simple expedient of subtracting the stresses associated with ordinary bending (plane sections remain plane) from the total stresses found by the theory of bending with shear lag.

Equations 48 and 49 converge extremely slowly (60 terms were required to obtain a reasonably accurate answer for a concentrated load) and they would be of no practical use by themselves. Because shear lag is a local effect, however, it is possible to estimate its effect by considering the forces applied to a beam to be divided into a number of discrete loads each spread over a short distance. Any distribution of load may be represented approximately in this manner. To meet the needs of practical men, equations were derived in article 14 of the Appendix, which represent the additional stresses in the stiffener associated with shear lag caused by the application of a load W spread over a distance Δ along the beam. These equations may be written:

$$p_{sw} = \frac{W B h}{I} \frac{S}{200}$$

$$p_{sc} = \frac{W B h}{I K} \frac{S}{200}$$

where

p_{sw} = Additional stress in stiffener at its junction with the plate.

p_{sc} = Additional stress in stiffener at centroid of area of stiffener alone.

W = Load spread over distance Δ.

B = Breadth of plate between stiffeners.

h = Distance between centroid of stiffener alone and middle of thickness of plate.

I = Moment of inertia of cross section of stiffener alone.

R = Bt / 0·91 A

t = Thickness of plate.

A = Area of cross section of stiffener alone.

$$K = 1 + \frac{h^2}{k^2}$$

k = Radius of gyration of area of cross section of stiffener alone.

S is given by a complicated expression - equation 52 on page 21 of the Appendix. The important case in practice is that of a panel of plating with many stiffeners, and for this case values of S were calculated. A value of Poisson's ratio equal to 0·3 was used, but normal variations of this quantity have little effect in practice. It was found that S is independent of the ratio L/b provided that L/b is greater than 4. (The quasi-effective breadth is usually expressed in terms of L/b). Values of S are expressed graphically, for a concentrated load and three values of Δ, in fig. 2 of the Appendix. The figure shows the variation of S along the stiffener from the centre of the load, in units of distance measured in terms of breadth of plate. S is shown for one side of the centre of load only; its variation on the other side is identical. The distribution of stress across the plate is of the same character as that shown in fig. 20 of the Appendix (which is drawn for the experiments), but in practice it is usually sufficient to know the stresses in the stiffener. The stress varies linearly across the stiffener so that the values found for the two specified points enable one to find the stress at any other point in the stiffener.

There is a quicker method when it is desired to know the shear lag effects associated with water pressure. In article 4 of the Appendix it is demonstrated in a very elementary fashion that the shear lag stresses due to water pressure at a given depth were the same as those due to a uniform load per unit length equal to that at the depth considered. The additional stresses due to shear lag associated with a uniform load may be calculated directly by use of the following equations:

$$p'_{sw} = \frac{w B^2 h}{I} \frac{S'}{400}$$

$$p'_{sc} = \frac{w B^2 h}{I K} \frac{S'}{400}$$

where p'_{sw} and p'_{sc} = Additional stresses associated with a uniform load.

w = Load per unit length (measured <u>along</u> the beam).

The other symbols have the same meaning as before and values of S' are given in Table II on page 8 of the Appendix, which were calculated from equation 55 on page 22. These equations may be used to calculate the additional stresses associated with a uniform load or a load which varies linearly like water pressure against a vertical beam. If, in addition, there are concentrated or other loads, the stresses due to shear lag associated with these may be estimated using the previous pair of equations, and the results added together to give the total additional stress.

Thus the system of equations developed enables one to estimate the effects of shear lag in any beam, however loaded. Unlike the quasi-effective breadth method, it is not necessary to have a large

number of charts - one for each sort of bending moment diagram - and the method is altogether more logical because it treats separately the stresses which depend upon two different types of action.

A short theoretical investigation was undertaken in an attempt to evaluate the importance of shear lag in practical shipbuilding and this is summarized in article 16 of the Appendix. The results simply confirmed the conclusions of previous authors, but they also demonstrated that for the spacing of stiffeners usually encountered in practice shear lag is unimportant, except possibly in way of a relatively concentrated load.

16) Effect of Shear Lag on the Analysis of Continuous Beams by Moment Distribution.

In Chapter I of this thesis some problems concerning the strength of ships were solved by use of the moment distribution method. In addition to the work described in the Appendix a short investigation was carried out to examine the effects of shear lag on this method and some remarks on the subject are set out below.

It has already been shown that shear lag is negligible in practice, except in way of a relatively concentrated load. The most obvious occurrence of a concentrated load in practice is in panels of plating which are stiffened by two sets of beams which intersect at right angles. These often consist of large numbers of hydrostatically loaded small stiffeners with one or more deep girders affording them support at intervals. The point at which shear lag may be expected to be important is in the plate flanges of the light stiffeners where they intersect the heavy girders. The reactions at the girders may be considered to be comparatively large negative loads applied to the stiffeners at points of maximum bending moment. Such a set of beams is analysed in Section 5 of Chapter I, where for example, the relatively small bulkhead stiffener BE is assumed to be supported by heavy transverse girders at C and D. A further example is to be found in Chapter IV.

When analysing the small stiffeners, they are treated as continuous beams over the supports and the moment distribution process is applied at each support. It is assumed in this process that at each step the change of slope is the same on each side of each support, but in the presence of shear lag the usual equations for stiffness, carry-over factor etc., which satisfy this condition may need modification. The amount of the modification would depend upon the relative magnitude of the concentrated load. Several possible methods of adapting the moment distribution method to the situation appear to be possible:

a) The Fourier series type of solution of the shear lag problem could be used to develop equations for finding the stiffness and carry-over factor of each span of the continuous beam. There is an objection to this, viz: the theory can only be applied when the end cross sections of each span are either free to warp or completely restrained against warping. By

this means only the upper and lower limits of the required quantities could be found.

b) One could calculate the quasi-effective breadths of plate in way of the concentrated load (assuming an approximate magnitude), analyse the beam on this basis, make a closer estimate of the load and then adjust the breadths and repeat the process if necessary.

c) It would be possible to develop an equation which would allow for the extra change of slope associated with shear lag near the ends of each span and to modify the moment distribution technique to take account of it, so that as the relaxation proceded the shear lag effect could be adjusted to correspond to the magnitude of the concentrated load.

In fact, however, all of these methods would be cumbersome to apply and it would probably be better to adopt a different method of analysis. Wilson's method of analysing continuous beams (ref. B 3, article 90) could be adapted for this purpose. The method consists of finding the reactions at the intermediate supports by equating the upward deflections caused at every support by all the supporting forces, to the downward deflections which the load would cause at those various points if the beam were supported at the ends only. Deflections of any amount at one or more of the supports can be taken into account very simply by this method. If the two sets of deflections are calculated by equations 40 or 44 of the Appendix, shear lag throughout the beam is allowed for automatically. When using Wilson's method it is necessary to find the deflections more accurately than is the case in other methods and although the equations for deflection with shear lag converge rapidly it is necessary to use several terms of the series.

In order to assess the practical importance of the effect of shear lag on the moment distribution process, Wilson's method was used to find the bending moments in a uniformly loaded continuous beam, 250 inches long, supported at four equidistant points. The cross section was identical to that of the bulkhead stiffener of the ship mentioned in Chapter IV, in which the 6 in. angle bar stiffeners were 25 in. apart. (This example was chosen in view of the experimental results described in Chapter IV and will be referred to in that Chapter).

It was found that the effect of shear lag was very small indeed. The reactions at the middle two supports were decreased by 0·03 % and the two end reactions were increased by 0·1 %. The bending moment at the two middle supports was decreased by 0·4 % so that the net increase of bending moment at the centre of the middle span was 1·4 % (the latter was about one third of the maximum bending moment at the middle two supports). Although it is not a good thing to argue from the particular to the general, this stiffener is representative of normal shipbuilding practice and it is reasonable to conclude that for stiffened plating of average proportions shear lag may be neglected. The moment distribution process may be applied as usual, neglecting shear lag, and the additional stresses associated with shear lag may be estimated afterwards if necessary.

CHAPTER III

ANALYSIS OF THE EXPERIMENTS AT GLENGARNOCK ON SHIP STRUCTURAL MEMBERS.

17) History.

For some years past a considerable amount of experimental work has been going on at Glengarnock to examine the behaviour of stiffened plating. Specimens consisting of a plate 2 ft. wide stiffened by a typical ship stiffener are loaded in a specially constructed testing machine under conditions as near as possible to those in a ship. This part of the thesis is a record of an examination of the results of the first 300 tests carried out at Glengarnock, in order to determine what precautions must be taken when using the theory of bending in practice, and to draw general conclusions from the test results.

The experiments were commenced in 1939 by a sub-committee of the Welding Research Council, later the British Welding Research Association, and the work continued throughout the War. Shortly after the War the investigation came under the aegis of the British Shipbuilding Research Association and is still going on. A summary of the main objectives and the experimental procedure will be found in ref. G5. The tests were carried out by the authors of refs. G1 to G9 inclusive and I was neither able to take part in them nor to influence their course in any way. The B.S.R.A. and the investigators themselves gave me all the help they could; permission was readily granted to enable me to examine the actual figures recorded during the experiments and the investigators could not have been more willing to co-operate.

It soon became clear, however, that the investigators could throw little light on reasons for the observed behaviour of the specimens. Hardly any theoretical analysis had been done and a fair idea of the "practical" outlook of the people in charge may be obtained by reading their reports (refs. G1 to G15 incl.). I decided to disregard their opinions entirely and to treat the results on their merits. An attempt was made to modify the usual method of applying the theory of bending until it fitted the facts as reported. The principle was adopted that the theory should be as simple as possible and the most elementary assumptions were used unless comparison with experiment showed that they required modification. Full use was made of the work described in Chapters I and II.

18) Preliminary Work.

The experimental procedure was to increase the load applied to the specimens until rough measurements indicated maximum stresses in the neighbourhood of 12 or 14 tons/in^2. On removal of the load some permanent set was usually observed, which was taken to indicate that a certain amount of yielding had taken place at stress concentrations,

riveted joints and welds, etc. (A small amount of this is known to cause no harm). No further yielding takes place unless the load is raised above the previously applied maximum but the same maximum load was re-applied two or three times to ensure elastic behaviour of the structure. The stresses and deflections quoted by the investigators in their reports (refs. G2 to G9) are those read during the final applications of load. (Generally strains were read during one load cycle and deflections during the next cycle in order to avoid the use of both sets of instruments simultaneously.)

The first essential was to plot the measured stresses (strains x Young's modulus) as ordinates with loads as abscissae. In general the stresses were proportional to load but there were exceptions. Fig. 7 shows a typical set of graphs of the individual stresses at four positions across the web of the 6 inch channel bar measured during test 91.

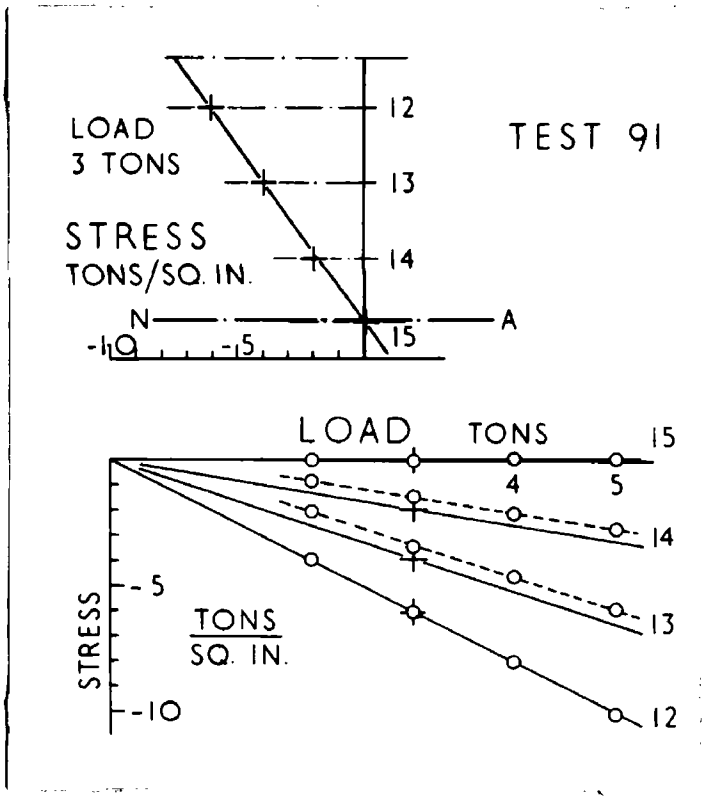

Fig. 7.

The points plotted for gauges 12 and 15 in the lower diagram lie on straight lines through the origin. Those for gauges 13 and 14 lie on straight lines which do not pass through the origin. Concerning the latter, it was decided that more weight should be given to the four measured stresses at 2, 3, 4 and 5 tons load than to the zero measurement, and it was assumed that the true stresses lay on a line passing through the origin with the same slope as that of a line passing through the four measured stresses, as shown by dotted lines in fig. 7. (The location of the average line was not always so simple; in some experiments there was considerable scatter of the readings). The mean measured stress was then read from each line at a

convenient load (3 tons in this particular case) and these were used to draw a diagram of stresses across the section of the beam as shown in the upper diagram of fig. 7.

Before using the measured stresses to determine the bending moments, it was necessary to compute the geometrical properties of cross section of the various specimens. Much had been written about the positions of neutral axes and corresponding effective breadths of plate of the specimens (refs. G2 to G9 incl.). Variations of the latter between 15 inches and 30 inches had been recorded whereas the actual breadth was 23·5 inches (nominally 24 in.). It had been suggested that shear lag in the plate might be responsible for the variations but an investigation described in article 16 of the Appendix to this thesis showed that this was not so. It was found that the increases in stress at mid-span caused by shear lag (expressed as percentages of the stresses due to bending) were never more than 4% at the plate and 1% at the table of the tee bars and most other cross sections. Exceptionally there were greater increases and the maximum increase occurred in the 6 inch deep flat bars in which increases were never more than 10% at the plate and 0·7% remote from it. The latter figures refer to flat bar specimens which were very heavily constrained and in these specimens the theoretical point of zero stress was moved in a direction away from the plate by about 0·05 inch. The corresponding movements in other specimens were all less than this. It followed that the variations of the position of the point of zero stress observed at Glengarnock (which amounted to as much as one inch in some of the larger tee bars), must be due to some cause other than shear lag. In fact, for all practical purposes, shear lag in the specimens used at Glengarnock was negligible.

Examination of the measured stress distribution across the webs of a considerable number of specimens showed that the measured position of zero stress could not be expected to define the position of neutral axis in the majority of cases, for the following reasons:

i) Measured stresses varied up to ± 0·3 ton/in.² from the mean line, and the position of zero stress could not be found accurately from them.

ii) Tension or compression in the specimens due to restraint of the end structure added direct stresses to stresses due to bending. This effect was negligible compared with the maximum stress in the specimen, in most cases, but a small tensile or compressive stress could cause an appreciable shift of position of zero stress in the web.

iii) Tilting of specimens added transverse bending stresses to those due to bending in a vertical plane and there was a slight movement of the position of zero stress due to this.

It was therefore assumed that the <u>full</u> breadth of plate associated with each stiffener was effective. It was also assumed that there was no difference between the behaviour of riveted and welded specimens since the riveting of the faying flange to the plate was under very low stresses at all times. The corresponding geometrical properties of the cross sections of the specimens are given in Table VI. It was

TABLE VI

GEOMETRICAL PROPERTIES OF CROSS SECTIONS OF SPECIMENS INCLUDED IN ANALYSIS

Ref.	Scantlings (inches)	Type	Thick-ness of Plate (in.)	Properties of Sections I ($in.^4$)	I/y ($in.^3$)
A	12 x 2 x 0·75/0·42	T	0·32	269·3	30·3
B	ditto	T	0·44	297·5	31·35
C	ditto	T	0·63	331·5	32·65
D	12 x 8 x 0·75/0·42	T	0·32	514·7	75·7
E	ditto	T	0·43	585·0	78·3
F	ditto	T	0·61	647·7	81·4
G	12 x 3½ x 3½ x 0·40/0·60	CH	0·42	357·3	38·3
H	12 x 3½ x 3½ x 0·46/0·60	CH	0·41	370·6	40·6
I	12 x 3½ x 0·40/0·54	IA	0·42	356·1	36·8
J	12 x 3½ x 0·40/0·60	IA	0·42	346·0	38·1
K	12 x 3½ x 0·45	BA	0·42	346·8	37·6
L	12 x 0·45	BP	0·42	337·3	37·4
M	12 x 4 x 0·5	FP	0·41	359·0	40·5
N	10 x 1·125	FB	0·42	256·4	31·85
P	9 x 3 x 3 x 0·32/0·44	CH	0·42	139·8	18·5
Q	9 x 3 x 0·32/0·44	IA	0·42	137·9	18·5
R	9 x 3 x 0·40/0·38	T	0·42	136·4	18·55
S	9 x 3 x 0·44	BA	0·42	145·8	19·25
T	9 x 0·44	BP	0·42	142·7	19·1
U	6 x 3 x 3 x 0·30/0·38	CH	0·38	49·8	9·54
V	6 x 3 x 0·30/0·38	IA	0·38	49·3	9·55
W	6 x 3 x 0·38	BA	0·38	37·6	6·97
X	6 x 0·40	BP	0·38	38·9	7·27
Y	6 x 3 x 0·45	OA	0·41	29·3	5·32
Z	6 x 0·45	FB	0·38	29·3	5·36

assumed that these properties of the cross sections were constant throughout the length of the specimens, except in way of brackets. This table of values was used throughout the analysis and when comparing theory with measured results no evidence was found to justify rejection of the assumptions upon which it was based.

During the first series of experiments (ref. G2) an important decision had been made, viz: that tests on single specimens would give the same results as tests on three stiffeners side by side. Mr. Turnbull stated:

> "Originally it had been intended to test specimens consisting of a plate stiffened by a single stiffener but there was some doubt as to whether or not the deflections and stresses derived from a specimen with a single stiffener could be considered as truly representative. It was, therefore, decided in the first instance to test specimens with three stiffeners, and then to cut them up so as to give three separate specimens each having a single stiffener.
>
> The results indicated that the deflections of the individual stiffeners of the intact three-stiffener specimens were similar and that the behaviour of three separate stiffeners tested together were almost identical with that of the intact specimen and gave similar deflections for the side and centre specimens.
>
> It is therefore considered that the results of single stiffener specimens are suitable for the purposes of the investigation."

The tests referred to were carried out on three identical specimens and the conclusions are no doubt valid in this case, but it was also inferred that correct results would be obtained when three specimens having <u>different</u> geometrical properties of cross sections were tested side by side. The actual order of testing the specimens was as indicated in Table VII. Each line shows three specimens tested simultaneously; the letters refer to the sections identified in Table VI and the numbers below each letter refer to the tests carried out. It will be observed that in some of the early tests specimens having ratios of stiffness up to 2:1 were tested side by side, but after about test 90 the three specimens of each set had nearly the same stiffness. In the early tests, therefore, the possibility of interaction of different specimens through the end structures had to be considered. In some of the later tests attempts were made to reduce tilting of unsymmetrical stiffeners by connecting the adjacent plate edges together (see Section 23). It is probable that under these circumstances there was a tendency for load to be transferred from one specimen to another. The magnitude of these effects could not be determined, but it appeared that many of the discrepancies between theory and measurement could have been caused by interaction between the specimens in one form or another. As these were secondary effects they were ignored when formulating the theory upon which the analysis was based, but sometimes in later work these possibilities had to be considered when deciding whether the results of one or two of a group of experiments should be given more or less weight than the remainder.

On the assumption that the specimens acted

TABLE VII

ORDER OF TESTING SPECIMENS

G	G 1-3, 9-22	G
B	B 4-8	B
A 27-29	B 24-26	D 30-32
L 45-54, 58	(0)* 55-57	K 53-44, 59, 60
F 67-69	C 61-63	E 64-66
(0)* 73, 76	I 86-90	N 81-85
U 91-96, 105-119	X 101-104, 129-138	V 97-100, 120-128
W 159-148, 168-175	Y 149-158, 176-186	Z 159-167, 187-194
P	P 195-215	P
H	H 216-233	H
S 234-240	T 234A-240A	S
Q 241-247	R 241A-247A	Q
J	J 248-261	J
M	M 262-289	M
-	Z 294-300	-

* (0) indicates 10 inch specimens not included in analysis.

independently, there were three essential elements in each test (Ref. G1):

i) The stiffener and its associated plate acting as a beam.

ii) The end structures which tended to resist changes in slope of the ends of the stiffener.

iii) The bracket or other connection between the stiffener and end structures.

The measurements were nearly all made on the stiffeners; records elsewhere were confined to a few deflections of the end structures. The most fruitful source of information was the strains measured in the stiffeners. The calculated section modulus and the stresses found from the measured strains were used to deduce the net bending moment acting on the beam at any point. The net bending moment is the sum of the bending moment calculated on the assumption that the ends of the beam are simply supported, and the bending moment associated with the moments of constraint applied by the end structures to the ends of the specimen. In nearly all the tests the structures at each end of a given specimen were identical so that the bending moments due to constraint were constant along the span. Fig. 8 shows the bending moment diagram for two typical identical specimens, one loaded on the stiffener side of plate and the other on the clear side. The full line represents the bending moments calculated from the distribution of loads shown in fig. 2 of ref. G5 on the assumption that the load applied by each ram was distributed evenly over the 14 inch long wooden pad (shown in fig. 1 of the same reference) and that the ends of the specimen were simply supported. The experimental values were plotted at a distance from the free bending moment line equal (to scale) to the measured net bending moments at the positions where strains were measured. It will be observed that the experimental points lie on a straight line (within the limits of experimental error) and the distance of this line from the base represents the bending moments associated with constraint at the ends of the specimen. In this manner the constraining moments present in each experiment were determined.

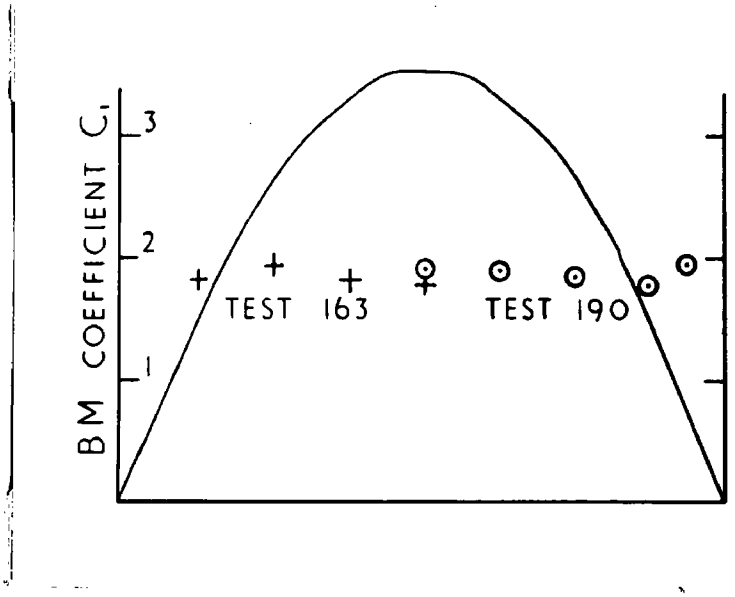

Fig. 8.

The next step was to correlate deflections computed from the bending moment diagrams by integration, with measured deflections. This was a straightforward matter when the specimen had a constant cross section throughout its length. It is well known, however, that the ordinary theory of bending does not apply to a beam where the cross sections are not approximately uniform along its length and it could not be expected to apply in way of brackets. Very few opportunities had been taken to measure strains in the brackets, but the results given by Mr. McCallum (ref: G9) indicated that the distribution of stresses was similar to that predicted by the tapered beam theory. The stresses within the brackets were all very low except near their toes and it was clear that this would not be a very rewarding field for research. In order to keep the theory as simple as possible it was necessary to make assumptions about the overall behaviour of brackets. Considering only welded brackets meantime, the very low stresses and great depth of the brackets compared with the beams indicated that the deformation of the brackets was very much less than that of the beams clear of the brackets. In fact a bracket behaved approximately as a rigid plate over most of its area. At the toes of a bracket there was some deformation and it was necessary to allow for this. It was therefore assumed that the bracket was rigid from its heel to within a distance from its toe equal to two thirds of the depth of stiffener, but that it had no effect on the cross section beyond that point. In other words it was assumed that the bracket rotated as a unit when the beam was loaded, possible distortion near its toe being accounted for by assuming complete rigidity over only part of its nominal length. The distance over which the bracket was assumed to be rigid will be referred to as the effective length of bracket. That this assumption gave results very near the truth was born out by the analysis as a whole. Comparison with experiments 294 and those subsequent to it (ref. G9) showed that measured deflections and those computed from bending moments were within a few thousandths of an inch throughout the length of the beams(which - alone in these experiments- were simply supported so that measured bending moments could be checked). In general, computed and measured deflections agreed very well if the cross section of the specimen was symmetrical about its web. Measured deflections tended to be greater than those computed, especially in the deeper sections but when the deflections associated with shear deformation of the webs of the stiffeners (computed by the method described by Timoshenko in ref. B1) were added, agreement was better. Examples will be found in fig. 15 in Section 24. Unsymmetrical specimens tended to twist under load and this caused additional deflections which are discussed in Sections 22 and 23.

Fig. 9 shows how the brackets affected the bending moments and deflections. It was convenient to express the bending moments in the standard form:

$$M = C_1 \frac{WL}{24}$$

where W was the total load applied to the specimen and L was its length (16 feet in every case) and C_1 was a numerical constant. If the specimen was freely supported at its ends the bending moment at midspan due to the Glengarnock loading was given by $C_1 = 3{\cdot}516$. If the specimen was completely fixed at both ends the fixing moment was given by $C_1 = 2{\cdot}342$ when the specimen had a uniform cross section throughout its length. As the effective length of bracket was increased the end moment required for complete fixity was also increased and the left hand diagram of fig. 9

shows the values of C_1 for the fixing moments plotted on a base of ratio of effective length of brackets to total length of specimen. It will be observed that there was a considerable increase in the moment required for complete fixity as the size of bracket was increased.

Fig. 9.

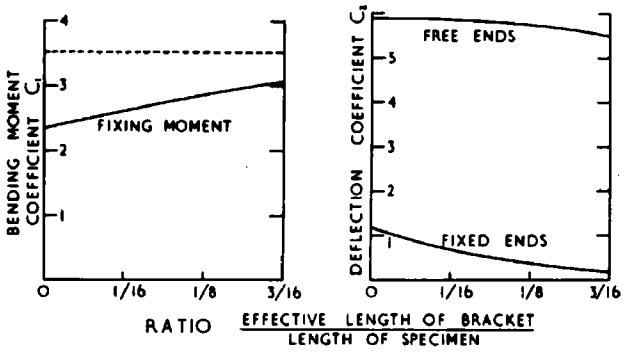

Similarly it was convenient to express the deflections δ in the form

$$\delta = C_2 \frac{WL^3}{384EI}$$

where I was the moment of inertia of specimen at mid-span and the other symbols had the same meaning as before. At mid-span of a uniform beam with the Glengarnock loading $C_2 = 5{\cdot}887$ when the ends were freely supported, and $C_2 = 1{\cdot}199$ when the ends were completely fixed. The right hand diagram of fig. 9 shows the values of these coefficients as the effective length of brackets was increased. It will be observed that the deflection with freely supported ends was not affected much, but that the deflection with completely fixed ends was considerably reduced as the effective length of brackets was increased.

Fig. 9 also demonstrates clearly the importance of the degree of constraint in determining the bending moments and deflections. The effect of constraint was one of the most important factors which had to be taken into account in the analysis and this will be discussed in Section 20.

19) Classification of Experiments.

The experiments fell broadly into five main groups and are classified in Tables VIII to XII. In the left hand column of these tables the cross sections tested are identified by the letters used in Table VI and the second column indicates whether the load was applied to the stiffener, or the clear side to the plate of the specimens. The symbol * indicates a scalloped specimen. The type of end connection or size of bracket is indicated at the top of the remainder of the columns; two columns are given for each, one for riveted connections and one for welded ones denoted by R and W respectively. For details of the structure in any

TABLE VIII

SCHEDULE OF TESTS ON SPECIMENS WITH BRACKETLESS END CONNECTIONS.

STANDARD BASE STRUCTURE

		Pads	Short Lugs		Long Lugs		Extension Pieces		
		W	R	W	R	W	Free	R	W
A	C	27							
B	C	24							
C	C	61							
D	C	30							
E	C	64							
F	C	67							
G	C		11						
	S		13						
H	C		216	217				218	219
I	C	86							
	S	88							
J*	C	249							
K	C		40						
	S		34	35					
L	C	50							
	S	46							
M	C	263							
M*	C	277							
N	C	81							
	S	83							
P	C		196	198				197	200
Q*	C	290,292							
U	S		91						
V	S	97							
W	C		169		171			170	
	S		139		144		141	140	142
X	S	101							
Y	C		177		179			178	
	S		149		154		151	150	152
Z	C	188				190			189
	S	159				163	161		160

TABLE IX

SCHEDULE OF TESTS ON SPECIMENS WITH EQUAL SIDED BRACKETS.
STANDARD BASE STRUCTURE

		Size of Bracket (inches)											
		15		21		27		30		36 x 28	36 x 30	35	
		R	W	R	W	R	W	R	W	W	W	R	W
A	C									29			
B	C									26			
	S									7,8	4		
C	C										63		
D	C									32			
E	C										66		
F	C										69		
G	C							14	15	16	17		
	S							1	5				
H	C	220	221	222	225	224	225					226	227
I	C										87		
	S										89		
J*	C						253					254	255
K	C							43	44				
	S							36	(37)				
L	C								54		55		
	S										48		
M	C						267					268	269
M*	C						281					282	283
N	C										82		
	S										84		
P	C	202	203	206	207	209	210					212	213
Q	C	242	243			244	245					246	247
Q*	C						291,293						
R	C	242A	243A			244A	245A					246A	247A
S	C	235	236			237	238					239	240
T	C	235A	236A			237A	238A					239A	240A
U	S	110	112			93	95						
V	S						99						
W	C	172		173		174						175	
	S	145		146		147						148	
X	S						103						
Y	C	180		181	182	183	184					185	186
	S	155		156		157						158	
Z	C		191		192		193						194
	S		164		165		166						167

TABLE X

SCHEDULE OF TESTS ON SPECIMENS WITH UNEQUAL SIDED BRACKETS.

STANDARD BASE STRUCTURE

	Size of Brackets					
	35 x 45		35 x 55		55 x 64	
	R	W	R	W	R	W
H C					228	229
J* C	256	257	258	259	260	261
M C	270	271	272	273	274	275
M* C	284	285	286	287	288	289
P C					214	215

* Indicates scalloped specimen.

TABLE XI

SCHEDULE OF TESTS ON BRACKETED SPECIMENS WITH REINFORCED BASE.

	Size of Brackets					
	15 x 15	27 x 27	30 x 30		Angle	36 x 30
	W	W	R	W	W	W
B S				6		
G S					21	
I S						90
K S			38	59	60	59
L S					58	49
N S						85
U S	113	96			116,117	
V S	125	100			126,127	
X S	134	104			137,138	

Y

TABLE XII

SCHEDULE OF TESTS ON SPECIMENS WITH ENDS OF STIFFENERS SNAPED

		Angle of cut at end of Stiffener measured from plate (degrees)				
		25	30	60	75	90
A	C	28				
B	C	25				
C	C	62				
D	C	31				
E	C	65				
F	C	68				
G	C	9,10				
	S	12				
J*	C			248		
K	C					41,42
	S					33
L	C	52				51
	S	47				45
M	C			262		
M*	C			276		
P	C				195	
Q	C			241		
R	C			241A		
S	C			234		
T	C			234A		
U	S			92		
V	S		98			
W	C				168	
	S				143	
X	S		102			
Y	C				176	
	S				153	
Z	C				187	
	S				162	

particular test the reader is referred to the statistical reports (refs. G2 to G9), where a diagram of the arrangement of each test will be found. The test machine itself is described in ref. G1. Each table shows along the rows the identification numbers of the experiments carried out on each cross section, and down the columns the identification numbers of the experiments carried out on each type of end connection.

Experiments analysed but not included in the tables were as follows:

Tests 105 to 109, 114 to 115, 120 to 124, 129 to 133, 135 to 136, 199	End connections at each end not identical.
Tests 250 and 251, 264 and 265, 278 and 279	Ends connected to standard base by "gussets."
Tests 20 and 22	Ends connected to standard base by angle brackets.
Tests 294 to 298	Specimens freely supported at ends.
Tests 2 and 5	Base struts released.

Some tests were carried out with the connections halfway between the riveted and fully welded conditions, e.g: only the toes of a bracket were welded and a test carried out, and then a further test was carried out after welding had been completed. Intermediate experiments of this nature have also been omitted from the tables, but these tests were analysed and the results are mentioned where significant.

The following experiments were not included in the analysis:

Test 23	12 in. x 4 in. tee bar specimen.
Tests 55 to 57, 70 to 80	10 inch non-standard cross sections.
Test 299	6 inch flat bar with non-standard end connections.

The results of the tests on specimens with welded end connections will be discussed at some length in following Sections. From these alone a great deal can be learned about applications of the theory of bending to the structural members of ships. Riveting is not so important in shipbuilding as it used to be, and consideration of the experiments on specimens with riveted connections will be deferred until Section 28.

20) Method of Analysis.

With the assumptions mentioned in Section 18 it was possible to apply the theory described in Chapter I of this thesis. When applied to a symmetrically loaded symmetrical structure like the majority of the specimens tested in the Glengarnock machine, equation 9·7 used as described in Section 11, gives values of the indeterminate bending moments M_c associated with constraint at the ends of the specimen:

$$M_c = \frac{\beta}{a}$$

If M_s = Bending moment associated with applied load if specimen was simply supported at its ends.

E = Young's modulus of elasticity.

I = Moment of inertia of cross section between brackets.

L = Total length of specimen.

e = Effective length over which brackets are assumed to behave rigidly.

- the value of β was given by:

$$\beta = -\int_{-(\frac{L}{2}-e)}^{\frac{L}{2}-e} \frac{M_s}{EI}\,dx \qquad (20\cdot1)$$

If K_ϵ is the stiffness of one end structure, and if $F_\epsilon = 1/K_\epsilon$

- the value of a was given by:

$$a = \int_{-(\frac{L}{2}-e)}^{\frac{L}{2}-e} \frac{1}{EI}\,dx + 2F_\epsilon$$

$$= \frac{L-2e}{EI} + \frac{2}{K_\epsilon} \qquad (20\cdot2)$$

Hence

$$M_c = \frac{-\int_{-(L/2-e)}^{\frac{L}{2}-e} \frac{M_s}{EI}\,dx}{\frac{L-2e}{EI} + \frac{2}{K_E}} \qquad (20{\cdot}3)$$

It may also be of interest to find the value of the ratio M_c/M_f where M_f is the constraining moment associated with complete end fixity. Complete fixity implies that $F_E = 0$ and it is easy to show that:

$$\frac{M_c}{M_f} = \frac{K_E}{K_E + \frac{2\,EI}{L-2e}} \qquad (20{\cdot}4)$$

It is clear from this equation that the constraining moment is proportional to the moment M_f required to fix the ends of the beam completely against changes of slope. The ratio M_c/M_f is a function of the ratio between the stiffness K_E of the end structure and the bending stiffness of the specimen, the latter being expressed by

$$K_s = \frac{2\,EI}{L-2e}$$

Equation 20·4 is illustrated graphically in fig. 10 which covers the range of values encountered in the tests. A logarithmic scale was used for the abscissae.

Fig. 10

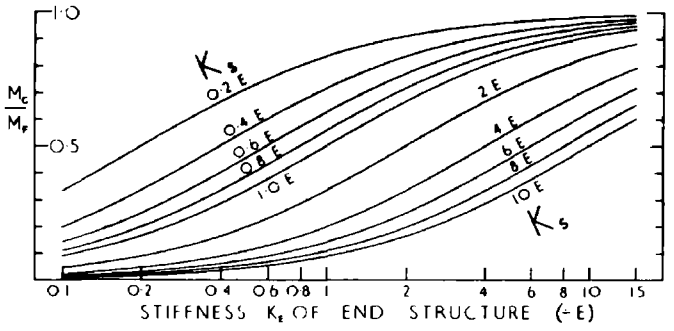

All the quantities on the right hand side of equation 20·3 were easily calculated except the stiffness K_E of the end structures. The values of M_c could be found from the experiments, however,

and it was then possible to solve equation 20·4 for K_ε:

$$K_\varepsilon = \frac{M_c}{M_f - M_c} \cdot \frac{2EI}{(L - 2e)} \qquad (20{\cdot}5)$$

The method of analysis was to find experimental values of K_ε in this way, and to use them as a basis for comparison between the effectiveness of different arrangements for obtaining end constraint. In many cases equation 20·5 made it possible to obtain several estimates of K_ε of a given end structure, one for each experiment in which that end structure was used.

An almost complete catalogue of the K_ε values for welded end structures was made (see Sections 21, 24 and 25) and from these it is possible to find theoretically the bending moments acting on any size or shape of specimen, thus extending the range of usefulness of the experiments without further experimental work (see Section 26). The possibility of calculating K_ε from first principles is discussed in Section 27.

21) Experiments on Specimens With Bracketless End Connections (Welded).

These were considered first because the specimens had constant cross sections throughout their length and were, therefore, the simplest experiments to analyse theoretically. The tests in this category are summarized in Table VIII on page 62.

The largest group of experiments was that shown in the first column, in which the ends of the specimens were welded to pads on the end structures. For each test the strains measured at each position were first plotted on a base of load and the mean increase in strain per unit increase in load was estimated. From these figures the stresses and hence the bending moments acting on the beams were calculated, and this information was used, as described on page 59, to find the constraining moments. Using the known or calculated quantities on the right hand side of equation 20·5 a value of the stiffness K_ε of the end structures was estimated from the results of each test. It was found that the values of K_ε varied considerably but that they fell into quite well defined groups depending upon the size of end connection. The average value of K_ε for 12 inch connections was estimated to be 1·0 E ton in./radian and that for 6 inch connections was 0·15 E ton in./radian. Values of K_ε found experimentally for welded pads at the ends of specimens of different sizes were plotted and are shown in fig. 11. With the help of this diagram it would be possible to estimate the bending moments and deflections of any stiffener less than 12 inches deep with its ends welded to pads in the Glengarnock machine.

The theory indicates that for a given value of K_ε the variation of constraining moment depends upon the moment of inertia of cross section of the specimen. To illustrate this Table XIII was prepared and shows the theoretical stresses and deflections of all the 12 inch

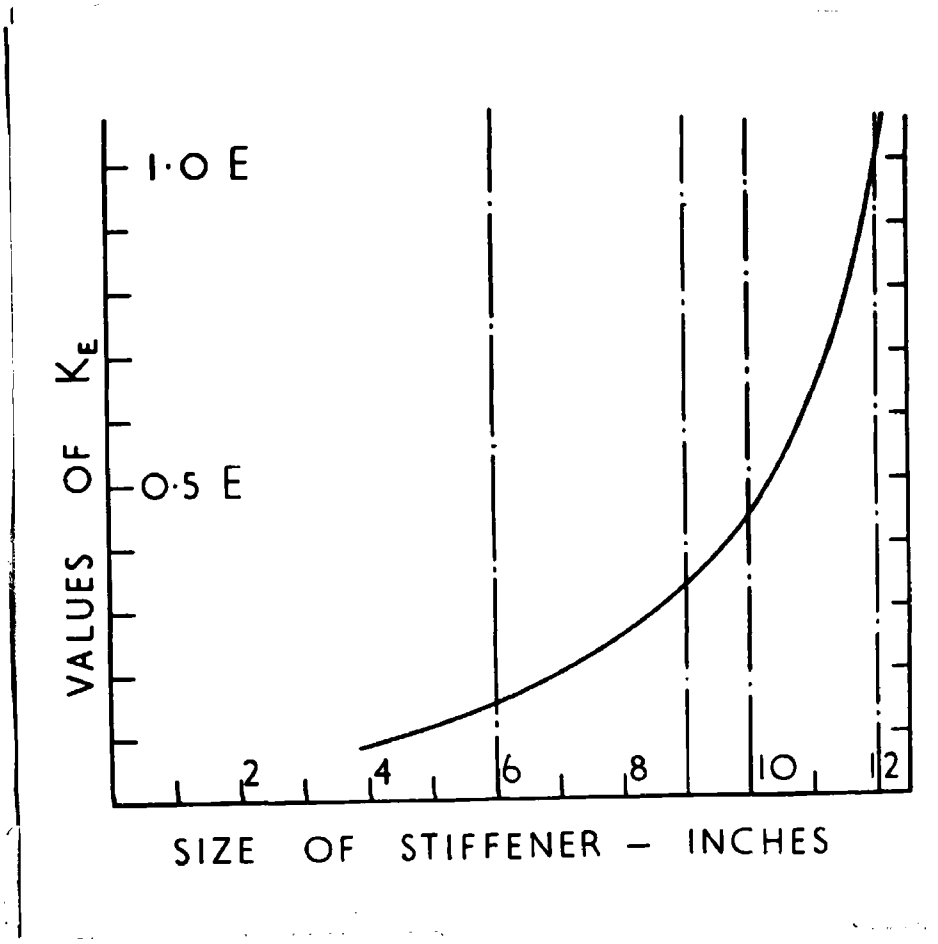

Fig. 11. Stiffness of End Structure from Experiments on Specimens connected to it by Welded Pads.

specimens tested at Glengarnock with welded pads, assuming $K_E = 1{\cdot}0$ ton in. per radian, compared with the values actually measured at midspan. The variation of stiffness of the specimens was not great but was sufficient to indicate the validity of equation 20·3. (A better example of the application of the theory will be given in Section 24). The table demonstrates the following points:

a) Constraint of stiff specimens was less than that of more slender specimens, as predicted by theory.

b) The stresses in specimens with symmetrical cross sections agreed fairly well with theory.

c) The stresses in specimens with unsymmetrical cross sections agreed with theory within limits, but there was a considerable departure from the theoretical distribution of stress over the cross section, the stress near the junction of flange with web being greater than it would be in a similar symmetrical specimen. The theory which accounts for this is described in Section 22.

TABLE XIII

COMPARISON OF THEORETICAL STRESSES AND DEFLECTIONS WITH THOSE MEASURED DURING TESTS ON SPECIMENS WELDED TO PADS ON END STRUCTURE.

Theoretical Stiffness of End Structure K_E = 1·0 E ton in./radian. associated with 12 inch stiffeners.

Cross Section		I (in.⁴)	$\frac{M_c}{M_F}$	Stresses at 12 tons load. (tons/in²) Theory	Experimental Heel	Av.	Toe	Deflections (inches) Theory Bending only	Theory With shear	Expt.	Test
A	(C)	269·3	0·263	9·19		9·9		0·286	0·300	0·386	27
B	(C)	297·5	0·244	9·02		8·9		0·264	0·278	0·310	24
C	(C)	331·5	0·224	8·26		8·6		0·242	0·256	0·295	61
I	(C)	336·1	0·222	7·81	9·4	9·1	9·0	0·238	0·253	0·340	86
	(S)				-10·2	-8·9	-7·3			0·328	88
L	(C)	337·3	0·222	7·69		7·3		0·237	0·250	0·272	50
	(S)					-8·1				0·260	46
D	(C)	514·7	0·157	3·99		4·3		0·164	0·178	0·230	30
E	(C)	585·0	0·141	3·91		3·7		0·148	0·162	0·156	64
F	(C)	647·7	0·129	3·79		3·7		0·136	0·150	0·142	67

For each test, the measured stresses and deflections were plotted on a base of load, and mean lines drawn through the points obtained. The experimental values quoted were read from the mean lines at 12 tons load.

d) The theoretical deflections calculated by bending theory were slightly less than the measured deflections. When the theoretical deflections due to shear strain in the webs were added agreement was better, but in several cases this addition did not account for the whole of the difference.

The remaining specimens to be considered in this Section were constrained either by long lugs or by extension pieces. The only welded long lugs were those fitted to the 6 inch flat bar (Z) and an analysis of experiments 163 and 190 showed that the end stiffness K_E in these experiments was 0·75 E tons in./radian. The end stiffness of the same specimen with extension pieces was 2·25 E tons in./radian. The end stiffness associated with larger stiffeners and extension pieces was much greater and it was clear that this was accounted for by the fact that the extension piece was the same size as the specimen itself. The values of end stiffness were as shown in Table XIV.

TABLE XIV

VALUES OF END STIFFNESS K_E ASSOCIATED WITH EXTENSION PIECES.

	Specimen	Stiffness K_E tons in./radian	Test
H	12 inch Channel bar	7·35 E	219
P	9 inch Channel bar	7·5 E	200
W	6 inch Bulb angle	5·0 E	142
Z	6 inch Flat bar (Angle bar similar)	2·25 E	(160 (189

It should be noted that both H and P were unsymmetrical specimens and the anomalous values of K_E may be associated with the difficulty of estimating the bending moments when the stress across the flange showed a considerable variation. The difference in behaviour between symmetrical and unsymmetrical sections noted above was common to all the experiments. It was desirable to examine the theoretical explanation and this will be discussed next.

22) Behaviour of Specimens with Unsymmetrical Cross Sections.

Throughout the experiments it was observed that although the symmetrical specimens behaved according to the simple beam theory those with unsymmetrical cross sections did not. In the latter there was a tendency to twist under load and the stress in the flange was decreased at its outer edge and steadily increased across the flange until it was well above that calculated by the bending theory where the flange joined the web. This behaviour was due to the action of shearing forces in the beams at right angles to their longitudinal axes.

Consider a beam cross section consisting of elements of plate at right angles to each other, for example a vertical web with horizontal flanges. In each flange there is a resultant force F along the beam due to the bending moment at a distance x from the origin, which, if M varies, will be increased to $F + \delta F$ on the section distant $x + \delta x$ from the origin. The increase δF represents the longitudinal shearing force on the flange where it joins the web and this force is equal to the integral of the shearing stresses in a longitudinal direction across the flange multiplied by the area over which they act. It is well known that shearing stresses acting on an element of material in one direction are accompanied by equal complementary shearing stresses at right angles to that direction. The integral of these shearing stresses in the flange multiplied by the area over which they act represents a horizontal force perpendicular to the longitudinal axis of the beam. There are similar forces in all the elements which make up the cross section. The sum of the vertical forces is equal to the increase δV in vertical shear force over the distance δx along the beam. In a symmetrical cross section the horizontal forces in the various elements cancel out giving a net zero force. In an unsymmetrical cross section, however, there are unbalanced horizontal forces which form a couple tending to twist the beam. If the applied vertical force is displaced horizontally so that, together with the resultant vertical force associated with shear stresses across the section, there is a couple which balances the moment of the couple tending to twist the beam, there will be no torsion and the beam will bend about its neutral axis (in a manner similar to a beam with a symmetrical cross section). This argument could also be applied to loading in a plane perpendicular to the one discussed above, and clearly there must be one point in the cross section of every beam through which loads applied to the beam must pass if twisting is to be avoided. This point is known as the shear centre and its location must be found whenever bending of an unsymmetrical cross section is considered. The theory is not so well known as it should be but some of the modern textbooks on strength of materials, such as those by Den Hartog (ref. B5) and Salmon (ref. B2), include a short discussion of the main points. The textbooks only deal with the simplest cases but Stelling in 1929 (ref. T3) gave a general semi-graphical method which might be useful in the more difficult ones. Some excellent experiments were carried out on channel bars by Seely et al (ref. T1) in 1930. More recently Terrington (ref. T2) published a summary of the theory.

For the present analysis a simple relationship was developed for the position of shear centre in the unsymmetrical cross sections which were used at Glengarnock, viz: an inverted angle bar welded to a plate (or its riveted counterpart - a channel bar riveted to a plate).

The shape of cross section to be considered is shown in fig. 12. The theory

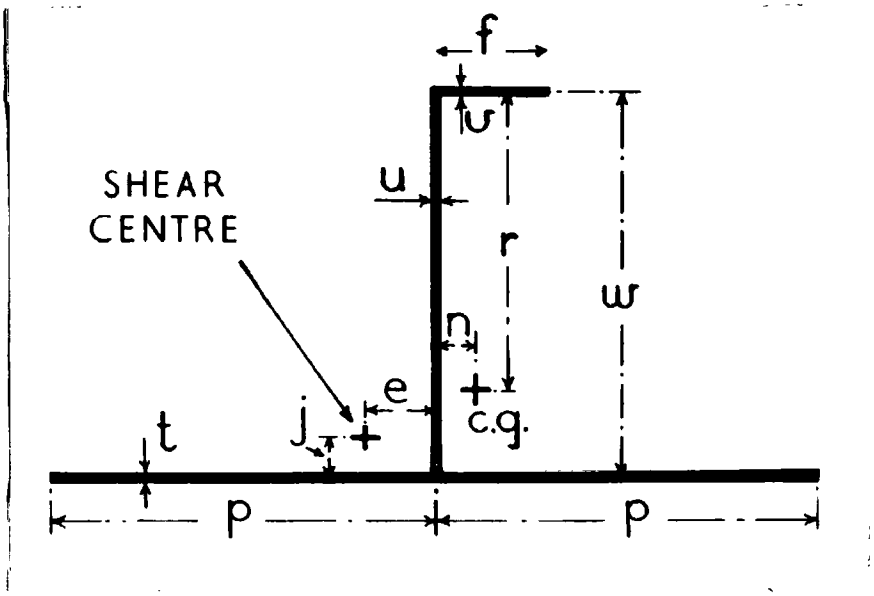

Fig. 12

was confined to sections of this shape, and it was found that to clarify its presentation it was convenient to let the symbols represent only numerical values of the quantities concerned and to indicate their direction in the text. By considering the shearing stresses across the section it can be shown that under the action of shearing force the following forces act in a direction perpendicular to the longitudinal axis of the beam:

A) If the beam is bent about the horizontal neutral axis through the centroid without twisting (assuming that with the cross section as shown in fig. 12 the plane of the paper is vertical), and if there is shearing force V per unit length of beam acting down:

   i) The horizontal forces P_A in the plate cancel each other, giving zero resultant force.

   ii) A horizontal force F_A acts in the flange from left to right (as drawn).

   iii) A vertical force W_A acts in the web in an upwards direction.

B) If the beam is bent about a vertical axis through its centroid, without twisting, and if there is a shearing force S per unit length of beam from left to right:

   i) A horizontal force P_B acts in the plate from right to left.

   ii) A horizontal force F_B acts in the flange from right to left.

   iii) A vertical force W_B acts in the web in a downwards direction.

It is clear that the shear centre in this cross section must be above the plate and to the left of the web (whereas the centroid of the cross section is to the right of the web). Let e be the numerical value of the horizontal distance of the shear centre measured from the middle of the plane of the web and let j be the vertical distance of the shear centre above the mid-plane of the plate. Then for bending without twisting, the forces V and S pass through the shear centre, and by taking moments about this point a pair of simultaneous equations for e and j are obtained:

$$F_A(w - j) - W_A e = 0 \qquad (22{\cdot}1)$$

$$P_B\, j - F_B(w - j) + W_B e = 0 \qquad (22{\cdot}2)$$

It is assumed that the thickness of each component of the cross section is small compared with its other dimension and the work is simplified by replacing the actual cross section by one approximately equivalent to it. Let w be the distance between the mid-thickness of the flange and mid-thickness of the plate and let u be the thickness of the web such that (wu) is equal to the cross sectional area of the actual web. Let f be the distance between the mid-thickness of web and the remote edge of the flange and let v be the thickness of flange such that (fv) is equal to the cross sectional area of the actual flange. Let 2p be the breadth of plate and let t be the thickness of plate. Then the equivalent section will have a cross section as shown in fig. 12. Also let:

r = Numerical value of distance of centroid of section from plane of flange.

n = Numerical value of distance of centroid of section from plane of web.

I_x = Moment of inertia of cross section about horizontal axis through its centroid.

I_y = Moment of inertia of cross section about vertical axis through its centroid.

I_{xy} = Product of inertia of cross section about horizontal and vertical axes through its centroid.

I_p = Moment of inertia of plate alone about vertical axis through centroid of plate alone.

By integrating the shearing stresses across the section the following equations are obtained for the forces:

$$P_A = 0$$

$$W_A = \frac{V}{I_x}\frac{w}{6}\left[(6fv - 3uw)r - uw^2\right]$$

$$F_A = \frac{V}{I_x}\frac{f^2 v\, r}{2}$$

$$P_B = \frac{S}{I_y}\frac{2tp^3}{3}$$

$$W_B = \frac{S}{I_y}\frac{w}{2}\left[(f - 2n)fv - nuw\right]$$

$$F_B = \frac{S}{I_y}\frac{v f^2}{6}(2f - 3n)$$

By considering the calculation of moment of inertia and product of inertia of the cross section it may be shown that these equations are equivalent to:

$$P_A = 0 \qquad P_B = \frac{S}{I_y} I_p$$

$$W_A = \frac{V}{I_x} I_x = V \qquad W_B = \frac{S}{I_y} I_{xy}$$

$$F_A = \frac{V}{I_x} I_{xy} \qquad F_B = \frac{S}{I_y}(I_y - I_p)$$

Substituting in equations 22·1 and 22·2, and solving, it is found that:

$$e = \frac{I_p I_{xy}\, w}{I_x I_y - I_{xy}^2} \tag{22·3}$$

$$j = \frac{\left[I_x(I_y - I_p) - I_{xy}^2\right] w}{I_x I_y - I_{xy}^2} \tag{22·4}$$

It will be observed that in sections of normal proportions j is very small and it may usually be assumed to be zero.

It was found that the shear centres in the unsymmetrical cross sections tested at Glengarnock were about one inch from the webs of the channel bars and inverted angle bars, on the opposite side of the web from the centroid of cross section. For example in the 12 inch inverted angle bar (I) the distances were $e = 0{\cdot}94$ inch and $j = 0{\cdot}14$ in., and in the 6 inch inverted angle bar (V) the distances were $e = 0{\cdot}96$ inch and $j = 0{\cdot}04$ inch.

With one or two exceptions, the loads were applied in the planes of the webs of the stiffeners. The calculation of the resulting stresses and deflections involved the following steps:

1) The applied load R at any section was replaced by an equal and parallel load R' acting through the shear centre, and a twisting moment T equal to the moment of the load (in the plane of the web) about the shear centre.

2) The stresses and angle of twist of the specimen associated with the twisting moments T were calculated by the method described below.

3) The load R' was resolved at the shear centre into rectangular components R'_u and R'_v, each parallel to one of the principal axes of the cross section (taking account of the twist of the specimen relative to the direction in which R' was applied).

4) The flexural stresses and deflections associated with R'_u and R'_v were calculated in the usual way using the principal moments of inertia I_u and I_v of the cross section, and superimposed to find the effect of R' acting at the shear centre.

5) The stresses and deflections found in (2) and (4) above were added (algebraically) to find the total stresses and deflections due to the loading.

In the Glengarnock analysis steps 1, 3, 4 and 5 were straightforward but to calculate step 2 it was necessary to develop equations which applied to the cross sections and loading used. The treatment given by Timoshenko (ref. B1) for the simple cases of I and channel beams loaded at midspan was extended, and an outline of the theory applied to an inverted angle bar welded to plating is given below. In order to simplify the computation it was assumed that the loads R exerted by each ram of the testing machine were applied at discreet points along the specimen instead of each load being apread uniformly over a distance of 14 inches as was assumed in the calculation of bending moments.

Considering any one pair of the loads, their action was to apply a constant torque along those parts of the specimen between their point of application and the ends of the specimen, but there was, ofcourse, no torque along the specimen between the two loads. If the cross section had been circular the torques would have been resisted entirely by shear and there would have been no stresses between the two sections at which the loads were applied. With any other cross section, however, the applied torques are resisted by bending actions as well as those associated with shear. In the Glengarnock specimens, although no

torque was applied between the two loads which formed each symmetrical pair, the flange, web and plate were subjected to bending all along the specimen, and these bending actions were responsible for the unusual distributions of stress over the cross sections of the specimens at midspan.

By symmetry, the cross section at midspan must remain plane during twisting and it was convenient to take the origin of co-ordinates at midspan. (When the specimen twisted the co-ordinate system rotated with the section at midspan, and the actual rotation of the midspan cross section was calculated by finding theoretically the rotation of the ends of the specimen with respect to the cross section at midspan). The mathematical treatment was the same as for a cantilever built in at the origin and subjected to torques applied at specified positions along its length.

Let:

ϕ = Angle of twist at any cross section of beam.

θ = $d\phi/dx$ = Angle of twist per unit length of beam.

T_1 = Torque balanced by shearing forces associated with torsion.

T_2 = Torque balanced by shearing forces associated with bending of the components of the cross section.

The cross section of the beam was divided into a number of narrow rectangles and the dimensions of the cross section were taken to be those shown in fig. 12. Then:

$$T_1 = C\,\theta \qquad (22{\cdot}5)$$

where C is the torsional rigidity of the bar calculated in the usual manner (ref. T4) from the properties of the narrow rectangles into which the cross section had been divided:

$$C = \frac{(fv^3 + wu^3 + 2pt^3)\,G}{3} \qquad (22{\cdot}6)$$

In order to determine T_2 , bending of the flange, web and plate must be considered. Rotation of the cross section takes place about the shear centre. (If it did not the shear centre would be displaced whereas it has been postulated that this is not so). For this reason the shear centre is also known as the centre of twist. Rotation of the cross section about the shear centre causes bending of the flange, web and plate, about their respective centroids and the shearing stresses at their junctions build up a force in each component. Referring to fig. 13, which shows a short length dx of the beam, and using the signs appropriate to the directions of the axes shown, it is found that:

Fig. 13

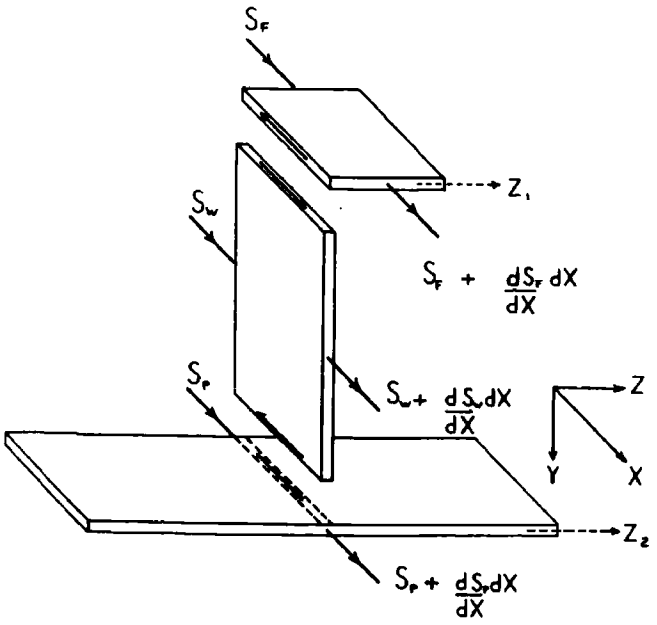

a) In the flange:

Longitudinal strain in flange due to force S_F in flange.	= +	$\frac{S_F}{f\ v\ E}$	(22·7)
Deflection of flange.	= z_1 =	$(w - j)\ \phi$	(22·8)
Curvature of flange.	= $\frac{d^2 z_1}{dx^2}$ =	$(w - j)\ \frac{d^2\phi}{dx^2}$	(22·9)
Longitudinal strain in flange at web-flange junction due to bending of flange.	= +	$\frac{f}{2}\ (w - j)\ \frac{d^2\phi}{dx^2}$	(22·10)

b) In the web:

Longitudinal strain in web at web-flange junction due to bending of web.	= +	$\frac{w}{2}\ e\ \frac{d^2\phi}{dx^2}$	(22·11)
Longitudinal strain in web due to force S_w.	= +	$\frac{S_w}{w\ u\ E}$	(22·12)

Longitudinal strain in web at web-plate junction due to bending of web = $-\frac{w}{2} e \frac{d^2\phi}{dx^2}$ (22·13)

c) In the plate:

Longitudinal strain at web-plate junction due to bending of plate. = 0 since joint is at N.A. of plate.

Longitudinal strain due to force S_p. = $+\frac{S_p}{2pt\ E}$ (22·14)

By equating strains at the web-flange junction the following equation is obtained:

$$+\frac{f}{2}(w-j)\frac{d^2\phi}{dx^2} + \frac{S_F}{fvE} = +\frac{w}{2} e \frac{d^2\phi}{dx^2} + \frac{S_w}{wuE} \qquad (22\cdot15)$$

and by equating strains at the plate-flange junction:

$$\frac{S_p}{2pt\ E} = -\frac{w}{2} e \frac{d^2\phi}{dx^2} + \frac{S_w}{wuE} \qquad (22\cdot16)$$

For equilibrium of the cross section:

i) The total longitudinal force on the cross section must be zero

i.e: $S_F + S_w + S_p = 0$ (22·17)

ii) The total moment of longitudinal forces about any point on cross section must be zero. In particular, taking moments vertically about plate:

$$w S_F + \frac{w}{2} S_w + M_w = 0 \qquad (22\cdot18)$$

where M_w is moment due to bending of web.

By solving equations 22·15, 22·16 and 22·17 it was found that:

$$S_w = \frac{\{f^2v(w-j) - fvwe + 2ptwe\}}{2(fv + wu + 2pt)} wu\ E\ \frac{d^3\phi}{dx^3} \qquad (22\cdot19)$$

$$S_F = \frac{\{w^2ue + 4ptwe - 2ptf(w-j) - wuf(w-j)\}}{2(fv + wu + 2pt)} fv\ E\ \frac{d^3\phi}{dx^3} \qquad (22\cdot20)$$

$$S_p = \frac{\{f^2v(w-j) - w^2ue - 2fvwe\}}{2(fv + wu + 2pt)} 2pt\ E\ \frac{d^3\phi}{dx^3} \qquad (22\cdot21)$$

Note that $M_w/I_w = E\ e\ \frac{d^2\phi}{dx^2}$ where I_w = Inertia of web alone about its own centroid.

so that:

$$M_w = \frac{w}{6}\left\{S_w - \frac{u\ w}{2pt} S_F\right\}.$$

and equation 22·18 was satisfied. By integrating the shear stresses in the web it was found the the total force in the web was zero.

Now, the bending moment acting in the flange. $= E\ \frac{vf^3}{12}\ (w-j)\ \frac{d^3\phi}{dx^3}$

and by integrating the associated shear stresses it was found that the total shear force in the flange

$$= \frac{f}{2}\ \frac{dS_F}{dx} - (w-j)\ \frac{vf^3}{12}\ E\ \frac{d^3\phi}{dx^3} \qquad (22\cdot22)$$

Similarly, total force in plate

$$= \frac{2\ E\ j\ tp^3}{3}\ \frac{d^3\phi}{dx^3} \qquad (22\cdot23)$$

On substituting for S_F it was found that these two forces were equal and acted in opposite directions. They therefore formed a couple, the moment of which was equal to one of them multiplied by the the distance between them, viz: w. This is the part of the torque applied to the beam which was balanced by shearing forces due to bending of the flanges, that is to say it is T_2.

But the total torque on the cross section is

$$T = T_1 + T_2$$

By using equations 22·5, 22·6, and 22·22 with 22·20, or 22·23, and writing $d^2\theta/dx^2$ for $d^2\phi/dx^2$ it is found that this equation can be written:

$$\frac{d^2\theta}{dx^2} - \frac{\theta}{k^2} = - \frac{T(x)}{C\,k^2} \qquad (22\cdot25)$$

where

$$k^2 = + \left\{ \frac{(8pt + 4wu + fv)(w - j)f - (wu + 4pt)3we}{12(fv + wu + 2pt)} \right\} \frac{f^3 vw\, E}{C}$$

or

$$k^2 = + \frac{2\,E}{3\,C} w\, j\, tp^3$$

For small bars on wide plates it is better to use the first expression.

T(x) is the applied torque per unit length. In the Glengarnock machine the function T(x) is defined to be:

$$\begin{aligned} T(x) &= 0 && 0 < x < \alpha \\ &= T && \alpha < x < \beta \\ &= 2T && \beta < x < \omega \\ &= 3T && x > \omega \end{aligned}$$

where T is the torque due to the load applied by one ram

acting through the horizontal distance between the shear centre and the line of action of the load, and the rams are placed at distances α, β and ω from mid-span of the specimen.

The solution of equation 22·25 by the usual methods would be difficult because $T(x)$ is discontinuous. The equation would normally have to be solved for each range of x separately and 6 of the 8 arbitrary constants in the solutions would have to be evaluated by using the conditions of continuity at α, β and ω. This is avoided by solving the equation by means of the Laplace transformation, which has remarkable properties for simplifying this type of problem.

Although the solution will apply to both halves of the specimen, the origin was chosen to be at mid-span because the loading was symmetrical about this point. Each half of the specimen may be considered separately and it is convenient from the mathematical point of view to assume that $T(x)$ is zero at all points to the left of the origin. (The solution derived for the right hand half of the specimen applies, however, to the left half by symmetry). It is assumed that θ is sectionally continuous in every finite interval in the range $x \geqslant 0$ and that θ is of exponential order as $x \to \infty$. (As in most engineering problems these assumptions are obviously justified). The Laplace transform of such a function is obtained by multiplying the function by $\exp(-sx)$ and integrating the product with respect to x, from zero to infinity. The transform is then a function of the new variable s. Applying this theory to the differential equation 22·25 it is transformed into the following algebraic equation:

$$s^2.f(s) - s\left[\theta\right]_{x=0} - \left[\frac{d\theta}{dx}\right]_{x=0} - \frac{f(s)}{k^2}$$

$$= - \frac{T}{k^2 C}\left\{\frac{\exp(-\alpha s)}{s} + \frac{\exp(-\beta s)}{s} + \frac{\exp(-\omega s)}{s}\right\} \qquad (22\cdot26)$$

By symmetry, the cross section at $x = 0$ remains plane and hence $\left[\theta\right]_{x=0} = 0$. The value of $\left[d\theta/dx\right]_{x=0}$ is unknown and may be represented by the constant A, the value of which will be found later. Equation 22·26 may then be written:

$$(s^2 - 1/k^2).f(s) = A - \frac{T}{k^2 C}\left\{\frac{\exp(-\alpha s) + \exp(-\beta s) + \exp(-\omega s)}{s}\right\}$$

Or, solving for f(s) and rearranging by means of partial fraction:

$$f(s) = \frac{A}{(s^2 - 1/k^2)}$$

$$\frac{T}{C}\left\{\frac{1}{s} - \frac{s}{(s^2 - 1/k^2)}\right\}\left\{\exp(-\alpha s) + \exp(-\beta s) + \exp(-\omega s)\right\}$$

(22·27)

The function f(s) is the Laplace transform of $\theta(x)$ and the value of the latter is given by the inverse transform of equation 22·27, which may be found by the methods described in refs. M3 and M4.

It is:

$$\theta = Ak \sinh(x/k) + \frac{T}{C}\left[1 - \cosh\frac{x-\alpha}{k}\right]_{\alpha}$$

$$+ \frac{T}{C}\left[1 - \cosh\frac{x-\beta}{k}\right]_{\beta} + \frac{T}{C}\left[1 - \cosh\frac{x-\omega}{k}\right]_{\omega}$$

(22·28)

where the terms in square brackets are taken to be zero when the value of x is less than the subscript outside the bracket.

The derivative of equation 22·28 is

$$\frac{d\theta}{dx} = A\cosh(x/k) - \frac{T}{C\,k}\left[\sinh\frac{x-\alpha}{k}\right]_{\alpha}$$

$$- \frac{T}{C\,k}\left[\sinh\frac{x-\beta}{k}\right]_{\beta} - \frac{T}{C\,k}\left[\sinh\frac{x-\omega}{k}\right]_{\omega}$$

(22·29)

Hence, at mid-span (i.e: when $x = 0$)

$$\frac{d^2\phi}{dx^2} = \frac{d\theta}{dx} = A$$

It may now be seen that equations 22·7 to 22·14 can be used to find the stresses at mid-span, which are associated with twisting. The determination of the constant A from the remaining boundary condition will be discussed shortly.

The angle of twist of the specimen with respect to the section at mid-span was obtained by integrating equation 22·28 or by dividing its Laplace transform, equation 22·27, by s and finding the inverse transform.

$$\phi = k^2 A\left\{\cosh(x/k) - 1\right\} + \frac{T}{C}\left[(x-\alpha) - k\sinh\frac{x-\alpha}{k}\right]_{\alpha} + \frac{T}{C}\left[(x-\beta) - k\sinh\frac{x-\beta}{k}\right]_{\beta} + \frac{T}{C}\left[(x-\omega) - k\sinh\frac{x-\omega}{k}\right]_{\omega} \qquad (22\cdot30)$$

The angle of twist at the end of the specimen with respect to mid-span was found by putting $x = L/2$ in this equation. This is equivalent to the angle of twist at mid-span with respect to the ends of the specimen.

The constant A may be evaluated by using the boundary condition at $x = L/2$ (where L is the length of specimen between end structures). There are two cases to consider:

i) If the ends of the specimen are not free to warp the boundary condition is $\theta = 0$ when $x = L/2$. Substituting in equation 22·28 it was found that

$$A = -\frac{T}{k\,C}\left\{\frac{3 - \cosh\frac{L/2-\alpha}{k} - \cosh\frac{L/2-\beta}{k} - \cosh\frac{L/2-\omega}{k}}{\sinh(L/2k)}\right\} \qquad (22\cdot31)$$

ii) If the ends of the specimen are free to warp the boundary condition is $d\theta/dx = 0$ when $x = L/2$. Substituting in equation 22·29 it was found that

$$A = + \frac{T}{k\,C}\left\{\frac{\sinh \frac{L/2 - \alpha}{k} + \sinh \frac{L/2 - \beta}{k} + \sinh \frac{L/2 - \omega}{k}}{\cosh (L/2k)}\right\} \qquad (22\cdot32)$$

The actual end conditions are between these two theoretical extremes.

23) Application to Experimental Specimens.

The theory was used to find the distribution of stress over the cross section at mid-span of some of the unsymmetrical specimens. Fig. 14 shows (full lines) the theoretical stresses, plotted on an outline of the cross section of the 12 inch inverted angle bar "I" compared with the stresses measured during tests 86 and 88 (shown by circles). This cross section was chosen as an example because it was the only welded unsymmetrical cross section with ends welded to pads which was tested with loads applied to both clear and stiffener sides of the plate (see Table VIII).

The position of the shear centre was at the point marked "SC" and was found to be 0·94 in. left of the centre line of web (as drawn). The centre of area of the cross section was at the point marked "CG". The loads were applied through push rods equidistant from the web as indicated by the arrows. The theoretical stresses were calculated as described in the previous Section, after finding the bending moment at mid-span on the assumption that the end stiffness was $K_\epsilon = 1{\cdot}0\ E$ ton in. per radian, as shown in fig. 11. The bending moment at mid-span was resolved into components in the directions of the principal axes of the cross section, taking account of the angle of twist at each value of the applied load, and the stresses due to bending were calculated. The theoretical angle of twist at mid-span was 2·25° at 12 tons load (no experimental measurements), and the dotted lines in fig. 14 show the distributions of stress across the flanges at that load due to bending alone. It will be observed that the small change in the angle of the plane of the applied bending moment had an insignificant effect upon the distribution of stress, which agrees well with that calculated in the usual way and quoted in Table XIII.

Without considering twisting, the experimental points show that the stresses in the flanges of the two specimens were greater than those attributable to the calculated bending moment. The experimental values of stress near the neutral axis of the section show little evidence of axial forces on the cross section and it is clear that the actual applied bending moment was greater than the calculated one.

This discrepancy is not easy to account for, but it is probably associated with the fact that the 12 inch inverted angle bar "I" was tested as the middle one of three specimens, the outer two being 10 inch specimens, see Table VII.. Both of the outer specimens had approximately 2/3 of the stiffness of the middle one. It follows that with the same load applied to each specimen the change of slope at the ends of the 12 in. specimen would tend to be less than the changes of slope at the ends of the 10 in. ones. This difference between the changes of slope at the ends of the adjacent specimens would involve a twisting of the horizontal angle bar and associated plating of the end structures to which the specimens were connected, with the result that the constraining moment applied to the 12 in. specimen would be less, and that applied to the 10 in. specimens more, than the calculated values. The result would be an increase in the net bending moment at mid-span of the 12 inch specimen, as observed. (It should be noted that this explanation is purely conjectural. There is no positive experimental evidence for the suggested interaction between the specimens via the end structures. Very early during the period of my research I asked the B.S.R.A. committee which guided the experiments for permission to carry out tests in order to determine the extent of this effect - and others - but the request was rejected. No reason was given).

When the theoretical stresses associated with twisting were added to those due to bending, the theoretical stress distribution shown by full lines in fig. 14 (page 88) was obtained. If the difference discussed in the last paragraph is ignored, the agreement with the experimental stresses is quite good and confirms the validity of the theory described in Section 22. It will be observed, however, that in Test 86 the stresses associated with horizontal bending of the flange due to twisting were less than predicted by theory. On the other hand in Test 88 they were greater. It is suggested that the explanation lies in the fact that in Test 86 the flange of the angle bar was in <u>tension</u> and this would tend to reduce horizontal bending and deflection, whereas in Test 88 the flange was in <u>compression</u> and this would tend to increase horizontal bending and deflection.

Similar results are obtained if the theory is applied to other specimens. It was found that the values of the constant A given by equations 22·31 and 22·32 were almost identical and an average value was used to obtain the stresses. It may be concluded that the end conditions do not affect the stresses at mid-span significantly. When considering bracketed specimens it is sufficiently accurate to take as L the distance between the ends of the brackets, for the purpose of finding the stresses associated with twisting. In some of the tests there were discrepancies between theory and experiment which were not easy to account for theoretically. In particular, an attempt had been made during tests 195 to 247A to reduce the twisting by connecting the plating of the two outer specimens to the inner one (see ref. G7, page 6). Later, during tests 248 to 293 (ref. G8) the stiffeners had been mounted 24 in. apart on a strip of plating 72 in. wide, except three tests - namely 248A, 262A and 276A, in which the specimens were separate as in tests 1 to 194. By a comparison between the results of these tests and the results of tests 248, 262 and 276, in which the plating was continuous it was observed that making the plating continuous reduced the tilt (but did not eliminate it), reduced the deflections, and reduced the stress at the heel of bar and increased it at the toe, as might be expected. Although the stiffnesses

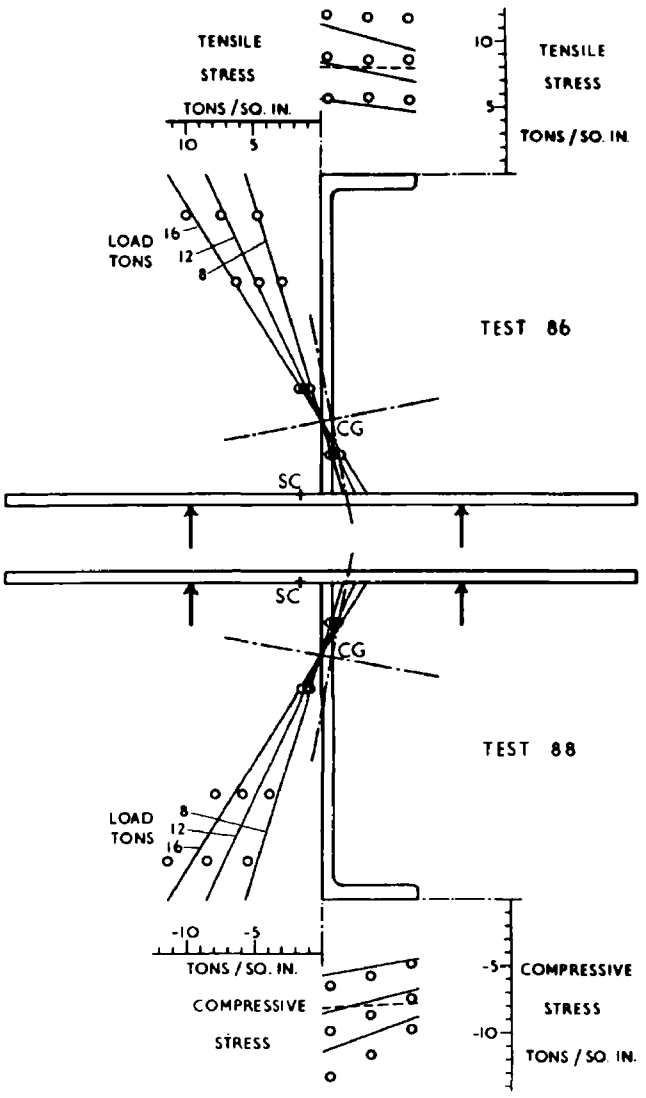

Fig. 14 Bending with twisting of a typical specimen.

Comparison between theoretical and measured stresses across section at mid-span.

of the specimens tested side by side in these tests were almost identical the two outer specimens had one cross section (usually unsymmetrical) whilst the centre one had another (usually symmetrical). This method of testing caused difficulties when an attempt was made to include the results in the present analysis. For example, two 9 inch inverted angle bars "Q" were tested one on each side of the 9 inch tee bar "R", with the plates connected by means of bolted strips. The flanges of the inverted angle bars pointed inwards towards the tee bar, and although the amount of twisting was reduced (not eliminated) some of the load applied to the two outer specimens must have been transferred to the inner one in the process, with consequent changes in the bending moments and deflections.

It may be concluded that the twisting of the specimens could be attributed to the cause described in the previous Section, and that the theory given accounts for the major change in stress distribution provided that the specimen was free to twist as assumed. If the unsymmetrical flange is in compression the twisting is increased, and if it is in tension the twisting is decreased. In general, the twisting and methods adopted to reduce it made the unmodified deflections an unreliable guide to the degree of constraint, but it was found that an estimate could be made of the net bending moment acting at mid-span by taking the bending stress at the flange to be the average of the measured stresses at the heel, and at the centre of the flange. The net bending moment so found could then be used as described on page 59 to find the constraining moments.

In practice where an area of plating is stiffened by a number of parallel unsymmetrical stiffeners, usually the flanges of the bars all point the same way. In this case the twisting will probably be considerably reduced without modification to the bending moments (except near the boundaries of the panel parallel to the stiffeners).

24) Experiments on Specimens with Equal Sided Welded Brackets on Standard Base Structure.

The experiments on specimens with equal sided brackets were the most comprehensive of all the groups tested at Glengarnock. The main reason for this was, ofcourse, that the experiments were designed in the first instance to compare welded with riveted construction and in the latter one is almost bound to fit brackets. The experiments in this category are indicated in Table IX. In this Section only the tests on welded brackets are considered; riveted brackets are discussed in Section 28. The method of analysis of the experiments was that described in Section 20 using equation 20·5. The cross sections of the specimens were constant along their lengths except in way of the brackets and the effective length of brackets was decided in each case by the criterion suggested in Section 18.

It was found that the measured value of end stiffness K_c was approximately 10·0 E tons in./radian for all welded brackets reaching to "adjacent floor" of the end structure. This was the largest group of specimens having the same value of K_c. Four symmetrical specimens having the widest possible range of moments of inertia - F, B, R and Z (see Table VI) - serve to illustrate the validity of equation 20·3 and a comparison between theory and experiment is shown in fig. 15. Using the experimental value K_c = 10.0 E tons in./radian and calculated values of the other quantities, the value of M_c was found for each of these specimens, using equation 20·3, and is indicated by full lines in the middle row of diagrams in fig. 15. These values of M_c were used to find the net bending moments and hence to calculate the stresses and deflections shown by full lines in the upper and lower rows of diagrams. The corresponding experimental values are shown by the circles, those in the middle row of diagrams being bending moments calculated from the flange stresses, plotted from the theoretical bending moment diagram for freely supported ends, in the manner described on page 59. The dotted lines

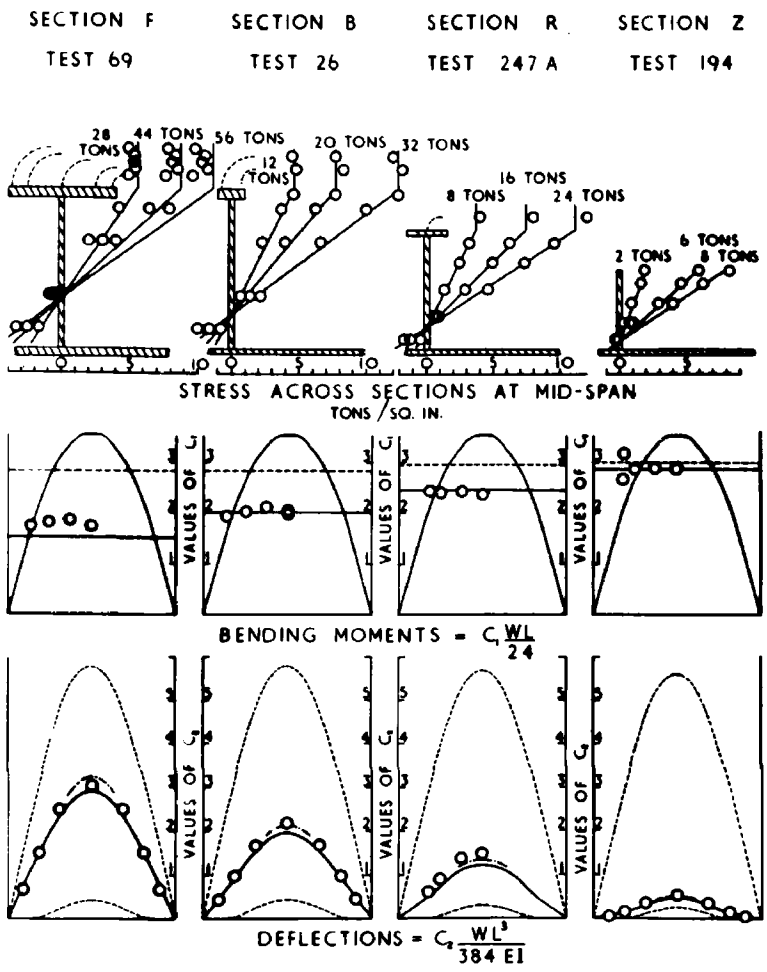

Fig. 15.

indicate bending moments for completely fixed ends, and deflections for for freely supported and completely fixed ends respectively. Although the end structure was the same in each case the end constraint varied considerably as the stiffness of the specimens was altered. The important point is that this was predicted by equation 20·3 and it may be concluded that the equation correctly describes the variations of constraint.

Fig. 15 also gives an indication of the accuracy of the theory of bending when variations of cross section along the length of a beam and of end constraint are taken into account. It is clear that the accuracy is good enough for practical purposes except that the measured deflections were generally slightly more than the theoretical figures associated with bending alone, as shown by full lines in fig. 15, but some of the difference could be accounted for by the addition of the theoretical deflections associated with shear strains in the webs of the stiffeners as indicated by the chain dotted lines. (The discrepancies noticeable in the experiment on section F may be explained partly by the fact that this specimen was tested with specimens C and E (see Table VII) which had considerably different stiffnesses and examination of the diagram of stress

across section F at mid-apan indicated that there was a considerable compressive force along the axis of the specimen.)

It may be concluded that, provided K_E could be calculated from the scantlings of the end structure, equation 20·3 could be used to estimate fairly accurately the constraining moments and hence the stresses and deflections of symmetrical specimens (and also of unsymmetrical ones by means of the theory in Section 22). The possibility of calculating K_E will be discussed in Section 27.

Meanwhile it is of considerable interest to continue to estimate values of K_E from the experimental results so that the various different end structures etc. may be compared. It was found that the values of K_E associated with other bracketed specimens again fell into groups. They varied according to the size of bracket and to the size of angle bar which connected the ends of the brackets to the "adjacent floor" of the end structure. The K_E values appeared to conform to a logical pattern and they are shown graphically in fig. 16.

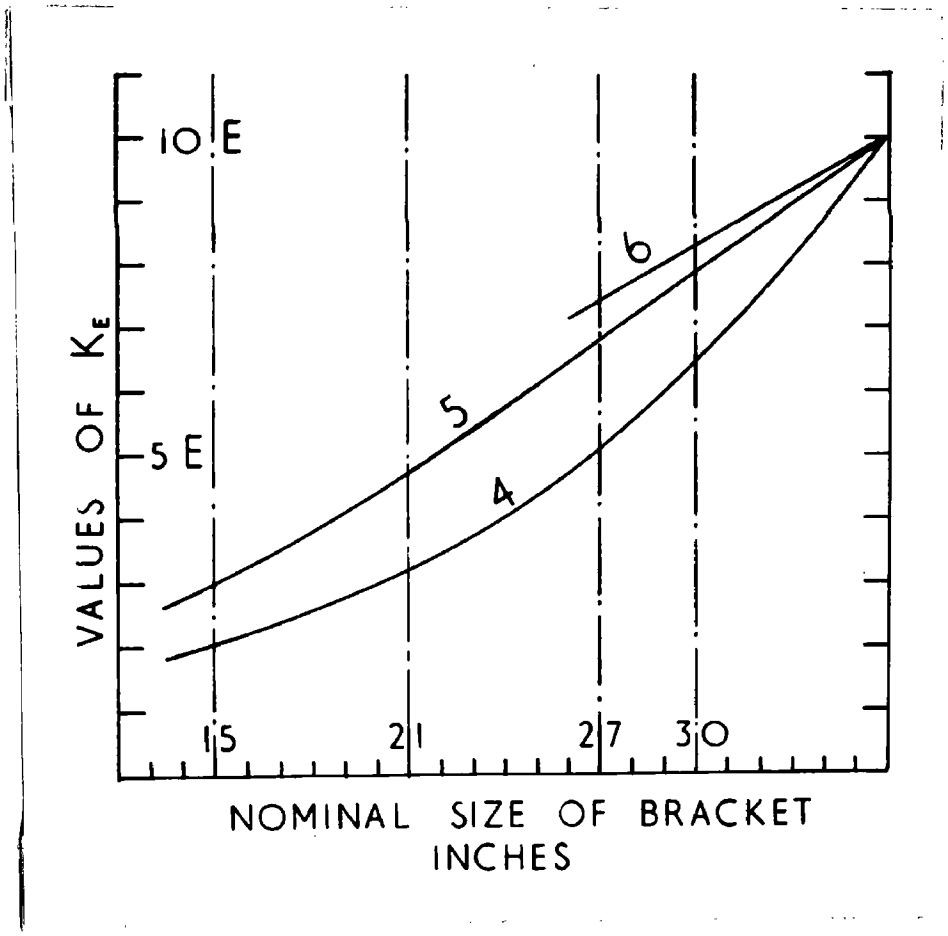

Fig. 16.

Values of stiffness K_E of end structure associated with welded brackets.

Three curves are shown which refer to brackets having 4, 5 and 6 inch bars between the bracket and adjacent floor of the end structure.

25) Experiments on Specimens with Brackets Welded to Reinforced or Weakened Base Structure.

The stiffness of the base structure could be altered as explained by Mr. Jensen in connection with fig. 5 of ref. G5. Only two experiments were carried out with the base struts released at both ends but an analysis of these and the experiments in which the struts were released at one end only, showed that the effect of this modification was not so great as might have been expected.

A larger number of experiments was carried out on specimens attached to ends reinforced by welding and these are shown in Table XI. An analysis of these experiments showed that compared with the end stiffness of the standard base structure (fig. 16), the values of K_ξ were increased by about 50% when the brackets reached to the "adjacent floor" but the increase diminished rapidly as the size of bracket was reduced, being about 25% with 30 inch brackets and only 10% with 27 inch brackets. When 15 inch brackets were fitted there was no significant increase in K_ξ when the base was reinforced.

26) Use of Results of Analysis to Predict Behaviour of Other Specimens in the Glengarnock Machine.

The analysis described above was concerned solely with 16 ft. long specimens which were symmetrical about mid-span, symmetrically loaded, and attached at each end to structures which were identical. The analysis has made it possible to deduce from the experiments, values of stiffness K_ξ of the end structures associated with the various forms of end connection (brackets, pads etc.) and enabled comparisons to be made of their effectiveness in producing end constraint. By means of the theory described in Chapter I of this thesis these results may be used to predict the behaviour of more complex specimens and of other specimens which might be tested. Indeed, within wide limits the behaviour of any welded specimen in the Glengarnock machine acted on by any given form of loading could be estimated.

The Glengarnock testing machine was built so that it could test specimens 8 ft., 16 ft. or 24 ft. long. So far it has only been used for specimens 16 ft. long and the analysis has been concerned with these alone. With the values of stiffness of end structure deduced, however, equation 20·3 may be used to find the theoretical bending moments if specimens of lengths other than 16 ft. were tested. It will be noted that if the length of specimen is increased, keeping the same structural arrangements at its ends, the ratio M_A/M_F will be increased but M_F decreased (and vice versa), see figs. 9 and 10.

If aluminium specimens were tested, equation 20·3 could be used to predict the results (due regard being paid to the different Young's modulus), provided that the end connections were made of steel. If the end connections were of aluminium, this would alter the stiffness of the end structure in a manner which would have to be determined. If the whole of the end structures were made of aluminium the equation could be used as before.

Equation 20·3 could also be used to find the bending moments acting in specimens with any other form of loading (e.g: uniform load, concentrated loads etc.), the only restriction being that the loads must be arranged symmetrically about mid-span, and that the ends must be structurally identical. If these conditions are not fulfilled it is necessary to use the more general theory described in Chapter I. There were only a few experiments carried out at Glengarnock in which the conditions mentioned were not fulfilled; these were concerned with specimens in which the end structure at one end differed from that at the other. To illustrate the application of the theory in Chapter I together with the results of the analysis described above, two examples have been chosen. In one of these, test 199, the specimen had a constant cross section throughout its length and the theory of Section 3 could be applied. In the other example, test 129, there was a bracket at one end but not at the other, and it was necessary to use the more complex theory of Sections 9 and 11.

The first example chosen was test 199, in which the 9 in. channel bar (P) was loaded with one end welded to a pad on the end structure while the other had a welded extension piece fitted. Thus the specimen was of constant cross section throughout its length but was connected to end structures which differed in stiffness:

Stiffness K_L at left hand end (Welded lugs - see fig. 11) = 0·34 E ton in./radian.

Stiffness K_R at right hand end (Welded extension piece - see Table XIV) = 7·5 E tons in./radian.

Moment of Inertia I of cross section (Table VI) = 139.8 $in.^4$

Hence

$$c_L = 0·1045 \qquad c_R = 0·720$$

For a specimen which had uniform cross section the bending moment required for complete end fixity was

$$M_F = 2·342 \frac{WL}{24}$$

Substitution into equations 3·4 and 3·5 of Chapter I of the thesis gave the results:

$$M_L = 0·376 \frac{WL}{24} \qquad M_R = 2·505 \frac{WL}{24}$$

Fig. 17A shows the theoretical bending moment coefficient C_1 of the equation

$$M = C_1 \frac{WL}{24}$$

The bending moments associated with the load applied to the beam assuming freely supported ends and with end constraint are shown separately, the latter being represented by a straight line.

Fig. 17 A.

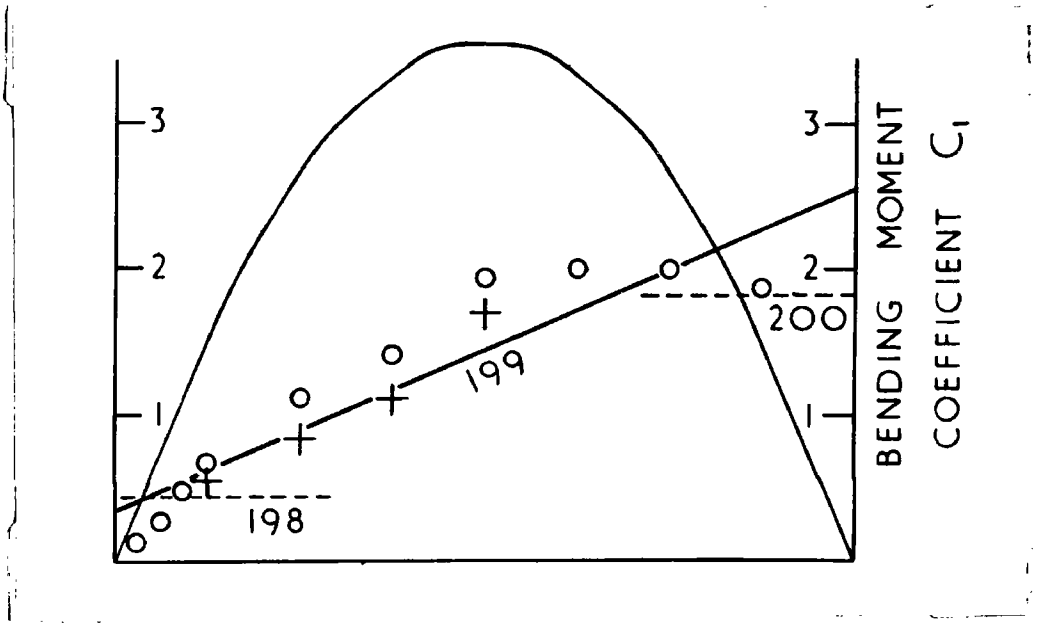

The measured bending moments acting in experiment 199 were first computed from the mean lines through graphs of load as abscissae and the "mean stress across flange" quoted in ref. G7, as ordinates. These were plotted so that their distances from the free bending moment line were equal to scale to the net bending moments and are shown in fig. 17 A as circles. One would expect these points to lie on a straight line which would represent the experimental bending moments associated with constraint. In fact the circles lie on a curved line. This can only be accounted for by the possibility that the "mean stress across flange" quoted includes part of the effect of twisting;(the cross section was an unsymmetrical one). When the load is not applied at the shear centre, the theory in Section 22 indicates that the bending moment acting at any cross section could be computed with fair accuracy from the mean of the measured stress at the heel of the flange and the measured stress at the middle of the flange. (See fig. 14). Bending moments were computed in this way at sections of the beam where all the readings were available, and were plotted in the same manner as before. These are represented by + symbols in fig. 17 A and it will be seen that they lie approximately on a straight line. The theoretical constraining moment line agrees quite well with the experimental constraining moments found in this way.

A more complex example was test 129 in which the

6 inch bulb plate (X) was attached by a welded pad to the end structure at its right hand end, and by a 27 in. welded bracket to the end structure at its left hand end, which was also reinforced by welding. The stiffnesses of end structures were:

Stiffness K_L at left hand end (27 in. welded bracket - fig. 16 increased 10% to allow for reinforcement, see Section 25) = 5·61 E tons in./radian

Stiffness K_R at right hand end (6 in. welded pad - see fig. 11) = 0·15 E ton in./radian

The moment of inertia I of the cross section clear of the bracket was 38·9 $in.^4$ (see Table VI), and referring to the theory in Sections 9 and 11 of Chapter I it was convenient to tabulate the calculation of a and i as follows:

TABLE XV

Item	E a	Lever about mid-span	E a L	E a L^2	E i
Specimen	4·34	+ 11·5	+ 50	570	10330
Flexibility of right hand end	6·66	+ 96·0	+640	61400	-
Flexibility of left hand end	0·18	- 96·0	- 17	1650	-
Total	11·18	+ 60·1	+673	63620	10330

$$E\,i = 10330 + 63620 - 60{\cdot}1 \times 673$$

Hence

$$a = 11{\cdot}18/E \quad \text{ton}^{-1}\ \text{in.}^{2}$$

$$i = 33450/E \quad \text{ton}^{-1}\ \text{in.}$$

Centroid of 1/EI diagram was 60·1 in. to right of mid-span.

Consider now the diagram of M_s/EI. It was known

from previous work that the area under the M_s diagram, was $0{\cdot}0972\ WL^2$ tons in.^{2} with its centroid at mid-span. When calculating the value of β the bracket at one end had to be accounted for, and this was done by assuming that the specimen was rigid over the effective length 23 inches in way of the bracket. Using the moment of inertia of cross section of the specimen equal to $38{\cdot}9$ in.^{4} along the remainder of the length, it was found that

$$\beta = -\int_{-(L/2-e)/2}^{(L/2-e)/2} \frac{M_s}{E\,I}\,dx = -\frac{11{\cdot}1}{E}\,\frac{WL}{24}$$

The centroid of this diagram was found to be $5{\cdot}1$ in. to the right of mid-span, i.e: $57{\cdot}0$ in. to the left of the centroid of the $1/EI$ diagram.

Equation 9·7 of Chapter I gave the following equation for the constraining moments in Test 129:

$$M_1 = \left[-\frac{11{\cdot}1}{11{\cdot}18} + \frac{(-11{\cdot}1)(-57)}{33450}\,x\right]\frac{WL}{24}$$

$$= (-0{\cdot}992 + 0{\cdot}0189\,x)\,\frac{WL}{24}$$

where x is measured (positive to right) from an origin $60{\cdot}1$ in. to the right of mid-span.

The terms in the bracket correspond to the coefficient C_1 in the equation

$$M_1 = C_1\,\frac{WL}{24}$$

The theoretical bending moments, represented by coefficient C_1, are shown in fig. 17 B. Again the experimental bending moments were plotted from the free bending moment line to give the experimental bending moments associated with end constraint.

The cross section of the specimen was almost symmetrical and little or no twisting was present. The experimental points (shown by + symbols) lie on a straight line as expected. The corresponding theoretical line is rather high and the most probable reason for this was that the estimated stiffness of end structure associated with

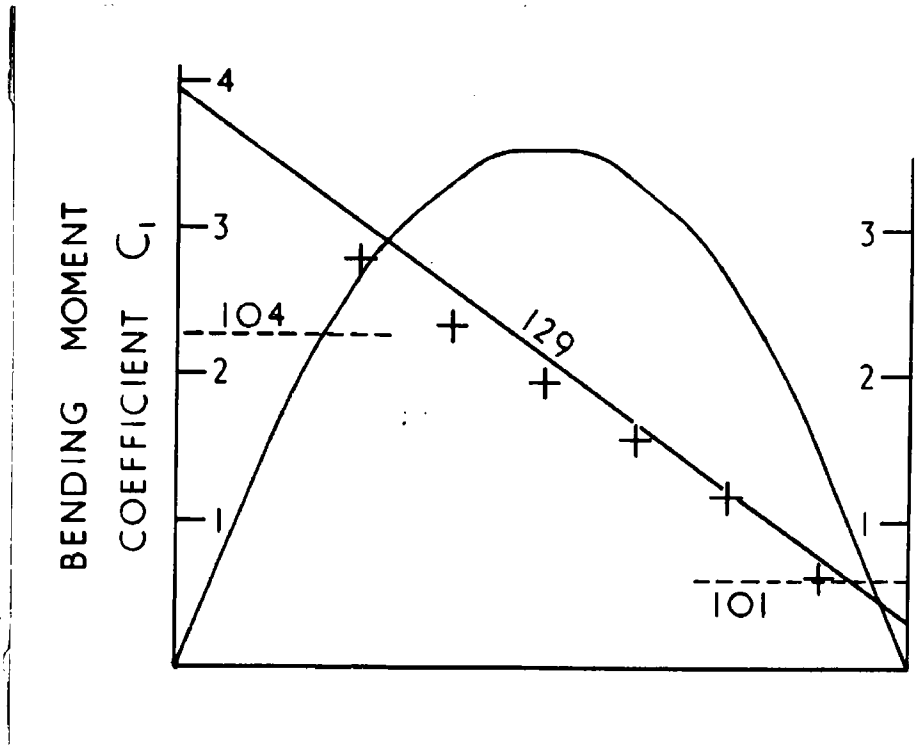

Fig. 17 B.

the 27 in. bracket was slightly too great.

In figs. 17 the theoretical constraining moments for the experiments in which both ends had equal stiffness are indicated by dotted lines. It will be observed that the common shipyard practice of joining the constraining moment thus found for one end of the beam, to the constraining moment found similarly for the other end, in order to find the constraining moment line for the intermediate case (as suggested in ref. X5 for example), gives incorrect results.

27) Calculation of Stiffness of the End Structures from the Scantlings.

It has been shown that the behaviour of the specimens can be accounted for by the theory described, but values of K_E were found experimentally. In order to calculate theoretically the constraint of beams in practice it would be necessary to estimate the values of stiffness K_E by consideration of the scantlings of the end structure. The complexity of the end structure, coupled with the lack of experimental evidence about its behaviour, rendered this task very difficult. This Section is a record of an attempt to estimate the stiffness of the end structures in the Glengarnock machine from first principles. It was assumed that the stiffness was derived from structure in the immediate vicinity of the ends of the specimens and that the form of end connection played a major part in determining the structural action. The estimated values of stiffness are compared with those found experimentally.

It was apparent that the stiffness of the end structure when the ends of the specimen were welded to pads, was derived

from a complicated action which involved bending of the plating of the end structure. Calculation of this was likely to lead to some difficult mathematics and the attempt to do so was abandoned. It is suggested that the experimental values in fig. 11 would serve as a useful guide for the estimation of values of K_ϵ in practice because it seems most unlikely that the stiffness arises from any action other than the local bending of the plate.

The calculation of end stiffness when the end structure was fitted with welded extension pieces was then attempted. It was assumed that any increase in stiffness of end structure above that associated with ends welded to pads, was derived from resistance of the end extensions to bending. The plating associated with the extension pieces was very wide compared with the dimensions of the stiffener and it was to be expected that there would be shear lag in the plate. Referring to fig. 7 of the Appendix to this thesis, however, it was clear that if the problem were to be solved by a Fourier series method the effective breadth of plating would be not more than 0·36 x (length of extension piece). If this breadth were used the moment of inertia so found would be the maximum which could occur and stiffnesses of end structure rather greater than the actual ones would be calculated.

Considering the 6 inch flat bar (Z) and using this criterion for the effective breadth of plate it was found that the stiffness was approximately 3·0 E tons in./radian, if the remote ends of the extension pieces were freely supported. To this value must be added the stiffness found for ends welded to pads only: 0·15 E tons in./radian. Comparing this theoretical figure with that found from experiments 160 and 189, viz: 2·25 E tons in./radian, it may be concluded that assumptions upon which the calculations were based yield results which are rather too large, as expected. (This conclusion was supported by similar results from an analysis of experiments 163 and 190 in which the ends of the 6 inch flat bar (Z) were constrained by "long lugs".) In experiments 160 and 189 the specimen was quite heavily constrained (M_e/M_p = 0·88) and the variation of stiffness of the end structure did not affect the stresses as much as it would if the constraint were less, so that this method could possibly be used in practice with sufficient accuracy in some cases. The stress at 6 tons load calculated using the value of end stiffness estimated theoretically was 12·4 tons/in^2 at the edge of the flat bar at mid-span, and the measured stresses at the same place in experiment 160 were between - 12·6 and - 13·7 tons/in^2 (measured on both sides of the bar) and in experiment 189 about 11·8 tons/in^2.

A similar calculation to that described in the last paragraph was carried out for the 6 in. bulb angle specimen (W) but comparison with results of experiment 142 showed that the calculated value of end stiffness was far too low. Reference to Table VII showed that the bulb angle specimen was tested between the flat bar on one side and the angle bar on the other. Examination of the diagram in ref. G5 showing the structure of this test, and a comparison with fig. 3 of ref. G1, showed that whereas the extension pieces of the outer specimens extended to the back plate of the end structure, the extension pieces of the middle specimen were welded to a diaphragm plate so that the extension pieces were about half as long as those fitted to the outer specimens. Using this shorter length a revised stiffness of end structure was calculated on the assumption

that the coefficient of constraint $c = 0{\cdot}5$ at the end of the extension piece welded to the heavy diaphragm. The calculated stresses were then very near the experimental ones; because of the high end constraint this again was not a very good check of the theory.

An attempt to apply the same theory to experiments 200 and 219, on sections P and H respectively (see Table VI), failed. The calculated stresses were too low. Analysis of the experimental figures showed that the end stiffness in experiment 219 was approximately one third of the calculated value. It is suggested that the discrepancy was not due entirely to the assumption of too great an effective breadth of plate in the end structure but might be accounted for either by shear in the webs of the short deep extension pieces or by relative deflections of the end structures at the ends of the extension pieces, or both. Unfortunately both the experiments in question were carried out on unsymmetrical specimens and the distribution of stresses across the flanges was far from uniform so that accurate comparison was impossible. In view of this the matter was not pursued further.

The majority of specimens were tested with a bracket which either reached to the bulb angle called the "adjacent floor" of the end structure, or was connected to it by a short angle bar or flat bar. When the bracket reached the "adjacent floor" it seemed reasonable to assume that the bracket acted as a rigid plate and that when load was applied to the specimen rotation of the bracket as a unit was resisted by a horizontal force, associated with deflection of the "adjacent floor", acting through a lever arm L_1. When the bracket did not reach to the "adjacent floor" but was connected to it by a short bar, the bracket would rotate an additional amount due to flexibility of the bar.

Let the load which would be required to cause unit deflection of the "adjacent floor" in way of the bracket be k tons /inch deflection, and let the distance between the "adjacent floor" and the point about which the bracket rotates be L_1 inches. Then the angle through which a rigid bracket reaching to the "adjacent floor" would rotate under a moment M is given by:

$$\theta_1 = \frac{M}{kL_1^2}$$

If a smaller bracket, of effective length b, is fitted and its toe is connected to the "adjacent floor" by a bar, there is an additional rotation because of flexure of the bar. It was assumed that the end of the bar was freely supported at the "adjacent floor" and that the moment of inertia of the cross section of the bar and associated plating was I_1 in.^{4} Then a little consideration on the lines indicated in Section 8 (I) of Chapter I of this thesis, showed that if the additional rotation of the bracket was θ_2 radians, under the same applied moment:

$$M = \frac{3\,EI_1L_1^2}{(L_1 - b)^3}\,\theta_2$$

Hence

$$\theta_1 + \theta_2 = \frac{M}{kL_1^2} + \frac{(L - b)^3 M}{3 EI_1 L_1^2}$$

This may be rearranged to give the following theoretical expression for the stiffness of end structure when a welded bracket is fitted at the end of a specimen:

$$K_\epsilon = \frac{M}{\theta_1 + \theta_2}$$

$$= \frac{k L_1^2}{1 + \frac{(L_1 - b)^3 k}{3 E I_1}} \qquad (27{\cdot}1)$$

To use this equation it was necessary to estimate values of k, L_1 , and I_1 . Examination of fig. 3 of ref. G1, showed that the value of k must depend considerably on the behaviour of the bulb angle and the short struts which comprise the structure of the "adjacent floor", and the work described in Section 25 had shown that a small amount of welded reinforcement had a very significant effect. It was therefore unlikely that any calculation of the deflection per unit load applied by the toe of the bracket would be successful. In view of this it was decided to take the value of the end stiffness of a bracket reaching to the "adjacent floor" to be that found experimentally in Section 24 and to deduce from this the value of k for the "adjacent floor" of the standard base structure of the Glengarnock machine.

i.e: $k L_1^2 = 10 E$

The point about which the bracket rotated must be very near to the plate of the specimen and as a first approximation the point of rotation was assumed to be at the level of the top of the plate, so that L_1 = 36 inches. Then equation 27·1 becomes:

$$K_\epsilon = \frac{10 E}{1 + \frac{(36 - b)^3}{389 I_1}} \text{ tons in./radian} \qquad (27{\cdot}2)$$

A difficulty now arose about the magnitude of I_t. The breadth of plate was so large that shear lag could not be neglected, but the shear lag theory in the Appendix did not deal with a beam which had a large part of its length rigid in way of a bracket. Referring to fig. 7 of the Appendix, however, it was clear that if the problem were to be solved by a Fourier series method the effective breadth of plating would be not more than 0·36 (L_1 - b). The magnitude of I_t calculated assuming this breadth of plate to be effective would be the upper bound of I_t and stiffnesses calculated using this value of I_t would be rather greater than the actual stiffnesses. Using this criterion for effective breadth of plate, values of I_t were found for each size of bracket connecting bar and equation 27·2 was then solved to find theoretical values of K_ε. The calculations were carried out for all sizes of brackets from 12 in. to 36 in., with 4 in., 5 in., and 6 in. bars connecting them to the "adjacent floor". The theoretical values of K_ε are shown by the full lines in fig. 18. The corresponding results deduced from the experiments were shown in fig. 16, and are repeated in fig. 18 as dotted lines. (The theoretical and experimental values were identical when the brackets reached to the "adjacent floor" because this was one of the assumptions upon which the theory was based).

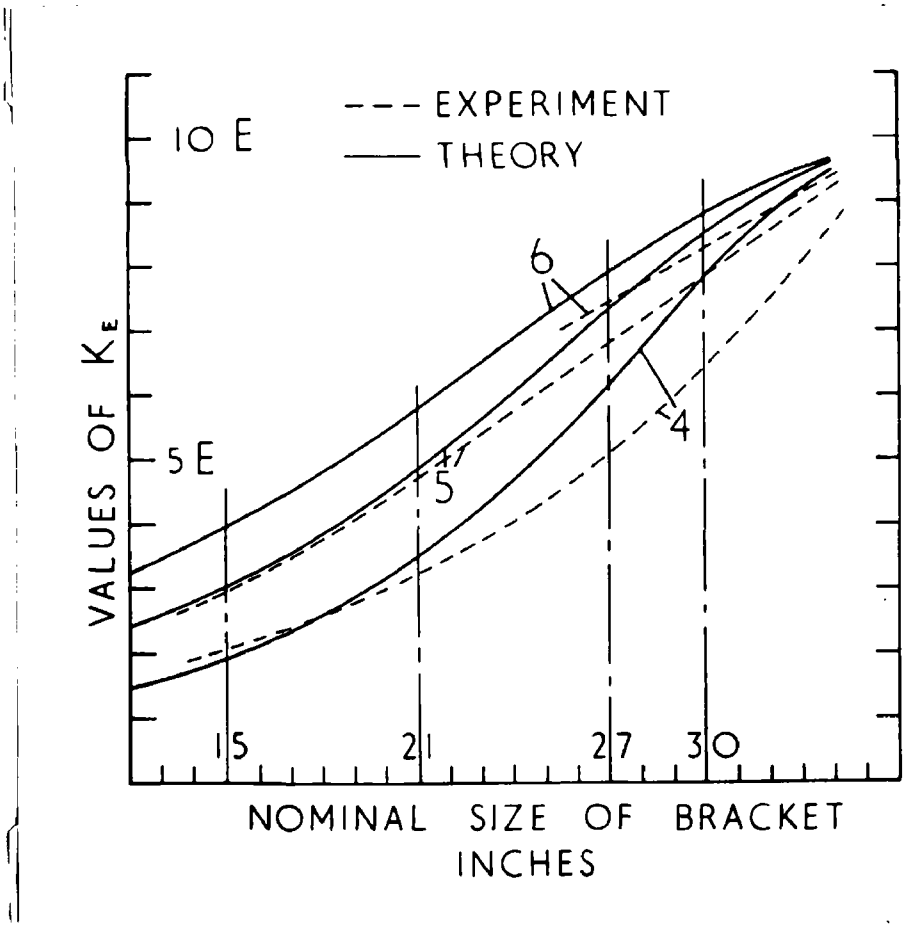

Fig. 18.

There is a remarkable similarity between the general character of the theoretical and experimental curves and agreement is particularly good when the smaller brackets are considered. The theoretical values of K_ε were always greater than the experimental ones as was anticipated when making the assumption regarding the effective breadth of

TABLE XVI.

COMPARISON OF THEORETICAL STRESSES AND DEFLECTIONS WITH THOSE MEASURED DURING TESTS ON SPECIMENS WITH WELDED BRACKETS.

Test No.	Nominal size of Bracket (in.)	Flange Stresses (tons/in.²) Theory	Measured H	Measured M	Measured T	Deflections (inches) Theory	Deflections (inches) Measured
Section H.		12 x 3 x 3 x 0·46/0·60 Channel bar.				Load 24 tons.	
227	35	7·7	7·9	6·8	6·0	0·216	0·245
225	27	8·6	8·4	7·7	6·5	0·243	0·273
223	21	9·6	9·7	8·6	7·3	0·284	0·285
221	15	10·9	9·9	9·8	9·8	0·330	0·360
Section P.		9 x 3 x 3 x 0·32/0·44 Channel bar.				Load 12 tons.	
213	35	5·6	6·2	5·4	4·5	0·161	0·172
210	27	6·8	7·5	6·7	6·1	0·206	0·212
207	21	8·0	9·3	8·0	7·0	0·255	0·246
203	15	9·45	11·2	9·6	9·3	0·318	0·352
Section Z.		6 x 0·45 Flat bar.				Load 6 tons.	
194	35	5·9	5·8	5·8		0·143	0·159
167				- 6·3			0·151
193	27	7·65		7·7		0·214	0·237
166				- 8·2			0·227
192	21	9·45		9·6		0·309	0·324
165				- 9·9			0·321
191	15	12·6		12·0		0·487	0·466
				- 12·0			0·445

plate for calculating I_t. The error was largest with 30 in. brackets and was as much as 20% in the case where the bracket was connected to the "adjacent floor" by a 4 inch bar. Even in this case, however, reference to fig. 10 showed that the maximum error in the ratio M_c/M_e would be only 10%. The error is probably due largely to the assumption of too great an effective breadth of plating, but it is possible that deflection of the bar itself due to shear deformation in addition to bending, also played its part in reducing the stiffness of the actual end structure.

An estimate of the accuracy of equation 27·2 by comparison with the experimental results may be obtained by considering Table XVI (page 102) in which the theoretical and measured stresses and deflections are side by side for experiments in which bracket size was varied from 35 in. to 15 in. As usual the measured stresses and deflections were plotted on a base of load, and mean lines drawn through the points obtained. The experimental values quoted were read from the mean lines at the load stated. The theoretical values of K_e were calculated from equation 27·2, and the theoretical stresses and deflections were calculated after finding the constraining moments from equation 20·3. Deflections associated with shear deformation of the webs of the stiffeners have been included. Note that sections H and P were channel bars and (as indicated in Section 23) they twisted when loaded so that measured deflections were increased and the stresses across their flanges were not uniform. H, M and T in Table XVI indicate heel, middle and toe, of the flange. Note also that the theoretical values were found entirely by calculation except the value of k which had to be estimated from experiments on specimens with brackets reaching to the "adjacent floor" of the end structure. It may be concluded that when brackets are fitted the stiffness of an end structure similar to that of the Glengarnock machine could be calculated with fair accuracy provided that an estimate could be made of the deflection per unit load of the structure to which the toe of the bracket was attached.

A general conclusion from the work described in this Section was that the stiffness of end structure could be calculated by using the theory described in Chapter I of this thesis, provided that the members within the end structure were not so short compared with their other dimensions that deformations due to shear strains became comparable with those due to bending.

28) Experiments on Specimens with Riveted End Connections.

In Chapter I it was assumed in Section 10, which dealt with flexible connections, that riveted joints would behave elastically. The experiments at Glengarnock on specimens with riveted brackets show that this assumption was fully justified. Fig. 19 (page 104) shows typical graphs of deflection measured during a series of experiments on the 9 inch channel bar (P) when attached to the standard end structure by 21 in. brackets. In test 204 each arm of the unflanged bracket was connected by four 3/4 inch diam. rivets. In test 205 the number of rivets was increased to seven and in test 206 a 3 in. flange was added to the brackets. It will be observed that in all cases deflection was proportional to applied load.

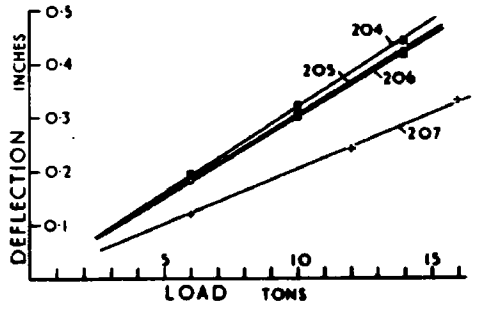

Fig. 19.

The increase in number of rivets caused a small decrease in deflections whereas the effect of adding flanges to the brackets was only slight. In test 207 the brackets were welded to both the specimen and the end structures and the decrease of deflection, corresponding to an increase in constraining moment, was substantial. It is clear that the additional flexibility associated with riveting must be taken into account in the analysis of the experiments in which this method of connection was used. To apply the theory described in Chapter I it seems reasonable to assume that most of the flexibility of the joints occurred near the toes of a bracket, because the rivets there experienced much higher forces than those near its heel. It was postulated, therefore, that there would be two regions of increased flexibility, one of which would result in a reduced stiffness K_{ER} of end structure, and the other could be allowed for by assuming additional flexibility F_B of the specimen near the toe of each bracket. It was assumed that the centre of the flexibility F_B associated with each bracket was located at the end of the length e over which the bracket was assumed to be rigid (see Section 18). An equation for the constraining moment similar to that derived in Section 20 could then be found as follows. As before the basic equation is:

$$M_c = \frac{\beta}{a}$$

In the case of a specimen with riveted connections to brackets at each end:

$$\beta = -\left\{ \int_{-(l/2-e)}^{l/2-e} \frac{M_s}{E\,I}\,dx + 2\,M_{sB}F_B \right\}$$

The first term in the brackets is the same as for a welded specimen and represents change of slope associated with the bending of the specimen. The second term represents the changes of slope at the toes of the two brackets, due to the flexibility of the riveted connections acted upon by the bending moments M_{sB} at distance e from the ends of the

specimen (the bending moment at this position being that which is associated with the load applied to the specimen on the assumption of simple supports at its ends).

The equation for a must also be modified to take account of the flexibility of the riveted connections, and it becomes:

$$a = \frac{L - 2e}{EI} + 2F_{ER} + 2F_B$$

Again the first term on the right hand side is associated with the bending flexibility of the specimen itself and is the same as for welded specimens. The second term represents the flexibility of the end structures (modified by the inclusion of the more flexible riveted connection to the bracket.). The last term takes account of the flexibility of the riveted connections between the toes of the brackets and the specimen.

The equation for the indeterminate bending moment M_c associated with end constraint may therefore be written:

$$M_c = - \frac{\left\{ \int_{(\frac{L}{2}-e)}^{\frac{L}{2}-e} \frac{M_s}{EI}\, dx + 2 M_{sB} F_B \right\}}{\frac{L - 2e}{EI} + 2F_{ER} + 2F_B} \qquad (28{\cdot}1)$$

Values can be calculated or estimated from results of any chosen experiment, for all the terms in this equation except F_{ER} and F_B. There are two unknowns, but only one equation. This difficulty could have been overcome if the step from the entirely riveted bracket to the entirely welded bracket had been made in two stages. For example, the connection between brackets and end structures could be welded first. The results of an intermediate test could then be used to find F_B on the assumption that the stiffness (or its reciprocal, the flexibility) of end structure was the same as for the all-welded specimens analysed in previous Sections. Alternatively, the connections between brackets and specimen could be welded first and the stiffness K_{ER} of the end structure with riveted bracket could be estimated by the methods described in previous Sections. In either case the welding of the bracket could then be completed to make an all-welded specimen. Unfortunately however, throughout the whole series of experiments welded specimens were converted from entirely riveted specimens in <u>one</u> step - by welding both arms of the brackets. An analysis of the type envisaged in this paragraph was therefore impossible.

An attempt was made to circumvent this difficulty by analysing the results of two tests simultaneously thus obtaining two independent estimates of the required quantities in equation 28·1, and

solving the resulting two simultaneous equations to obtain F_{ER} and F_B. The number of tests to which even this technique could be applied was found to be extremely limited because there were very few specimens which had identical riveted connections and end structures. A trial with specimens with equal sided riveted brackets (Table XI) soon demonstrated that the two simultaneous equations obtained from the results of two tests on specimens with nearly equal stiffness were "ill conditioned" and gave poor results. The 6 in., 9 in. and 12 in. specimens were connected by brackets to 4 in., 5 in. and 6 in. angle bars respectively in the end structures, so that identical end structures were only to be found when 35 in. brackets were fitted (in which case the size of angle bar probably did not matter). For the purpose of analysis, the following specimens with 35 in. riveted brackets were chosen:

12 in.	channel bar	H	Test 226
9 in.	channel bar	P	Test 212
6 in.	bulb angle	W	Tests 148 and 175

Using the average of the results of the tests on the 6 in. specimens, three equations were obtained. These were solved in pairs, yielding three values of each of F_{ER} and F_B, given in Table XVII.

TABLE XVII

Equations solved	F_B (radian/ton in.)	F_{ER} (radian/ton in.)	K_{ER} (ton in./radian)
H and P	0·46/E	0·128/E	7·8 E
H and W	0·27/E	0·13 /E	7·7 E
P and W	0·12/E	0·185/E	5·4 E

In the 6 in. and 9 in. specimens the brackets were connected by single rows of rivets, whereas in the 12 in. specimen there were two rows of rivets (reeled). This may account for the higher values obtained for K_{ER} in the solution of the two sets of equations which included the results from the 12 in. specimen. It should also be observed that in the equation obtained from test 226 the net bending moment in the region of the toe of the bracket was nearly zero so that the value of F_B had little effect on the result. In fact if F_B was assumed to be zero in this case, the equation associated with test 226 could be solved directly and it was found that K_{ER} = 7·5 E.

Summing up, it seems to be likely that if a 35 in.

riveted bracket with a single row of 3/4 in. dia. rivets is substituted for a 35 in. welded bracket, the stiffness of the standard end structure will be halved and in addition the flexibility of the riveted joint between the bracket and specimen is approximately 0·12/E radian/ton in. If the riveted bracket is connected by a double row of rivets (reeled), the stiffness of end structure will be reduced to about three quarters of the value it would have if the bracket was welded. The bending moment acting in the specimen near the toe of the bracket was too small to allow an estimate to be made of the flexibility of the riveted joint there.

The broad conclusion is, however, that no analysis of the type applied to welded specimens can be made of the experiments on specimens with riveted brackets. It is fortunate (from the point of view of practical usefulness of the analysis) that welded construction has long since proved its superiority over riveted construction, so that the need for comparison has disappeared.

29) Experiments on Specimens with Unequal Sided Welded Brackets on Standard Base Structure.

During tests to discover the optimum size of bracket (Table X) an apparently anomalous result was observed, viz: an increase in size of bracket did not necessarily result in a decrease in stress (Ref. G7, page 9). Although they were looking for the size of bracket which involved the least stress at mid-span, the investigators were surprised at this result and counçilled caution in accepting it until they had carried out further experiments. They need not have been surprised, however, because the result might have been anticipated theoretically. Table XVIII shows the theoretical effect on stress in a typical specimen, of increasing the size of brackets reaching to "adjacent floor" of the end structure. It will be noticed that as the effective length of bracket along the specimen was increased, the ratio M_c/M_F was decreased while M_F was increased. The relative rates of decrease and increase of these controlled the variation of constraining moment M_c and hence of stress. The latter reached a minimum in the case considered when the effective length of bracket was about 45 inches, (compare with fig. 2 of Ref. G7). It cannot be expected that the use of the idea of an effective length of bracket as defined in Section 18, would yield accurate results with brackets of the shape considered here but the general trend found in the experiments is reflected in the theoretical results. In the tests, the brackets smaller than 35 inches did not reach to the "adjacent floor" of the end structure and these had values of K_E less that 10·0 E ; the constraint was considerably less than with brackets of the same size along the specimen but reaching to the "adjacent floor" and the measured stresses are correspondingly higher (See Table XVI). Therefore, when the actual size of bracket was increased, the stress was rapidly reduced until a bracket reaching to the "adjacent floor" was fitted. After this the stiffness of the ends remained the same and further increases in size of bracket served only to stiffen the specimen, with the results shown in Table XVIII.

TABLE XVIII

EFFECT ON STRESSES OF INCREASING THE SIZE OF BRACKET REACHING TO THE "ADJACENT FLOOR" OF THE TEST MACHINE

9 inch Channel Stiffener (P). 12 tons load.

$I = 139{\cdot}8$ in.^{4} $I/y = 18{\cdot}5$ in.^{3} $K_E = 10{\cdot}0\ E$ tons in./radian

$M_F = 337{\cdot}5$ tons in. at mid-span for freely supported ends.

Effective length of bracket (in.)	$\frac{M_c}{M_F}$	M_F (tons in.)	M_c (tons in.)	Stress at mid-span. (tons/in.^{2})
12 *	0·858	251·0	215·4	6·60
24 *	0·836	273·8	228·7	5·87
36	0·811	293·7	238·1	5·37
48	0·774	309·3	239·5	5·30
60	0·720	321·0	231·3	5·74
72	0·631	331·3	209·0	6·94

* Denotes theoretical brackets reaching to "adjacent floor" but having no practical counterpart of this size in the experiments.

Before leaving this Section it should be noted that there seems to be little practical application for the work described. If a 12 inch channel bar with 35 inch equal sided brackets was fitted instead of the 9 inch channel bar with 64 inch brackets, it would occupy less space and reduce the maximum stress (at mid-span) by approximately 30 % (compare test 215 with test 227), and a similar substitution could be made in other cases where these unusual brackets were tested.

30) Observations on Some Additional Experiments.

When a long series of experiments such as those under consideration was undertaken, it was inevitable that a number of tests would be made which did not fit into the general pattern of the research, but which nevertheless, were related to it. During the Glengarnock experiments several auxiliary tests of this nature were carried out to find the effects of fitting unusual end connections, and of holes of various shapes in the stiffeners. Some tests were carried on until the specimens collapsed; it is a pity that there were not more of these. During the work described in previous Sections, the results of these additional tests were examined along with the rest, and some general observations on them are made in this Section. These observations may not be valid outside the range of loads applied to the specimens.

Several of the tests were concerned with different forms of end connection. Curved brackets were about as effective as straight ones (ref. G2). Brackets could be replaced by angle bars reaching to the "adjacent floor" (e.g: tests 58, 60) but this arrangement was improved if the end of the stiffener was also attached to a small bracket (e.g: tests 126, 127). The overall behaviour of brackets within the range of loads applied was not significantly affected by fitting them with flanges, but the latter reduced the stresses at the outer edges of the brackets and would probably help to prevent premature failure by buckling of the bracket. Specimens in which the ends of the stiffeners were not attached to the end structures experienced very little end constraint. Those in which the end of the stiffener was also snaped so that the angle between the snaped edge and the plating to which the stiffener was attached was less than 45°, experienced higher stresses locally at the snaped edge than at mid-span. (It may be noted in passing that when the ends of the stiffeners are free the force applied to the specimens must be reacted by shearing forces at the ends, which are carried by the plating alone). When the ends of a specimen were connected to the end structures by gussets (horizontal brackets) the constraint was little greater than if the end of the stiffener had been welded directly to the plating of the end structure without a bracket.

A small hole drilled in the flange of an inverted angle bar or channel bar (e.g: tests 87B, 90B, 119) had no significant effect on the overall behaviour of the specimen, within the range of loads applied, but caused a local stress concentration in the flange comparable to that which would be experienced by a flat bar in tension with a similar hole.

Scallops cut in the web of a stiffener (ref. G8) increased the stresses in the specimen, when tested at low loads, to the negligibly small extent which would be expected if the properties (I, I/y) of the cross section were calculated in the usual way, taking account of the material removed, but the decreased area of web caused an increase in deflections associated with shear strains in the web. Provided that sufficient material remained between the scallops to resist the shearing forces in the vicinity of the neutral axis of the cross section it appeared that their effect was negligible at low loads. Scallops may, however, cause premature failure of the specimen. The latter occurred when the loads were increased in test 293 and it is remarkable that, whereas in the

elastic range the specimen tended to twist in one direction, it finally failed by deformation in the opposite direction. This apparent anomally seems to have puzzled the investigators, but a likely explanation is as follows. Imagine the cross section of the specimen with plate at bottom and inverted angle above it with flange pointing to the right. The shear centre is to the left of the web and load applied vertically upwards in the plane of the web causes the specimen to twist in a counter clockwise sense. The twisting causes the flange to be bent to the left and it resists this action and applies to the web a force acting to the right. In addition to this the whole section is bent upwards and the flange of the bar is in tension; because the specimen is bent there are vertical components of the tension in the flange and these act to pull it downwards. Thus the forces in the flange act upon the top of the web so that it is pulled to the right and given a clockwise turning moment. Both of these tend to bend the web so that it would deform concave to the right. The web is thus acting as a cantilever and the vertical bending stresses are greatest at its joint with with the plate. Very little material is left between the scallops to resist this bending moment and the yield point of the material is soon reached as load is increased. Deformation of the web concave to the right rapidly increases when the material between the scallops yields and the specimen collapses by gross deformation of the cross section to the final form shown in fig. 1 of ref. G8.

31) Summary of Major Conclusions.

1) The ordinary theory of bending may be used to calculate the behaviour of structural members of ships in the testing machine at Glengarnock, within the elastic range of the material, provided that attention is paid to the following:

a) Variations of moment of inertia of cross section along the length of a beam must be taken into account when finding changes of slope, deflections etc: In particular, where brackets are fitted the beam in way of them may be considered to be rigid over most of the length of the bracket (e.g: over the effective length defined in Section 18, page 60).

b) The degree of constraint afforded by the structure to which the beam is attached must be estimated. This may be done with the aid of the theory described in Chapter I of this thesis, (provided that none of the structural members of the end structure is so short that deformations due to shear strains become comparable with those due to bending).

c) If the cross section of the beam is not symmetrical about the plane in which the loads are applied, the beam will twist (unless the load is applied through the shear centre of an unsymmetrical cross section). The stresses and deflections associated with torsion must be added to those due to bending. This effect is more serious when the load is applied on the

stiffener side, than when it is applied on the clear side of the plate.

d) Riveted connections are much less efficient than welded ones and in riveted construction the flexibility of the riveted joints must be taken into account. (It was not found to be possible, however, to estimate the flexibility of riveted joints from the results of the Glengarnock experiments).

2) In the range of specimens tested at Glengarnock a number of unimportant departures from results predicted by the ordinary theory of bending (used as in 1 above) were noted. It was thought that these were associated with the following:

a) Tension, and sometimes compression, acting along the length of a specimen, associated with restraint of the ends of a specimen by the end structures. (This was largest in bracketed specimens, probably because of displacement of the reactions at the end structures).

b) Deflections due to shear deformation in the webs of stiffeners.

c) Interaction between specimens tested side by side.

d) Deflection of plating due to loads applied to it, causing deformation of the cross section and hence changes of its bending stiffness.

e) Shear lag in the plating.

3) The amount of constraint at the ends of a beam depends upon the rotational stiffness of the end structures relative to the bending stiffness of the beam itself. To achieve a high degree of constraint the end of the beam must be anchored to a firm foundation by a stiff connecting member. One of these conditions alone is not enough.

4) The experimental values of end stiffness found in the analysis may be used together with equation 20·3 to compare the relative merits of the various sizes and types of end connections. Extension pieces provide a particularly neat method of achieving comparatively high end constraint and they have the advantage that they do not take up so much room as a bracket. On the other hand the magnitude of the constraining moment which can be achieved with extension pieces is limited, because it cannot be greater than M_F found when $e = 0$ (see for example fig. 9). By fitting a bracket it is possible to increase M_F, and if by this means the stiffness of end structure can also be made large compared with that of the stiffener, it is possible to achieve very high

constraining moments, and small deflections, (an example of which is test 194 shown in fig. 15). The fitting of large brackets is not necessarily a good thing, however, and it is often possible to design a bracketless specimen which is as strong even if it is less constrained at its ends, and which is lighter and takes up less room than its bracketed counterpart.

CHAPTER IV

EXPERIMENTS IN A SHIPYARD ON A TYPICAL BULKHEAD STIFFENER.

32) Introduction

It has been shown that the theory of bending, used as described, can account for the major phenomena observed in the Glengarnock experiments. There was some doubt about the applicability of these results to ships, however, because it seemed to be unlikely that the end structure of the Glengarnock machine could accurately represent the whole possible range of actual ship structures. For this reason it had originally been intended to include in the research described here, a series of experiments on a variety of actual ship structures in order to determine the range of end stiffnesses encountered in practice. It was found that this project was too ambitious and the attempt had to be abandoned.

Two experiments were carried out, however, at the shipyard of Messrs. Alex. Stephen and Sons, of Linthouse, during the summer of 1950, the first year of the three-year research period. Advantage was taken of routine tests on the deep tanks during the construction of two sister ships built to Lloyd's requirements; strain and deflection measurements were attempted on one selected stiffener of the bulkhead between the deep fuel tank and the engine room. It is the purpose of this chapter to describe some of the difficulties encountered, and to discuss the results of the second experiment during which some strain measurements and a reliable set of deflections were obtained.

33) Water-proofing of Strain Gauges.

The majority of stiffeners on the boundary bulkheads of ship tanks are within the tanks and are immersed during tests on the bulkheads, which are carried out by filling the tanks with water. Electric resistance strain gauges were the only available means of measuring remotely strains in the stiffeners, and to do so they had to be waterproofed. Preliminary experiments were carried out in the James Watt Engineering Laboratories. There appeared to be two methods: either to build a water-tight box around each gauge or to cover each gauge with an impermeable material. The first alternative was disregarded because it was considered that it would be most difficult to ensure water-tightness of any temporary hollow object stuck to steel under water pressure, and also because the presence of a substantial structure around the gauge might interfere with the stress distribution in the stiffener.

A small test beam submersible in a few inches of water was made, Teddington (British Thermostat) strain gauges were affixed and known changes of bending moment were applied. After a little perseverance readings accurate to $\pm$ 0·1 ton/in^2 were obtained (gauges dry) over

a period of several days. Several organisations were consulted and a number of experiments were carried out with various water-proofing substances. The following conclusions were drawn from these experiments:

a) Durofix (recommended by N. P. L. as the best adhesive for the strain gauges) does not adhere to steel in the presence of water.

b) Water-proofing substances having solvents stronger than acetone (the solvent of Durofix) tended to cause disintegration of the gauges as the solvent attacked the bonding.

c) Synthetic resins which require heat treatment were attractive (Catalin Ltd. recommended their Resin 999B which required 150° C for 35 minutes to set) but adequate heating and temperature control on board ship would be difficult and was beyond my capacity.

d) Synthetic resins which may be applied in the plastic state and set after addition of an (acid) accelerator could not be used because the acid appeared to attack the fine wires of the gauges.

e) Di Jell 171 (the substance universally used for damp proofing these gauges) was not completely water-proof after a short period of total immersion in water, but provided a good general protective covering and was easy to apply.

f) The most usual indication of the commencement of breakdown in the water-proofing was a steady movement of the point of balance of the Wheatstone bridge used for the measurements.

g) The procedure described in ref. W3 was too elaborate for this particular purpose.

A method recommended by the Royal Naval Scientific Service gave satisfactory results over several days and was finally adopted. This consisted of allowing the Durofix to set and then applying molten Okerin wax No. 561 up to 1/2 inch thick. The application of wax was comparatively simple on a horizontal surface, but to apply it to a vertical surface (e.g: bulkhead stiffener) was not so easy. The successful technique was to heat a soldering iron and to hold it touching the steel above the gauge. A stick of wax was allowed to melt gradually on to the soldering iron and the molten wax ran down the surface over the gauge where it solidified if not too hot. Considerable time and patience were required to build up a satisfactory coating.

34) First Shipyard Experiment

The first experiment on board ship was carried out on the bulkhead of an oil fuel bunker amidships in a cargo liner being built by Messrs. Alex. Stephen and Sons. The stiffener selected was a 6 x 3 inch inverted angle bar welded to the bulkhead inside the bunker - see

fig. 20A. The test head was about 25 feet above the top of the stiffener, which was 19 feet high and was continuous over three spans between top and bottom of bunker and two horizontal girders. Nine active strain gauges were stuck on the flange of the stiffener and each was accompanied by a dummy gauge for temperature compensation. These were connected by four-core cables, through a specially erected stand pipe, to measuring apparatus on the upper deck. (The top of the pipe was just higher than the test head and this obviated the necessity for water-tight glands). A deflection datum bar was made and knife edge brackets fabricated and welded outside the tank opposite the test stiffener.*

The strain gauges were affixed to the stiffener in the normal way but the weather was exceptionally wet and condensation in the tank over night prevented adhesion. The gauges were re-affixed and this time remained firm, after which they were allowed to dry out for three days and were then waterproofed. The filling and emptying of the tank were very slow operations and the gauges were immersed for about five days. There was a continuous apparent change of resistance of the gauges throughout the test, similar to that mentioned in f of Section 33 above, and it was not possible to obtain any strain readings. A good set of deflection readings was obtained but it was suspected that the datum bar had been accidentally moved during the test. After the test the gauge water-proofing was found to have been ineffective, partly because of damp enclosed by the water-proofing initially, and partly because of the entry of water along the holes in the wax where the wires entered. Many men were working in the tank until the last moment before test and although most of them gave me every consideration and assistance there were many strangers, particularly during the night, to whom I could not speak personally. At least two of the nine gauge positions were accidentally damaged by pulling the wires but the damage was not evident until the water-proofing was removed after the test.

---

*

This experiment would not have been possible without the magnificent co-operation which I received from all quarters. When I first approached the shipyard I found that the only suitable tank test for many weeks was due to start 15 days later, whereas I had no strain gauges or other apparatus immediately available. Within a few days (my diary shows) I was able to borrow strain apparatus from Lloyd's Register of Shipping, who also supplied strain gauges (which I later replaced), and Dr. J. Small of the Electrical Engineering Dept. of the University found a local firm who were able to supply 200 yards of four-core cable. The shipyard placed at my disposal one of their technicians who worked like a Trojan. With his aid, and the blessing of the ship manager, the gauge positions were prepared and the gauges stuck and water-proofed. The cable pipe (which passed through three decks) and deflection datum bar etc. were made and erected for me. Although the tank test commenced one day ahead of schedule, all these preliminaries were completed in time.

35) Second Shipyard Experiment.

The second experiment was carried out in the same shipyard on an identical stiffener in a sister ship of the one mentioned above. Much more time was available, and also construction of the ship itself was further advanced so that the intensity of other work was less than before. Previous experience had shown that natural drying out of the strain gauges was unsatisfactory; it was necessary to ensure that the gauges were absolutely dry before applying the water-proof material. Two 1000 watt fires were arranged to heat the gauges as they dried, one fire being employed at each gauge position. The gauges were affixed as early as possible in the day and heated, gradually increasing the air temperature to about 50° to 60° C late in the afternoon. (An initial low temperature avoids boiling the acetone solvent in the glue and creating bubbles in it). The gauges should reach full sensitivity after 24 hour's drying at normal temperatures, but experiments had shown that full sensitivity could be attained in about 6 hours by careful application of heat. The water-proof covering of wax was applied as late as possible but this had to be done before evening because the fires conld not be left burning all night. It was not found to be possible to build up a coating of wax greater than 1/8 inch thick in the time available and the protection was completed with Di Jell 171 which was gently heated to melting point during application. It was possible to complete two gauge positions per day in this manner, all wiring being arranged and soldering completed while the gauges were drying out. By good fortune no gauges were damaged, mainly because only a few workmen were in the tank and there was no night shift, so that I was able to explain to all what I was trying to do and obtain their co-operation.

The strain readings obtained during the second test were much better than the first, but gauges on the lower span and all but one on the middle span showed evidence of deterioration of the insulation (later confirmed by tests with a Megger) and no steady readings were obtained from them. The gauges on the upper span gave steady readings but the stresses were very small (as might be expected in this region) and one could hot be sure that they were not subject to error.

An examination of the gauges after the tank had been drained showed that the smallest bubble in the wax or the slightest scratch on the surface of the metal was sufficient to allow water under pressure to reach the gauge, but some gauges had failed although neither of these minor defects had been observed. The conclusion was drawn that it was impractical, with the recources at my disposal, to continue work of this nature with reasonable hope of success. It was therefore decided that the experiments should be abandoned in favour of a more profitable line of research.

Deflections were again read during the second test and a good set of readings was obtained. The measurements were made at approximately 9-inch intervals between a datum bar and the bulkhead plate opposite the web of the stiffener. The datum bar was a 3 x 3 inch angle bar suspended from crude knife edges at the top and pressed against a stop at its lower end. The measurements were made by inside micrometer, the advantages of which lay in the accuracy of the instrument used, and the fact that only one was required and no instrument was left in the ship

while measurements were not actually being made. Each set of readings - zero, loaded, and zero - was made twice independently and the figures agreed within 0·005 inch in nearly all cases.

The deflections of the horizontal girders had a very great influence on the deflections of the stiffener. The deflections of the girders, and consequently of the stiffener, in the second ship were about three times as great as the deflections in the first ship although the two structures were identical. The only explanation which can be offered is that the filling and testing of adjacent tanks influenced the deflections of the horizontal girders in the first ship, whereas in the second ship no other tanks in the vicinity contained water, but the suspected movement of the datum bar in the first ship may also have affected the results. Although the stiffeners had unsymmetrical cross sections no twisting was detected. The deflections measured are shown in Table XIX, on page 119.

36) Theoretical Analysis of Results.

Despite the failure to obtain reliable strain measurements, a comparison of the measured deflections with those predicted theoretically is of interest. The deflections of the stiffener were profoundly influenced by the deflections of the two horizontal girders which were supposed to support it. The main interest of the experiments was the degree of constraint at the top and bottom of the stiffener and, because this particular bulkhead presented a particularly difficult case of grillage analysis, it was considered to be sufficient to arrange that the theoretical deflected form of the stiffener would pass through two points at the heights of the two girders, at deflections from zero equal to the measured deflections of the girders at those two positions. With this premise, the bending moments and deflections were calculated for three conditions at the ends of the stiffener:

a) Ends completely fixed.

b) Ends partially constrained, as in the ship.

c) Ends simply supported.

The calculations for (a) and (c) were straightforward, but before (b) was started it was necessary to estimate the stiffness of the end structures. The stiffener and the structure in its vicinity are shown in fig. 20A. It was assumed that the constraint was derived only from structure very close to the ends of the stiffener. The double bottom was supported at many points by keel blocks on the building slip and it seemed to be reasonable to assume that the double bottom floor adjacent to the one beneath the bulkhead, would afford a comparatively rigid support for the end of the 3 in. flat bar by which the stiffener bracket was connected to it. Using the method described in Section 27 of Chapter III and by means of equation 27·1 of that Section, the stiffness of the end structure at the lower end of the stiffener was found to be just under 5·2 E tons in./radian. If the deck beam had been rigid the

TABLE XIX

DEFLECTIONS MEASURED IN SECOND SHIPYARD EXPERIMENT.

Distance above inner bottom.	Deflection from zero when load was applied.	Permanent deflection after load was removed.	Difference.
Inches	Inches / 1000	Inches / 1000	Inches / 1000
221	16	- 2	18
210	31	0	31
202	55	0	55
193	65	4	61
183·5	79	5	74
174·5	92	12	80
165·5	94	5	89
156	109	3	106
147·25	143	18	125
138·5	173	25	148
129·5	189	22	167
120	201	23	178
111·5	196	23	173
102·5	177	25	152
93·75	158	31	127
84	132	18	114
74·5	130	32	98
65·5	122	21	101
38·5	80	- 4	84
29·5	59	12	47
21·5	30	1	29

stiffness of the structure at the top of the stiffener would have had this value also, but it was necessary to allow for deflection of the deck beam. The beam ran across the ends of brackets of a number of identical stiffeners spaced 25 in. apart, but 50 in. on each side of the top of the test stiffener there were heavy longitudinal deck girders. It was assumed that the deck beam was fixed at these two girders and its deflection under equal loads applied to it by the three stiffener brackets between the girders was estimated. The stiffness K_E at the top of the stiffener was then calculated by use of equation 27·1 of Chapter III and was found to be slightly more than 4·0 E tons in·/radian. (The stiffeners of the bulkhead above the deck did not coincide with those on the test bulkhead and were left out of account in this calculation). Using these values of end stiffness the bending moments acting on the test stiffener were estimated by making a calculation similar to that described in Example 3 of Chapter I. It was assumed that shear lag was negligible and the deflections were adjusted so that, in way of the two horizontal girders, they were equal to those measured at these two positions during the second experiment.

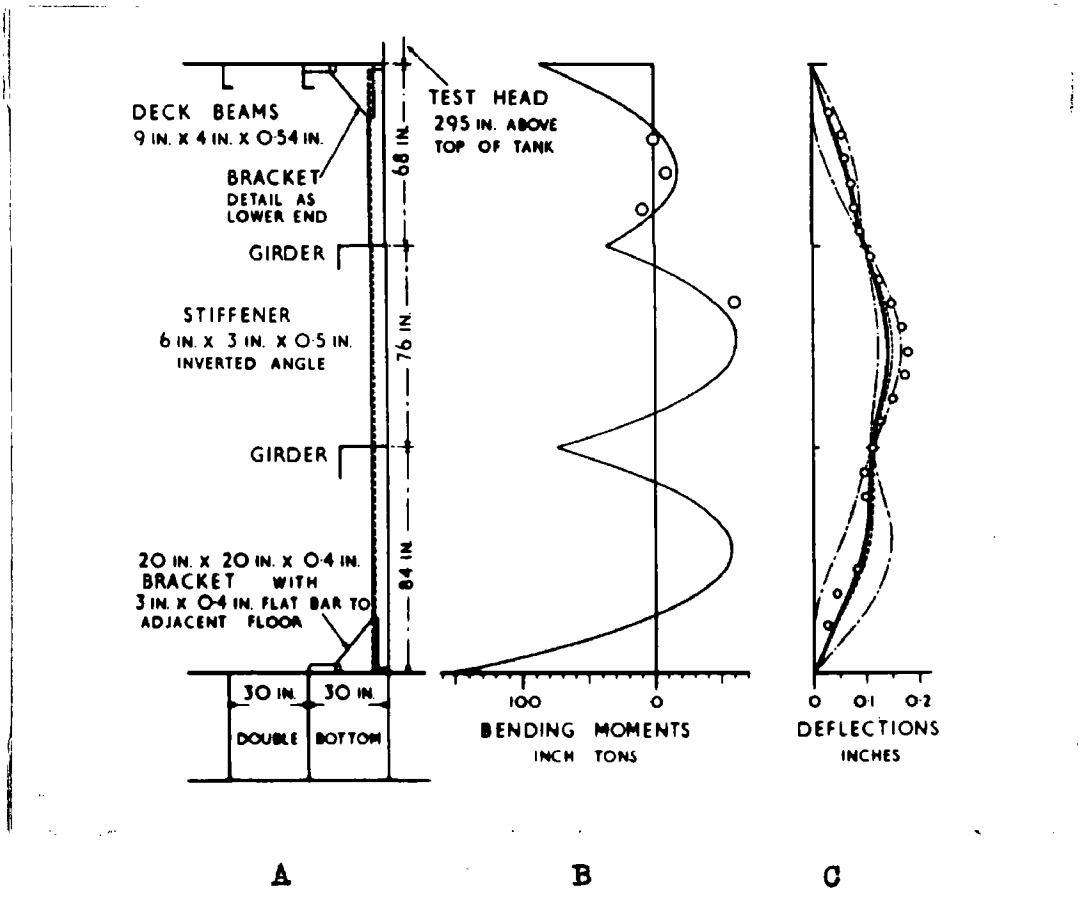

Fig. 20. Comparison between maasured and calculated bending moments and deflections - Second Shipyard experiment.

Fig. 20 B shows the calculated bending moment diagram for the partially constrained stiffener. The full line in fig. 20 C shows the corresponding deflections and the two chain dotted lines indicate the deflections for freely supported, and completely fixed ends. The circles in fig. 20 B represent bending moments calculated from the

stresses measured during the second experiment, but what agreement there is may be coincidental in view of the failure of other gauges lower on the stiffener. The deflections were more reliable and those measured during the second experiment are indicated by circles in fig. 20 C. The test load was, ofcourse, the first to be applied to the bulkhead and when it was removed there was some permanent set, although the maximum stresses were of the order of 5 tons/in^2. Following the Glengarnock practice, (see Section 18), the permanent deflections were deducted from those measured at maximum load and the differences so found are the deflections represented by circles in fig. 20 C.

At the top of the stiffener the measured and theoretical slopes of the bracket agree well and correlation between deflections over the upper span of the stiffener is quite good. At the lower end of the stiffener the actual constraining moment applied was evidently greater than that calculated on the basis of the assumptions mentioned above. The most probable explanation is that the weight of water acting on the inner bottom of the ship caused a change of slope at the lower end of the stiffener in the direction indicated by the experimental results. This could be accounted for theoretically as described in Example 1 of Chapter I but in this case the calculation would probably have to be concerned with the whole bottom structure of the ship in this vicinity treated as a grillage and some allowance would have to be made for the building blocks beneath the ship.

The deflections of the centre span of the stiffener were considerably greater than those to be expected from theory, but clearly the cause of this did not lie in errors in the estimates of constraint at the upper and lower ends of the stiffener. Additional deflections associated with shear deformation of the web of the stiffener only increased the theoretical deflections to those indicated by the dotted lines, and hence were not responsible for the discrepancy either. It was thought that possibly shear lag in the vicinity of the concentrated reactions in way of the two horizontal girders might have caused weakness of the stiffener in these regions. If this was so there would be a decrease in the constraining moments at each end of the centre span, which would involve larger deflections of the latter. An investigation of the effect of shear lag on bending moments in a continuous beam of similar proportions was carried out and is described in Section 16 of Chapter II. In this example the supports did not deflect at all and consequently the two centre reactions (corresponding to the horizontal girders in the ship) were considerably greater than in the ship and shear lag effects in the example would be greater than in the ship stiffener. The example clearly showed that shear lag was not responsible for the increased deflections. A possible explanation is that the axial load applied to the top of the stiffeners by the weight of structure above the bulkhead, caused an increase in deflections so that they were greater than those caused by water pressure alone, but this hypothesis could not be checked.

The measured permanent deflections (See Table XIX) indicate a weakness in the design. They are apparently associated with yielding of the main bulkhead plating in way of the slots cut in the horizontal girders to allow the stiffener to pass through. This could have been avoided by making some other connection between them.

CHAPTER V

ANALYSIS OF BEAMS IN SHIPS BY THE PLASTIC BENDING THEORY.

37) Introduction.

Although elastic analysis of the structures discussed in previous chapters was to a large extent successful, a number of difficulties have been noted particularly in Chapter IV. The plastic bending theory, originally introduced by Baker after the Steel Structures Committee of the 1930's had failed to reconcile elastic analysis of steel building frames with experiments (ref. X4), has now been extended to many fields of application (ref. L8) and has found wide acceptance in some of them. A natural question is whether this method would prove successful when applied to ships. The case for the application of plastic design theory in shipbuilding was forcibly put by Baker himself in 1951 (ref. L4). In fact the shipbuilder has no quarrel with the general philosophy and the design of columns and of riveted joints are examples of structural components of ships the strengths of which have, for many years, been based on the limiting loads which the components could sustain without failure. (The American term "limit design" seems more appropriate here than "plastic design"). It is the purpose of this chapter to examine more fully some of the problems which arise.

The first two chapters of this thesis were concerned with two special problems in the elastic bending theory which arise in shipbuilding, viz: the constraint at the ends of beams and, in panels of stiffened plating, the effectiveness of the plate as a flange of the stiffeners. Similar problems must be solved in order to apply the plastic design theory to structural components of ships.

38) Plastic Collapse of Partially Constrained Beams.

In his 1951 paper (ref. L4) Baker referred to beams which were partially constrained at the ends, saying ".... lack of complete fixity which makes nonsense of exact elastic analysis has no effect on the collapse load of the structure so long as the ends of the beams are so attached to the abutments that the full plastic moment of the section can be developed." He supported this statement with results of some experiments on partially constrained beams and said ".... these tests form a conclusive demonstration that the degree of stiffness of connexions has no effect on the collapse load of a structure." It is necessary to examine the application of this conclusion more closely and to find under what conditions the qualification at the end of the first statement quoted is applicable.

The plastic design theory is concerned with loads rather than deflections, but the criterion of failure is that small load increases above the critical value would produce much larger deflections than lower loads. To examine the effect of end constraint on the plastic collapse of beams an investigation was made of the relationship between deflections at mid-span and loads from zero to ultimate collapse in three possible cases. The results of the calculations are shown in fig. 21.

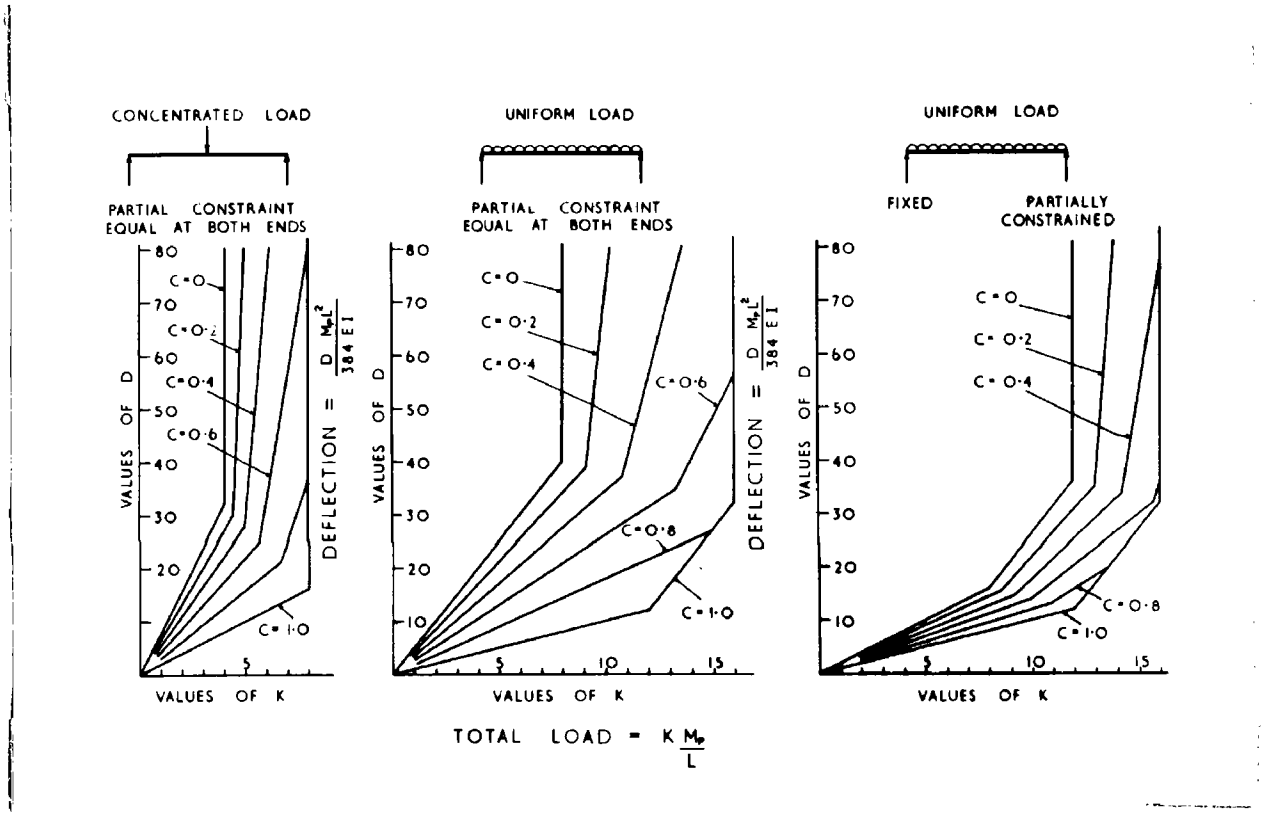

Fig. 21. Relation between Deflection and Load for Partially Constrained Beams.

The diagrams all have similar characteristics and using them as a basis, Baker's first statement quoted may be re-worded and expressed quantitatively as follows: "When the plastic design theory is used to calculate the ultimate collapse load of partially constrained beams, it may be assumed that the full plastic moment will be developed at each end of the beam and that large deflections will not occur before final collapse, provided that the coefficients of constraint at each end of the beam are greater than 0·5 approximately." Thus when the plastic design theory is applied it is necessary to estimate the coefficients of constraint at the boundary of the loaded part of the structure in exactly the same manner as in elastic analysis. In a great many cases it will be found that the coefficient of constraint is greater than 0·5 and for the purposes of plastic design these beams may be treated as completely fixed at the ends. If the coefficient at one end of a beam is less than about 0·5 it is necessary to examine the deflections reached just prior to collapse and for this purpose the simple method described by Symonds and Neal (ref. L5) can

be used. Although it is usually assumed that the construction of steel frames used in civil engineering is such that the coefficient is more than 0·5, the analysis of the results of the practical tests carried out at Glengarnock showed that this is not always the case in shipbuilding, and recent work by Roderick (ref. L7) showed that when stanchions are considered the constraint may be very important in civil engineering also.

It is difficult to estimate the positions at which plastic hinges will form in a curved member under loads applied in its own plane, and it may be noted in passing that the theory described in Section 9 may be used for this purpose. The usual elastic analysis would be carried out first and the position of the first plastic hinge can then be found from a knowledge of the properties of cross sections and the combined bending moments and direct forces acting. (The latter are important in curved members and must be taken into account). The additional load which may be withstood after the first plastic hinge has been formed can be calculated by means of a further "elastic" analysis in which the plastic hinge already formed is treated as a semi-rigid joint which has infinite flexibility. This leads to the position of the second plastic hinge. A similar calculation may be performed to find the further additional load before the third hinge forms and the position of the latter. The member is then statically determinate for the purpose of further analysis and the additional load it can withstand before final collapse as a mechanism may easily be determined. Once the properties of the $1/EI$ diagram have been calculated as described in Chapter I partial constraint may be taken into account, and little extra work is involved in the additional calculations.

39) Plastic Bending of Stiffened Plating.

The plastic theory of bending was developed originally for use in civil engineering and the cross sections normally considered have two axes of symmetry. Tee bar or flat bar stiffeners with wide plate flanges have only one axis of symmetry, however, and the plastic modulus of these will now be considered. The following analysis is based on the usual assumptions and idealization of the stress/strain diagram for mild steel. Almost without exception, the cross sectional area of plating associated with one stiffener in bending is greater than the sectional area of the stiffener alone and in what follows it will be assumed that this is so.

During elastic bending of the cross section the highest stress is at the fibres remote from the plate, because the neutral axis is near the plate. As the bending moment is increased the material at the extreme fibres of the stiffener will yield. Considering, for example, a tee bar stiffener, first the material in the table of the tee bar will become plastic and the stress over the whole of the table will be equal to the yield stress of the material. Then the plastic zone will extend down the web until the whole of this sustains the yield stress too. Meanwhile the stress in the plate is increased, but is still below the yield stress provided that the area of plate is greater than that of the stiffener. This may be proved by considering the equilibrium of the forces acting in the material of the cross section. If p_y is the yield stress of the

material it is clear that the direct force F_s acting over the cross sectional area A of the stiffener alone is:

$$F_s = A\, p_y$$

But for equilibrium, the sum of all the forces acting over the cross section must be zero, so that the direct force in the plating must be equal (but opposite in sense) to F_s and is given by:

$$F_p = 2bt\, p_p = -F_s$$

where p_p is the stress in the plate. Hence

$$p_p = -\frac{A}{2bt} p_y \qquad (39{\cdot}1)$$

Since it was assumed that $2bt > A$ the stress in the plate must be numerically less than the yield stress..

The two equal and opposite forces form a couple $Ah\, p_y$ which, (since bending stiffness of the plate may, as usual, be considered to be negligible), is equal to the moment of resistance of the section and, ofcourse, to the applied bending moment. This moment of resistance can only be increased if the two forces or the distance between them can be increased. But this cannot be done because the whole of the material in the stiffener has reached the yield point, and hence the limiting plastic moment is:

$$M_p = Ah\, p_y \qquad (39{\cdot}2)$$

The plastic modulus of beams which consist of symmetrical bars used as stiffeners of plating (under the conditions mentioned above) is given by:

$$Z_p = Ah \qquad \text{provided } 2bt > A \qquad (39{\cdot}3)$$

The ratio of the plastic modulus to the elastic modulus, known as the shape factor, for stiffened plating of the type discussed above is rather larger than the corresponding ratio in civil engineering in many cases.

40) Application to Shipbuilding.

The application of the plastic theory of bending to ship structural members would be advantageous (as opposed to the elastic theory) from the points of view both of simplicity of application and of the more rational criterion of strength. On the other hand there are serious

objections to its use in some circumstances.

It is very doubtful whether unsymmetrical stiffeners (e.g: the inverted angle bars or channel bars commonly used in merchant ships) could be made to behave in accordance with the idealized plastic theory used above. As was demonstrated in Chapter III, stiffeners of these shapes have a tendency to twist as well as bend under load, and they would fail by lateral "tripping" long before the full plastic modulus was developed unless special precautions were taken to prevent them doing so. It is clear that it will not be possible to apply plastic design methods until the shipbuilding industry can be supplied with an adequate range of rolled sections which are relatively free from this defect by reason of being symmetrical or nearly symmetrical.

There are many structural problems in shipbuilding, however, for which the use of plastic design methods would be unwise even if lateral instability could be avoided. Many parts of a ship sustain reversible loads, for example the inter-tank bulkhead analysed in Example 1 of Chapter I may be subjected to loads on either side, and elastic analysis would be required to ensure that no plastic hinge could form under normal working of the ship. (If plastic hinges were permitted to form under loads of opposite sense alternately, failure could occur after only a few cycles of load). In other cases elastic analysis must be used even when loading is normally in one direction only, because if a plastic hinge formed this would spoil the shape or appearance of the ship; the structures analysed in Examples 3 and 4 of Chapter I are typical of this.

CHAPTER VI

EPILOGUE

41) Review of Research.

The modern designer of structures has the choice of two general methods of deciding the strength of beams. He may either base his design on the ultimate collapse load calculated by means of the theory of plastic bending, or he may use an analysis based on the theory of elastic bending and keep the working stresses below a limit known from experience to be safe. The former method is more rational because the factor of safety against failure can be estimated whereas in the latter it is less well defined. The application of the plastic bending theory to shipbuilding was discussed briefly in Chapter V (page 123) but before it could be generally adopted shipbuilders would require experimental evidence of its applicability to ships. This would involve the loading of structures to failure, the cost of which could only be born by a large research organisation. Moreover, as discussed in Section 40 (page 126) there are many circumstances in the structural design of ships in which recourse must be had to elastic analysis. For these reasons the main body of the thesis was concerned with the elastic theory of bending which is in general use today.

The main purpose of the research was to decide which of the many possible variations of the elastic theory of flexure are important in practical shipbuilding. The research has shown that the use of the ordinary theory as described in the elementary textbooks (as is usual in shipyards), would rarely give accurate results in the design of the structural members of ships. Of the many possible reasons for this only a few are important, and the theories which deal with these aspects of the bending of beams have been extended and modified to make them more suitable for use in naval architecture. Departures from the usual theory of flexure which need to be taken into account are: the constraint at the ends of the loaded structural members (and the flexibility of riveted connections, if any), variations of the cross sections of the beams along their length, twisting of beams having unsymmetrical cross sections and, in very short members only, modifications of the bending theory associated with shearing strains. The main experimental evidence upon which these conclusions are based was an analysis of the extensive tests carried out by the shipbuilding research organisations at Glengarnock (See Chapter III, page 53). In addition an experiment was carried out in a shipyard and although this revealed difficulties which were not encountered in the Glengarnock work, it lent support to the conclusions at the end of Chapter III (See page 110).

The elementary teaching of strength of beams is usually confined to straight uniform beams, the ends of which are either completely fixed or freely supported. By far the most important modification which is required when applying the theory in shipbuilding is to take account of the actual degree of constraint at the ends of the beams. The first chapter of the thesis was devoted to an exposition of a new theory for taking account of partial constraint, which is simple to understand and

just as easy to apply as the corresponding theories which do not include the effects of constraint. The experiments discussed in the third and fourth chapters amply justify the basic assumptions of the theory and it is shown that quite an accurate estimate may be made of the constraint in practice, provided that the theory of flexure is applied correctly to all parts of the structure. In most cases the constraint may be estimated by considering no more than the structure in the immediate vicinity of the end of the beam. The theory may be applied to all welded types of beams met in shipbuilding, but where riveted connections are used further research would be required to determine the flexibility of the joints (See Section 28, page 103).

The cross sections of all the beams in a structure must be studied before any theoretical analysis is started. If the cross section varies along the length of a beam this fact must be taken into account in the analysis (See Sections 7 to 13, page 20). In particular, if welded brackets are fitted they may be regarded as rigid over an effective length defined in Section 18 (page 60). By fitting a bracket between a beam and a substantial structure at its ends it is possible to increase the constraining moment considerably (but this does not necessarily lead to the most economical design).

It is a misfortune of the present situation in shipbuilding that hardly any steel sections are rolled specially for the fabrication of welded ships. Shipyards are forced to build welded ships with rolled sections originally designed for riveted construction or to cut tee bars from I joists normally used for other purposes. This has led to extensive use of ordinary angle bars to stiffen panels of plating, by welding the edge of one flange to the plate so that it forms a web, with the other flange remote from the plate and parallel to it. The total cross section of the beam so formed is unsymmetrical and, in general, the load is not applied at its shear centre so that in addition to being bent the beam is also twisted, (See Sections 22 and 23, page 73). This constitutes a considerable weakening of the beam compared with its symmetrical counterpart, particularly when the stiffener is on the loaded side of the plating, and this situation is agravated when slots are cut in the web of the stiffener (See Section 30, page 109). It seems to be likely that compared with the effects measured at Glengarnock, the twisting would be reduced in a ship because of the restraint afforded by the continuous plating, but shipbuilders do not seem to have given the matter attention it deserves.

One of the fundamental assumptions of the ordinary theory of flexure is that cross sections which were plane before bending remain plane after bending. It is commonly assumed by naval architects that this is not so in wide plate flanges of stiffened plating. Research into this resulted in some advances in the theory and the first thorough experiments ever carried out on this subject confirmed the theoretical assumptions and illustrated the effects of shear lag (See Appendix and Chapter II). It was shown that deformations of the cross sections associated with shearing strains are normally negligible in practice, so that the plane sections assumption is usually justified. To cater for occasions when this is not so, however, a new method was developed by which the stresses due to bending and shear lag could be calculated independently. Beams should be analysed by the theory of bending ignoring possible shear

lag, and if necessary the additional stresses associated with shear lag in the plating may be estimated later by the method described in the Appendix.

Shearing deformation also occurs in the webs of stiffeners and this causes a slight increase of deflections. In Chapter III the latter were calculated by the usual method (ref: B1) but the correction rarely exceeded 10% of the maximum bending deflection. Usually the measured deflections of the Glengarnock specimens were greater than the corrected theoretical deflections (See Section 24, page 90), but in many cases the increases were associated with twisting of specimens with unsymmetrical cross sections. In the shear lag experiments described in the Appendix the usual correction for deflections due to shearing strains in the web was also found to be slightly too small. In short stocky beams the effects of shearing strains are important and this was found to be the case when attempts were made to estimate the stiffness of the end structure of the Glengarnock testing machine (See Section 27, page 97). It appears that further research into this aspect of the problem would be useful.

One of the anomalies in the use of the elastic banding theory is that although the structure is designed so that the general level of stress is well below the yield stress, a clause requiring considerable ductility of the material is nearly always included in its specification. This is necessary because although the general stress level is low, it will be much higher around the stress concentrations which are almost inevitable in practical construction (e.g: near the toes of brackets), and if the material was not ductile it might fracture before the general level of stress had reached a reasonable working figure. It is shown in the theory of plastic bending (ref. L1) that when a load is applied such that part of the structure yields, the behaviour of the structure is elastic during its recovery when the load is removed, and during subsequent applications of load provided that they do not exceed that already applied. For this reason, when carrying out experiments to verify an elastic theory the strains and deflections during the first application of load may not correlate well with the theory, but readings made during subsequent unloading and during subsequent applications and removals of load should do so. (This principle guided the investigators at Glengarnock - see page 53 - and it was adopted in the analysis discussed in Chapter IV). Conversely, if a comparison with the plastic bending theory is required, the experiment must be carried out during the first application of the load. In any case, however, readings should always be taken during the first load application, because unexpected weaknesses may be revealed which would not be detected in subsequent experiments. An interesting example was the permanent deflections measured over the middle span of the stiffener discussed in Chapter IV (See page 121).

42) General Conclusions.

With the provisos mentioned in the last Section the elastic theory of flexure may be used with confidence to calculate the stresses and deflections in the structural members of ships. In other words, the conclusions in Section 31 (page 110) regarding the Glengarnock results appear to hold also in practice.

This does not mean, however, that the strength of any beam in a ship may always be calculated easily by the elastic bending theory. For example, the experiments discussed in Chapter IV indicated that in order to estimate the bending moments in the bulkhead stiffener it would be necessary to calculate the deflections in way of the two heavy horizontal girders and to do so would involve consideration of the whole bulkhead as a grillage of intersecting beams. There was also the anomaly of the relatively large deflections measured in the centre span of the stiffener, which remained unexplained.

In general, the plastic bending theory is easier to use than elastic analysis and provides a more logical basis for design. There appears to be considerable merit in applying it wherever possible, provided that the objections mentioned at the end of Chapter V (page 127) do not apply.

- 00 -

REFERENCES.

Author's publications.

A 1 YUILLE. I. M. "On the Constraint at the Ends of Ships' Structural Members." Trans. I.N.A. 1952.

A 2 YUILLE. I. M. "Shear Lag in Stiffened Plating." Trans. I.N.A. 1955.

Books on Structural Analysis.

B 1 TIMOSHENKO. S. "Strength of Materials." Two volumes. (Nostrand 1940).

B 2 SALMON. E. H. "Materials and Structures." Part two - "Theory and Design of Structures." (Longmans 1938).

B 3 MORLEY. A. "Strength of Materials." (Longmans 1940).

B 4 MORLEY. A. "Theory of Structures." (Longmans 1948)

B 5 HARTOG. J. P. den "Strength of Materials." (McGraw-Hill 1949).

B 6 CROSS. H. and MORGAN. N. D. "Continuous Frames of Reinforced Concrete." (Wiley).

B 7 MAUGH. L. C. "Statically Indeterminate Structures." (Wiley 1946).

B 8 WILLIAMS. C. D. "Analysis of Statically Indeterminate Structures." (International Textbook Co.).

B 9 GRINTER. L. E. "Theory of Modern Steel Structures." Vol. II - "Statically Indeterminate Structures and Space Frames." (Macmillan 1937).

B10 GRINTER. L. E. (Ed.) "Numerical Methods of Analysis in Engineering." (Macmillan 1949).

B11 PIPPARD. A. J. S. and BAKER. J. F. "Analysis of Engineering Structures.". (Arnold 1943).

Column Analogy.

C 1 CROSS. H. "The Column Analogy." Univ. of Illinois, Bull. 215. 1930.

Elasticity.

E 1 TIMOSHENKO. S. "Theory of Elasticity." (McGraw-Hill 1934).

E 2 SOUTHWELL. R. V. "An Introduction to the Theory of Elasticity for Engineers and Physicists." (Oxford Univ. Press 1941).

E 3 PRESCOTT. J. "Applied Elasticity." (Longmans 1924).

E 4 COKER. E. G. and FILON. L. N. G. "Treatise on Photo-elasticity." Especially Chapter II. (Cambridge Univ. Press 1931).

Glengarnock Results.

(i) Statistical Reports.

G 1 TURNBULL. J. First Interim Report: "Description of the Testing Apparatus." Trans. Inst. Welding. 1939.

G 2 TURNBULL. J. Second Interim Report: "Investigation of the Welding of Ships' Structures." Trans. Inst. Welding. 1940.
(The field results from which this report was compiled were no longer available).

G 3 TURNBULL. J. Third Interim Report: "Investigation of the Welding of Ships' Structures." Trans. Inst. Welding. 1943.
(The field results from which this report was compiled were made available to me by courtesy of B.S.R.A.).

G 4 TURNBULL. J. Fourth Interim Report: "Investigation of the Welding of Ships' Structures." B.W.R.A. Report Ref. F.E. 3/34/26. 1945.
(The field results from which this report was compiled were made available to me by courtesy of B.S.R.A.).

G 5 JENSEN. C. J. G. First Interim Report under B.S.R.A. (Confidential). "Investigations at Glengarnock on the Strength and Stiffness of Ships' Structural Members." B.S.R.A. Report No. 1. 1947.

G 6 JENSEN. C. J. G. and HADJISPYROU. A. G. Second Interim Report under B.S.R.A. (Confidential). "Investigations at Glengarnock on the Strength and Stiffness of Ships' Structural Members." B.S.R.A. Report No. 16. 1948.

G 7 HADJISPYROU. A. G. Third Interim Report under B.S.R.A. (Confidential). "Investigations at Glengarnock on the Strength and Stiffness of Ships' Structural Members." B.S.R.A. Report No. 61. 1950.

G 8 HADJISPYROU. A. G. Fourth Interim Report under B.S.R.A. (Confidential). "Investigations at Glengarnock on the Strength and Stiffness of Ships' Structural Members." B.S.R.A. Report No 86. 1951.

G 9 McCALLUM. J. Fifth Interim Report under B.S.R.A. (Confidential). "Investigations at Glengarnock on the Strength and Stiffness of Ships' Structural Members." B.S.R.A. Report No. 133. 1954.

(ii) Papers to Institutions under the title "Ship Structural Members."

G10 Part I ADAM. J. L. Trans. I.N.A. 1940.

G11 Part II LILLICRAP. C. S. and JENSEN. C. J. G. Trans. I.E.S. Scotland. 1943-4.

G12 Part III LILLICRAP. C. S. and JENSEN. C. J. G. Trans. N.E. Coast I.E.S. 1944-5.

G13 Part IV JENSEN. C. J. G. Trans. N.E. Coast I.E.S. 1948-9.

G14 Part V HADJISPYROU. A. G. and LACKENBY. H. Trans. I.E.S. Scotland. 1951-2.

G15 Part VI McCALLUM. J. Trans. N.E. Coast I.E.S. 1954-5.

Riveted Joints.

J 1 RATHBUN. J. C. "Elastic Properties of Riveted Connections." Trans. Am. S.C.E. 1936.

J 2 WILLIAMS. D. "Load Distribution in Riveted and Spot-Welded Joints." Trans. I. Mech. E. 1951.

Limit Design and the Theory of Plastic Bending.

L 1 BROEK. J. A. v. den "Theory of Limit Design." (Wiley 1948).

L 2 PARTRIDGE. F. A. "Application of the Plastic Theory to the Design of Mild Steel Beams and Rigid Frames." Mechanical World. March 1952.

L 3 FREUDENTHAL. A. M. "Inelastic Behaviour of Engineering Materials and Structures." (Wiley 1950).

L 4 BAKER. J. F. "Shortcomings of Structural Analysis." Trans. N.E. Coast I.E.S. 1951-2.

L 5 SYMONDS. P. S. and NEAL. B. G. "The Interpretation of Failure Loads in the Plastic Theory of Continuous Beams and Frames." J. Aero. Sciences. Jan. 1952.

L 6 YOUNG. D. H. "Rational Design of Steel Columns." Trans. Am. S.C.E. 1936.

L 7 RODERICK. J. W. "Tests on Stanchions Bent in Single Curvature about both Principal Axes." British Welding Journal. May 1955.

L 8 PRAGER. W. "The Theory of Plasticity. A Survey of Recent Achievements." I. Mech. E. James Clayton Lecture 1955.

Mathematics.

M 1 FRANKLIN. P. "Fourier Methods." (McGraw-Hill 1949).

M 2 SOKOLNIKOFF. I.S. and E. S. "Higher Mathematics for Engineers and Physicists." (McGraw-Hill 1941).

M 3 CARSLAW. H. S. and JAEGER. J. C. "Operational Methods in Applied Mathematics." (Oxford 1941).

M 4 CHURCHILL. R. V. "Modern Operational Mathematics in Engineering." (McGraw-Hill 1944).

Relaxation Methods.

R 1 CROSS. H. "Analysis of Continuous Frames by Distributing Fixed End Moments." Trans. Am. S.C.E. 1932.

R 2 SOUTHWELL. R. V. "Relaxation Methods in Engineering Science." (Oxford Univ. Press 1940).

R 3 BUTTERWORTH. S. "Structural Analysis by Moment Distribution." (Longmans 1949).

R 4 SHEPLEY. E. "Continuous Beam Structures." (Concrete Pub. 1942).

R 5 KLOUCEK. C. V. "Distribution of Deformation." (Author's limited edition, distributed by Orbis Ltd., Czechoslovakia. - Copy in library of I.E.S. Scotland).

R 6 WESSMAN. H. E. and KAVANAGH. C. "End Restraints on Truss Members." Trans. Am. S.C.E. 1950.

R 7 VEDELER. G. "Calculation of Beams." Trans. I.N.A. 1950.

Shear Lag.

S 1 PIETZKER. F. "Festigkeit der Schiffe." (Springer, Berlin 1911).

S 2 KARMAN. Th. v. "Beitrage zur Technischen Physik und Technischen Mechanik." (Festschrift August Foppl) (Springer, Berlin 1923). (Quoted extensively in ref. E 1).

S 3 METZER. W. "Die Mittragende Breite." Luftfahrtforschung 1929.

S 4 MILLER. A. B. "The Effective Width of a Plate Supported by a Beam." Selected Engineering Paper No 83, Inst. Civil Engineers. Also Luftfahrtforschung 1929.

S 5 CHWALLA. E. "Die Formeln zur Berechnung der 'vollmittragenden Breite' dunner Gurt- und Rippen-platten." Der Stahlbau, Berlin 1936. (Der Stahlbau is bound as a supplement to Die Bautechnik).

S 6 SANDORFF. P. E. "Bending Rigidity and Column Strength of Thin Sections." Trans. Am. S. Mech. E. 1947.

S 7 WINTER. G. "Stress Distribution in, and Equivalent Width of Flanges of Wide, Thin-wall Steel Beams." N.A.C.A. Tech. Note 784. 1940.

S 8 YOUNGER. J. E. "Mechanics of Aircraft Structures." (McGraw-Hill 1942).

S 9 SCHADE. H. A. "The Effective Breadth of Stiffened Plating under Bending Loads." Trans. Am. S. N.A. and Mar. E. 1951.

S10 ORR. J. "Shear Lag by Relaxation." International Assoc. for Bridge and Structural Engineering, Zurich 1947.

S11 KUHN. P. and CHIARITO. P. T. "Shear Lag in Box Beams - Methods of Analysis and Experimental Investigations." N.A.C.A. Report 739. 1941. (And three previous papers by Kuhn given in bibliography).

S12 MUCKLE. W. "Built-up Girders - Effective Breadth of Plating attached to Rolled Sections." Shipbuilder Oct. 1955. (This paper was published after the research was complete, but may be of interest - particularly in connection with ref. 13 below).

S13 LOCKWOOD-TAYLOR. J. "Theory of Longitudinal Bending of Ships." Trans. N.E. Coast I.E.S. 1924-5.

S14 HARTMAN. E. C. and MOORE. R. L. "Bending Tests on Panels of Stiffened Flat Plating." Aluminium Research Laboratories, Technical Paper No 4, Aluminium Company of America. 1941.

S15 REISSNER. E. "Least Work Solutions of Shear Lag Problems." J. Aero. Sciences. 1941.

S16 SCHNADEL. G. "Die Mittragende Breite im Kastentragen und im Doppelboden." Werft und Reederei. 1928.

Torsion of Beams, Shear Centre.

T 1 SEELY. F. B., PUTNAM. W. J. and SCHWALBE. W. L. "Torsional Effect of Transverse Bending Loads on Channel Beams." Univ. of Illinois Bulletin 211. 1930.

T 2 TERRINGTON. J. S. "Torsion Centre of Girders." Engineering 26/11/54.

T 3 STELLING. E. G. "Verdrehungsfeste, dreiflachlige Bruckentrager...." Der Stahlbau, Berlin 1929. (Der Stahlbau is bound as a supplement to Die Bautechnik). See also Eng. Ab. I.C.E. No 41:97.

T 4 GRIFFITH. A. A. and TAYLOR. G. I. "Problem of Flexure and its Solution by the Soap Film Method." Tech. Rep. of the Adv. C'ttee for Aeronautics, Vol 3 No 399 (R and M) 1917-8.

Wire Resistance Strain Gauges.

W 1 LEE. G. H. "Introduction to Experimental Stress Analysis." (Wiley 1950).

W 2 AUGHTIE. F. "Electric Wire Resistance Strain Gauges." Trans. I Mar. E. 1946.

W 3 TANNAHILL. A. L. "Application of Electric Resistance Strain Gauges." Engineer 10/6/49.

W 4 DOBBIE. W. B. and ISAAC. P. C. G. "Electric Resistance Strain Gauges." (English Univ. Press 1948).

Extra Referances.

X 1 ------- "Hogging and Sagging Tests - M.V. Neverita." Admiralty Ship Welding Committee, Report R 1. 1946.

X 2 HAY. W. I. "Some Notes on Ships' Structural Members." Trans. I.N.A. 1945.

X 3 PARKES. E. W. "The Stress Distribution near a Loading Point in a Uniform Flanged Beam." Phil. Trans. Roy. Soc. A 244 1952.

X 4 ------- Reports of the Steel Structures Research Committee. First Report 1931. Second Report 1934. Final Report 1936.

X 5 ROSSEL. H. E. and CHAPMAN. L. B. (Ed.) "Principles of Naval Architecture." (Am. S. N.A. and Mar. E. 1942).

- - - - - - - - - - - - -